

# **Response time sensitivity of glaciers using the Open Global Glacier Model**

**From idealised experiments to an estimate for Alpine glaciers**

Master's Thesis

in Atmospheric Sciences



Submitted to the  
Faculty of Geo- and Atmospheric Sciences  
of the  
University of Innsbruck

in Partial Fulfillment of the Requirements for the Degree of  
Master of Science

by  
Lilian Schuster

Advisor  
Fabien Maussion, PhD

Innsbruck, March 2020



# Abstract

Shrinking glaciers are an iconic impact of past and ongoing climate change. Since glaciers adjust slowly to a changing climate, there is an imbalance between the current climate and their geometry: Present and future glacier extent largely depends on past climate variability, turning glaciers into a "delayed" sensor of climate change. A measure that is often used to describe how fast glaciers react to climate change (here defined as a step change in temperature,  $\Delta T$ ) is the e-folding response time, i.e. the time in which 63% of the adjustment between an initial and a perturbed equilibrium glacier state occurs. Estimating this response time from known glacier characteristics would be very useful, but this is impeded by the complex non-linear response of glacier dynamics to climate perturbations. Therefore, we rely on a numerical model to attempt to disentangle the factors affecting the e-folding response time.

Using the Open Global Glacier Model (OGGM), we perform idealised glacier experiments to estimate the response time sensitivity to climatic or geometric glacier characteristics. Starting with idealised glacier geometries, the experiments are improved to include more realistic and complex bed geometries. We compute the temporal evolution (1862–2003) of the response time of the Hintereisferner, Ötztal Alps, using initial equilibrium glacier states with similar lengths as the observations and the HISTALP climate dataset. Furthermore, we conduct general response time estimates for 3863 alpine glaciers using initial equilibrium glaciers with similar areas as measured in 2003.

For a large temperature perturbation  $\Delta T$ , the response time of the Hintereisferner decreases over time along with decreasing glacier length. For smaller  $\Delta T$ , the response time is longer, commencing with a slight increase and then followed by a decrease. This initial paradoxical increase is most likely due to melting of the glacier into a bedrock depression. For idealised glaciers of constant width and a single flowline, we could attribute increased response times to such a bedrock depression. The response time of alpine glaciers for smaller  $\Delta T$  is more variable between the glaciers and mostly longer, for  $\Delta T=+0.1^\circ\text{C}$  in median 53 years and 50% of the glaciers between 42 and 121 years compared to for  $\Delta T=+1^\circ\text{C}$  in median 20 years and 50% between 14 and 29 years. Moreover, the response time is shorter for steeper glaciers or higher mass balance gradients for alpine glaciers as well as in idealised experiments. For large  $\Delta T=+1^\circ\text{C}$ , the response time appears to increase linearly with the mean ice thickness. Glacier size parameters such as volume, area or length do not have a direct influence on the response time of alpine glaciers. Most alpine glaciers are steeper in their upper part, which might explain why applying larger  $\Delta T$  results in rather shorter response times. This effect is most prominent for flat initial equilibrium glaciers, possibly because the response time is more sensitive to perturbed equilibrium slope changes on flat glaciers compared to already relatively steep glaciers. Besides the large response time sensitivity on the applied perturbation  $\Delta T$ , we find discrepancies between different model set-ups and studies.

Therefore, we conclude that the response time is only a relative measure under simplified "laboratory conditions", and its interpretation as an absolute number is delicate. Despite the vagueness of its definition, it is a simple tool to compare the glaciers' response to climatic change and to diagnose which geometric and climatic parameters control the response behaviour. Furthermore, the response time and its changes with  $\Delta T$  could be used to cluster worldwide glaciers into specific groups of response time, and these insights could improve calibrations of numerical global glacier models. Whether the response time has a predictive value for other aspects of glaciology such as the current rate of volume change has to be studied in the future.

## Contents

<b>Abstract</b>	i
<b>Contents</b>	ii
<b>List of Tables</b>	v
<b>List of Figures</b>	v
<b>1 Introduction</b>	1
1.1 Motivation . . . . .	1
1.2 Response time of glaciers . . . . .	1
1.3 Study questions and outline . . . . .	2
<b>2 Basics, History, and Definition of Response Time</b>	4
2.1 Reaction of glaciers to a climatic change . . . . .	4
2.2 Response time using analytical and scaling approaches . . . . .	5
2.3 Details on numerical response time definition of our study . . . . .	9
2.4 Response time estimates of real glaciers in the literature . . . . .	11
<b>3 Methods</b>	14
3.1 Applied software (OGGM), used parameters, and datasets . . . . .	14
3.2 Approach to estimate response times of real glaciers that are in a large disequilibrium with the current climate . . . . .	17
<b>4 Results and Analysis</b>	19
4.1 Idealised glacier experiments: response time sensitivity . . . . .	19
4.1.1 Simplest reference idealised model . . . . .	19
4.1.2 Constant bed width . . . . .	21
4.1.3 Changing bed widths . . . . .	25
4.1.4 Changing bed slopes with a constant bed width . . . . .	25
4.1.5 Lessons from the idealised glacier experiments . . . . .	28
4.2 Response time for different Hintereisferner glacier states . . . . .	30
4.2.1 Idealised Hintereisferner with one flowline, linear mass balance, rectangular bed shape, and a constant width for different initial ELA . . . . .	30
4.2.2 Attempt to capture the Hintereisferner response time temporal evolution . . . . .	31
4.3 Response time of Alpine glaciers . . . . .	38
4.3.1 Total volume & area response time of the entire Alpine glacier ice mass and distribution of response time estimates for individual glaciers . . . . .	38
4.3.2 K-Means clustering for changes in the response time between the different temperature perturbations . . . . .	41
4.3.3 Most important geometric and climatic parameters that control the response time and a rough predictive model . . . . .	43
<b>5 General discussion</b>	50
5.1 In-depth comparison to Ze20 . . . . .	50
5.2 Comparison to literature and in between the experiments . . . . .	53
5.2.1 Relation between glacier size and response time . . . . .	54
5.2.2 Relations of glacier slope and mass balance gradient to the response time . . . . .	54
5.2.3 Relation between applied climatic perturbation and response time . . . . .	55
5.2.4 Relations between other variables and response time as well as comparison to Jo89 . . . . .	56

5.2.5 Direct comparison of response time estimates of real glaciers from other studies to our study . . . . .	57
5.3 Volume against length e-folding response time and e-folding against asymptotic approach . . . . .	58
5.3.1 Comparison between e-folding volume and length response time . . . . .	58
5.3.2 Comparison between e-folding and asymptotic volume response time . . . . .	60
5.3.3 Comparison between e-folding and asymptotic length response time . . . . .	61
5.4 Uncertainties, limitations and possible improvements . . . . .	61
<b>6 Conclusion and Outlook</b>	<b>64</b>
<b>A Appendix</b>	<b>66</b>
Abbreviations & Symbols . . . . .	66
A.1 Idealised experiments: resolution sensitivity & asymptotic response times . . . . .	68
A.2 Hintereisferner: applied climate and length-preserving temperature bias (1862–2003) . . . . .	69
A.3 Alps: $A$ -calibration and the asymptotic response time estimates . . . . .	70
<b>Bibliography</b>	<b>72</b>
<b>Acknowledgments</b>	<b>79</b>
<b>Eidesstattliche Erklärung</b>	<b>81</b>



## List of Tables

2.1	Summary of analytical and scaling approaches . . . . .	7
4.1	Model setup parameters of idealised reference glacier . . . . .	20
4.2	Summary of studied dependencies of the response time for idealised glaciers . . . . .	29
A.1	List of abbreviations . . . . .	66
A.2	List of symbols . . . . .	67

## List of Figures

2.1	Illustration of three-stage model from Roe and Baker (2014) . . . . .	9
3.1	OGGM flowline estimation of Hintereisferner . . . . .	15
4.1	Model initialisation and applied climatic step change: volume and length evolution for idealised reference glacier . . . . .	20
4.2	Idealised glacier experiments with constant slope and width: slope and MB gradient	21
4.3	Idealised glacier experiments with constant slope and width: additional parameters	23
4.4	Idealised glacier experiments with constant slope but changing widths . . . . .	25
4.5	Idealised glacier experiments with changing slopes and constant width . . . . .	26
4.6	Response time of idealised constant-width one-flowline Hintereisferner-like glacier states with a linear mass balance . . . . .	31
4.7	Ice thickness map and vertical profile of Hintereisferner for 1862 and 2003 . . . . .	33
4.8	Temporal evolution of length-preserving equilibrium Hintereisferner states (1862–2003): Response time with geometric and climatic conditions . . . . .	34
4.9	Response time evolution of Hintereisferner for different climatic perturbations and by applying the estimate of Jo89 . . . . .	35
4.10	Temporal evolution of the entire Alpine ice mass: initiation and estimation of response time . . . . .	39
4.11	Distribution of individual e-folding response times of Alpine glaciers . . . . .	40
4.12	K-Means clustering of Alpine glaciers for changes in the response time between different temperature perturbations . . . . .	41
4.13	Scatterplot of response time against different geometric and climatic glacier states with indicated correlation . . . . .	44
4.14	Best predictors and goodness of fit for different predictive models for Alpine glacier response time estimates . . . . .	46
4.15	Scatterplot of random forest regression (all $\Delta T$ ) versus our Alpine glacier response time estimates . . . . .	46
5.1	Comparison of different mean Alpine glacier response time estimates: OGGM (HISTALP & CRU) against Ze20 . . . . .	51
5.2	Scatterplot response time estimates of Alpine glaciers above 1 km length . . . . .	51
5.3	Comparison of rule of thumb relation from Ze20 to our modelled response time of Alpine glaciers . . . . .	53
5.4	Scatterplot of Jo89 versus e-folding response time for Alpine glaciers . . . . .	56
A.1	Resolution sensitivity of response time for idealised glaciers . . . . .	68
A.2	Scaled volume & length evolution of an idealised glacier of constant slope with exponential & sigmoidal fit . . . . .	68
A.3	Hintereisferner: climate anomalies 1862–2003 . . . . .	69
A.4	Applied temperature bias for length-preserving Hintereisferner (1862–2003) . . . . .	69
A.5	$A$ -parameter tuning to fit to the Alps total volume of Farinotti <i>et al.</i> (2019) . . . . .	70
A.6	Ratio of asymptotic to e-folding response time estimates for Alpine glaciers . . . . .	70
A.7	Scaled volume & length evolution of Hintereisferner with exponential & sigmoidal fit	71
A.8	Scaled volume & length evolution of Vernagtferner with exponential & sigmoidal fit	71



## 1 Introduction

### 1.1 Motivation

Shrinking mountain glaciers are an iconic feature of past and ongoing climate change. While a large part of global glacier mass loss since 1850 is related to natural climate variability, i.e. a retreat from the 19<sup>th</sup> century maximum at the end of the little ice age, about 70% of global glacier mass loss from 1991 to 2010 can be attributed to anthropogenic causes (Marzeion *et al.*, 2014a).

Mountain glaciers (here: all glaciers except for the Greenland and Antarctic ice sheets) contributed between 25% and 30% of the observed sea level rise from 1961 to 2016 (Zemp *et al.*, 2019). The contribution of mountain glaciers is relatively high despite their low ice mass proportion (about 0.8%; Oppenheimer *et al.*, 2019, Fig. 4.4). This is due to their faster response to the changing climate: mountain glaciers typically adapt to climate change within a few decades, while ice sheets need millennia (Cuffey and Paterson, 2010, hereinafter referred to as Cu10). Because of the current pace of climate change, glaciers are still reacting to past warming: if climate change would stop now and today's climate would remain stable, 36% of the present-day glacier ice mass would still melt (Marzeion *et al.*, 2018). This amount is called "committed mass loss" because it is a response of both actual and past warming.

On a regional level, melting glacier ice can be an important water source during summer months. Glacier runoff depletion in the dry and warm season can therefore cause problems in the water availability for certain regions (Kaser *et al.*, 2010). In addition, the number and volume of potentially hazardous moraine-dammed lakes in e.g. the Himalayas, which have the potential to produce devastating Glacial Lake Outburst Floods (GLOFs, Richardson and Reynolds, 2000), is increasing as glaciers retreat in response to climatic warming. How fast the runoff of individual glaciers diminishes after reaching peak water depends among other things on the magnitude of the warming and on the time it takes for glaciers to respond to changes in climate (e.g. Huss and Hock, 2018). The response to a mass balance change of a glacier is taking place at a finite velocity; therefore a glacier can be in a strong disequilibrium between the climate and its geometry (e.g., Zekollari and Huybrechts, 2015; Marzeion *et al.*, 2018).

Each individual glacier responds differently to climate change, due to its specific geometry and to regional climatic characteristics such as amount and seasonality of precipitation. Important parameters are the glacier surface slope, the change of mass balance with altitude and glacier elevation range (e.g. Oerlemans, 2001; Zekollari and Huybrechts, 2015; Zekollari *et al.*, 2020, hereinafter referred to as Ze20).

It is necessary to get a better understanding of how individual glaciers respond to a changing climate for predicting their future evolution. A possible starting point is to compare the response time between individual glaciers against their specific climatic and geometric characteristics. The response time estimates describe the response behavior of glaciers for similar climatic changes under "laboratory conditions". Hence, they enable to cluster glaciers into similar behaving groups. Subsequent studies could analyse whether the response time has a predictive value for other aspects of glaciology, such as a possible relation to the current rate of volume changes that are for example estimated by geodetic methods. Further, this scale could be used as a calibration parameter for mass balances of neighbouring glaciers in numerical models, or to improve analytical models. In addition, future research could analyse whether there is a relation between the reconstructability of past glacier states and the current response time of a glacier (Eis *et al.*, 2019).

### 1.2 Response time of glaciers

As the climate does not change abruptly but continuously and glaciers are nowadays nowhere in equilibrium, it is not possible to "observe" the theoretical construct of response time directly (Oerlemans, 2007). Past literature used different approaches to estimate the response time by

analytical simplified equations or by scaling, e.g. as a ratio of the maximum ice thickness to the mass balance at the terminus (Jóhannesson *et al.*, 1989, hereinafter referred to as Jo89), or as a ratio of a length scale to an ice velocity scale (Oerlemans, 2001). However, these approaches use different assumptions and some describe rather the response of the entire volume, while others describe the length response. A mass balance change in the accumulation area has to travel first through the glacier before it reaches the terminus. Hence, ice volume is more directly affected by changes in the specific mass balance than area or length of a glacier. Thus, the volume response time is shorter than the area or length response time (e.g. Oerlemans, 2001).

Further, regional or even global response time estimates were computed mostly by scaling approaches without explicitly including ice dynamics and using very simplified glacier geometries (e.g. Haeberli, 1995; Raper and Braithwaite, 2009; Bach *et al.*, 2018).

Analytical more accurate expressions, as e.g. the three-stage-model of glacier length evolution of Roe and Baker (2014), can provide clear physical insights into dependencies of geometric characteristics on the glacier response for idealised geometries. Nevertheless, they give only limited information for complex glacier geometries as the used assumptions are not valid.

More information of a glacier's geometry and climate is accounted for in numerical flowline models. To the best of our knowledge, numerical flowline model studies use the static e-folding approach to estimate a response time of a glacier: this value describes the time that a glacier in equilibrium with its initial climate needs to complete all but a factor of 1/e of its adjustment into its new perturbed equilibrium after a sudden change in the mass balance (Cu10). The e-folding response time scale is also used in our study, mostly for adjustments in the glacier volume.

Until recently, response time estimates using numerical modelling were rare and were applied only for single or a few glaciers (e.g. Oerlemans, 2001; Anderson *et al.*, 2008; Zekollari and Huybrechts, 2015). Due to the growing data availability, computing power and the development of new models in the last decade, it became possible to estimate response times of individual glaciers on a regional or global scale. Ze20 generated a first regional-scale glacier response time inventory with a flowline model for all Alpine glaciers above one kilometre length. Using statistical regression, they propose a “formula” to reconstruct the glacier response time as a function of glacier surface slope of the lowest 80% of elevation of the glacier and the glacier's elevation range.

Nevertheless, the response time is only vaguely defined and no overview among the studies exists. The sensitivity of response time for different geometric and climatic characteristics of glaciers has not yet been studied in detail with numerical flowline models. According to Zekollari and Huybrechts (2015) for the Morteratsch glacier, Switzerland, the e-folding response time depends strongly on the magnitude of applied climatic perturbation step change. The applied perturbation decides on the transient geometry of the glacier that is brought into the perturbed equilibrium state and therefore influences how fast a glacier responds. However, it is unclear how the response time changes for an individual glacier as it grows or shrinks, and how the response time generally varies for different climatic perturbations, experimental setups and models.

### 1.3 Study questions and outline

The aim of this thesis is to further investigate the concept of glacier response time, assess its sensitivity to the various factors listed above and, importantly, to discuss the limitations inherent to the concept of a “static” (or fixed) response time. To this end, we will use the open-source dynamical flowline model OGGM (Open Global Glacier Model, Maussion *et al.*, 2019a) to realize numerical experiments on both idealised and realistic glaciers. “Realistic” glacier experiments in our study are experiments that capture as much as possible of the true characteristics of the glaciers by using observed outlines, topographic maps, climate datasets and mass balance data

(see Ch. 3), hereinafter referred to as real glaciers.

After a literature review of the various analytical, scaling and numerical approaches used to compute glacier response time (Ch. 2), we examine the e-folding response time of idealised experiments and transfer the new insights to real glaciers (Ch. 4). Naturally, since real-world glaciers are much more complex, it becomes harder to identify the underlying mechanisms determining the response time. Therefore, we investigate the following three research questions that are built upon each other:

**1 (Ch. 4.1) What are the main drivers of glacier response time in idealised glacier experiments?**

We perform idealised flowline glacier experiments that give insights into how climatic and glacier-specific characteristics influence the response time. Among other things, we investigate the influence of glacier slope, the mass balance gradient, the equilibrium line altitude or the applied climatic perturbation. We start with the most idealised glaciers and go step by step to more complex bed geometries with changing bed widths or slopes, and bedrock depressions.

**2 (Ch. 4.2) How has the response time of the Hintereisferner glacier evolved in the last century and why?**

We compute the temporal evolution of the response time of the Hintereisferner based on equilibrium states that have lengths fitting to the observations from 1862 to 2003. In addition, we analyse the difference in response time evolution for different applied temperature perturbations. Hintereisferner is chosen as a case study because it has a relatively simple geometry and is a good representative of large valley glaciers in the Alps (e.g. Greuell, 1992). It is well observed and has glacier length records going back to the last 150 years (WGMS, 2017).

**3 (Ch. 4.3) How does the response time vary for Alpine glaciers and how sensitive is it to the applied temperature perturbation? What are the main factors that control the response time for Alpine glaciers?**

We estimate the total ice volume and area response time of Alpine glaciers as well as the response time of each Alpine glacier individually for four different temperature step change increase scenarios of  $\Delta T=+0.1^\circ\text{C}$  to  $\Delta T=+1^\circ\text{C}$ . We apply the K-Means clustering algorithm to group glaciers by their behaviour of how their response time changes for different  $\Delta T$ . The climatic and geometric characteristics of the initial equilibrium glaciers that can be related to the response of a glacier are estimated for the different scenarios. Furthermore, simple predictive models using multiple linear and random forest regression are evaluated.

Moreover, differences to the estimates of the Alpine glacier response time of Ze20 (Ch. 5.1) and to the general literature (Ch. 5.2) are discussed. In addition, the e-folding volume response time that was used in our study as default estimate is compared to a similar defined length response time and to the asymptotic approach, where the response time is defined as the constant of an exponential (sigmoidal) fit of the evolving volume (length) after the perturbation (Ch. 5.3). Problems and limitations are analysed in Ch. 5.4. Finally a conclusion and future possible research is presented in Ch. 6. In the appendix (A), a list of used abbreviations (Table A.1) and symbols (Table A.2) as well as some further analyses can be found.

## 2 Basics, History, and Definition of Response Time

First some important aspects and terminologies in glaciology and the reaction of a glacier to a changing climate are summarized (Ch. 2.1). Then, we describe the history of response time estimates using scaling or analytical approaches (Ch. 2.2), the used definition of response time for our study (Ch. 2.3), and the estimates of real glacier response times in the literature from numerical modelling studies and scaling approaches (Ch. 2.4).

### 2.1 Reaction of glaciers to a climatic change

In decades to centuries, compacted snow is transformed into solid ice in the accumulation area of a glacier (positive annual net mass balance) and, due to gravitation, moves downward into the ablation area (negative annual net mass balance) (Cu10).

The equilibrium line altitude (ELA) marks the approximate altitude where the mass balance over a year is zero and divides the accumulation from the ablation area.

Specific mass balances are expressed in  $\text{mm w.e. yr}^{-1}$  or  $\text{kg m}^{-2} \text{yr}^{-1}$  and vary mainly with the elevation. The mass balance increase with height in the ablation area is nearly linear and therefore a mass balance gradient (of the ablation area), i.e. a characteristic of the climate, can be computed. Typical values range between  $1 \text{ mm w.e. yr}^{-1} \text{m}^{-1}$  in dry climates (e.g. Axel Heiberg Island) and  $10 \text{ mm w.e. yr}^{-1} \text{m}^{-1}$  in maritime climates (in New Zealand), e.g. Oerlemans (2008). For Alpine glaciers, the mass balance gradient is around  $3\text{-}5 \text{ mm w.e. yr}^{-1} \text{m}^{-1}$  (Raper and Braithwaite, 2009). It is assumed that high ablation area mass balance gradients (of the ablation area) coincide with a stronger mass balance increase with height for the accumulation area. Hence, high mass balance gradients indicate situations with a lot of accumulation above the equilibrium line and a lot of ablation below it, resulting in larger ice transfer and higher flow rates in order to maintain a steady state profile (Hooke, 2019, hereinafter referred to as Ho19). Factors that influence the mass balance gradient include the change of temperature with height, the radiation balance, and the precipitation gradient, which is negligible according to Ho19.

Stresses on ice induce deformation, also called strain  $\epsilon$ . The rate at which strain occurs,  $\dot{\epsilon}_{ij}$ , in a given direction in ice depends on all stresses acting on the medium and therefore often the effective strain rate,  $\dot{\epsilon}_e$ , is used (Ho19). The effective strain rate,  $\dot{\epsilon}_e$ , is described through the Glen's flow law by the effective shear stress,  $\sigma_e$ ,

$$\dot{\epsilon}_e = A \sigma_e^n. \quad (1)$$

$A$  refers to the ice creep parameter that describes the viscosity of a medium, the smaller  $A$ , the stiffer is the medium (in this case ice).  $A$  depends on temperature, on the water content of ice (lower water contents result in lower values for  $A$ ) as well as on pressure, texture fabric, and impurities (Ho19). The ice creep exponent,  $n$ , depends on the creep mechanism operation and is often set to 3; however, lower values might be more appropriate for lower stresses. Glaciers move over their beds if the basal temperature is at the pressure melting point, i.e. sliding. Sliding theory is complex and often not accounted for in "simpler" models.

In a climate remaining constant for several centuries, glaciers would adjust their geometry such that the integral of the specific net balance over the glacier amounts to zero, as consequence the glacier would be in a steady state or equilibrium (Ho19). However, climate changes gradually with random fluctuations from year to year superimposed with a longer term warming trend in recent years (Cu10). As every glacier differs from another in its characteristics such as size, steepness, orientation, and local climate, the flow regime prescribes how a glacier reacts to a change in the climate (Cu10). Climatic changes influence the mass balance directly due to variations in precipitation, temperature, and radiation balance over the glacier. Discrepancies between specific net balance and local emergence or submergence velocity cause the glacier to change its geometry. In the case of a negative net mass balance, the ELAs raise and glaciers retreat into higher elevations until the net balance returns to zero (Ho19).

An important feedback that is known to directly influence the response time of glaciers is the normal increase in mass balance with elevation, the mass-balance-elevation feedback, which results in amplified thickening or thinning, i.e. Böðvarsson effect (Böðvarsson, 1955).

Changes in mass balance first affect the glacier's thickness. The thereby altered ice velocity propagates and diffuses downward and affects the mass transfer between accumulation and ablation area. Finally, the perturbation reaches the terminus where the commenced advance or retreat is reinforced (Ho19). If changes occur only in the upper part, it can take years until the signal has propagated to the terminus. The time required for full adjustment is hereby theoretically infinite.

In the case of a mass balance increase, the stability between the accumulation area, which is dominated by extension and particles driven down to the glacier bed, and the ablation area, which is dominated by compression and particles being driven upwards, is maintained through kinematic waves (Ho19). Those kinematic waves are not dynamic as waves in water but formed to conserve mass (or volume at constant density). They are waves of constant ice flux that move faster than ice (Ho19). Observing kinematic waves is difficult as local ice thickness and velocity change only by around 10% (van de Wal and Oerlemans, 1995).

The effect of a small change in the mass balance  $b$  can be analysed by applying a perturbation approach. The specific mass balance changes from  $b_0(x)$  to  $b(x, t) = b_0(x) + b'(x, t)$ . Index '0' corresponds to the initial equilibrium state and  $b'$  is the mass balance perturbation. The x-axis is here pointing downwards along the glacier bed. If the perturbation is small enough, second or higher order terms can be neglected. For a slab of ice with a constant slope and width, the ice thickness perturbation  $h'$  that changes over time can be expressed as

$$\frac{\delta h'}{\delta t} = \underbrace{b'}_{(i)} - \underbrace{\frac{\delta c_0}{\delta x} h'}_{(ii)} - \underbrace{(c_0 - \frac{\delta D_0}{\delta x}) \frac{\delta h'}{\delta x}}_{(iii)} + \underbrace{D_0 \frac{\delta^2 h'}{\delta x^2}}_{(iv)}, \quad (2)$$

with  $c_0 = (\frac{\delta q}{\delta h})_0$  as the kinematic wave speed,  $D_0$  as the diffusivity, and  $q$  as the ice flux. Hence, from this linearised theory approach, the ice thickness perturbation changes over time due to the following terms:

- (i) with a higher mass balance perturbation,  $h'$  increases over time
- (ii) results in the rate of change of  $h'$  decreasing or increasing exponentially
- (iii) represents a kinematic wave with constant  $h'$  moving with the speed  $(c_0 - \frac{\delta D_0}{\delta x})$
- (iv) describes diffusive dampening of the perturbation  $h'$

This information was taken out of Ho19, where the full derivation can be found. The original description is from Nye (1960).

## 2.2 Response time using analytical and scaling approaches

The response time of glaciers was estimated in the past mostly using analytical and scaling methods derived from simplified glacier geometries.

The first approach to define a response time applied the kinematic wave theory by neglecting diffusion and assuming a uniform longitudinal strain rate  $\frac{\delta h'}{\delta x} = 0$  (Nye, 1960). This simplifies Eq. 2 to

$$\frac{dh'}{dt} = b' - \gamma_0 h' \implies h' = \frac{b'}{\gamma_0} (1 - e^{-\gamma_0 t}), \quad (3)$$

with  $\gamma_0 = \frac{\delta c_0}{\delta x}$ . Here,  $h'$  approaches the value  $b'/\gamma_0$  asymptotically. In this simplified model the e-folding response time,  $\tau = \frac{1}{\gamma_0} = \frac{\delta x}{\delta c_0}$ , is inversely proportional to the longitudinal strain rates. The total time that would be required to attain a new steady state would be infinite (Ho19). Due to neglected diffusion, this approach severely underestimates the actual response time and unstable responses may develop. However, when adding diffusion, which occurs when fluxes are proportional to gradients (here the slope, see term (iv) in Eq. 2), the wavelength of the wave is increased and its amplitude decreased. Hence, the response time might be increased by more than an order of magnitude (Nye, 1963), resulting in a longer response time than available observations would be able to indicate (Jo89). It must be added here that the response time is only a theoretical construct and cannot be directly compared to observations. An approach of Oerlemans (2001) uses also the relation of response time being proportional to a length scale against a velocity. While the velocity is the speed of kinematic surface waves at the terminus in Nye (1963), it is a velocity based on simple geometric assumptions of the mass flux in Oerlemans (2001). More information is given in Table 2.1.

Jo89 suggested a practical measure of the volume response time scale,  $\tau_{V,Jh}$ , that is calculated as the ratio of a characteristic ice thickness scale,  $H^*$ , to the ablation rate value at the terminus, ( $b_t < 0$ ),

$$\tau_{V,Jh} = \frac{\delta V}{\delta B} = \frac{H^*}{-b_t}. \quad (4)$$

In the following, a short derivation is given for a simplified block glacier with a constant slope as done in Cu10: Assuming a glacier of total length  $L$ , and a mass balance perturbation occurring from an initial equilibrium state  $b_0(x)$  to a perturbed equilibrium state  $b_0(x) + b_1$ . The initial mass balance has to be independent of time for further integration and therefore the glacier has to be in equilibrium. The total volume of the glacier,  $V(t) = \int_L Y(x, t)H(x, t)dx$ , is described by its width,  $Y$ , and its height ice thickness,  $H$ . Using a simplified glacier on a long sloping surface with a constant thickness,  $\bar{H}$ , and constant width,  $\bar{Y}$ , and assuming small changes ( $dx \rightarrow \Delta x$ ), we can express the changing glacier volume by

$$\frac{dV}{dt} = L_1(t) \cdot \bar{Y} \cdot \bar{H} = \bar{Y} \cdot (L_0 b_1 - b_t L_1(t)) \quad (5)$$

with the length varying from  $L_0$  to  $L_0 + L_1(t)$ . In case of a glacier advance, the annual mass gain resulting from the perturbation,  $b_1 \cdot L_0$ , is assumed to be equal to the annual mass loss by ablation over the new part of the glacier,  $b_t \cdot L_1(t \rightarrow \infty)$ , under the condition that the glacier reaches its perturbed equilibrium. Rearranging Eq. 5 gives

$$\frac{dL_1(t)}{dt} + \frac{L_1(t)}{\tau_a} = b_1 \frac{L_0}{\bar{H}} \quad \& \quad \tau_a = \frac{\delta V}{\delta B} = \frac{\bar{H}}{-b_t}. \quad (6)$$

The e-folding response time of the simplified block glacier is described by  $\tau_a$  and the linear Eq. 6 can be solved by

$$L_1(t) = L_0 \frac{b_1}{b_t} \left[ 1 - \exp \left( -\frac{t}{\tau_a} \right) \right]. \quad (7)$$

In case of this geometric simplified derivation, the thickness scale,  $H^*$ , corresponds to the mean thickness. In the original publication of Jo89, the maximum ice thickness was chosen as thickness scale of real glacier shapes. This estimate of the response time of a glacier reaching a new steady state by Jo89 was already intended by the authors to only be an order of magnitude and is rather too short. The approach of computing the response time as a ratio of the difference in the steady state volume to the integral of mass balance perturbation,  $\tau \sim \frac{\delta V}{\delta B}$  of Jo89 (Eq. 4), is also used for other analytical formulations of the response time. Hereby, other studies use variations of

the applied simplifications, e.g. applying the ratio of a volume scale to a volume change rate for a response time estimate. The reasons for the underestimation of Jo89 and general limitations for most analytical or scaling approaches are described in the list below. Possible improvements from other studies are summarised in Table 2.1.

- [1] The estimate of Jo89 was done for a response with a **strong simplification of the real glacier geometry**. The ice thickness is the main geometric parameter for Jo89, but it is hard to estimate and not really clear whether the maximum ice thickness is the most appropriate ice thickness scale to use.
- [2] Jo89 **neglects the positive mass-balance-elevation feedback** that occurs if, due to an initial mass balance perturbation, the mass balance perturbation itself adjusts, because the glacier surface altitude changes. With this feedback, a second additional term has to be added to the mass balance perturbation,  $b' + \beta H'(x, t)$  with the mass balance gradient with altitude,  $\beta$ , and the ice thickness change,  $H'(x, t)$ . By this neglection, the response time is underestimated especially for flat glaciers where the surface slope can get significantly different from the bed slope (Harrison *et al.*, 2001).
- [3] In addition, in the so-called “one-stage models”, **any changes in the mass balance on the glacier are immediately converted towards a tendency on the terminus length** (Roe and Baker, 2014). In reality, adjustments due to e.g. a mass gain in the accumulation area take time, as the mass has to be transported to the ablation area, where the largest volume changes occur (Fig. 2.1). Most analytical approaches are one-stage models, hence assume that the glacier is perfectly plastic, which corresponds to the asymptotic case of a Glen’s law exponent with  $n=\infty$  (Eq. 1). For such a material, no deformation occurs for stresses below a certain threshold. For stresses above that threshold, the material deforms at a rate where the stress does not exceed the threshold (Ho19). Therefore, one-stage models predict much lower response times than higher-stage models or when using a numerical flowline model. This is most relevant for glacier length response times and if initial glaciers are not in equilibrium.
- [4] In order to linearise the equations, most approaches **assume small mass balance perturbation changes** from an initial equilibrium state. If applying it to larger perturbations, non-linear additional second or third-order terms should be added to the analytical derivations.

**Table 2.1: Summary of analytical & scaling response time ( $\tau$ ) approaches:** Parameters in equations are mass balance ( $B$ ) at the terminus ( $b_t$ ), thickness scale ( $H^*$ ), as spatial average ( $\bar{H}$ ) and maximum ( $H_{max}$ ), the mass balance gradient ( $\beta$ ) and the glacier volume ( $V$ ), area ( $S_A$ ), length ( $L$ ) and slope ( $s$ ). Changes between initial and perturbed equilibrium states are denoted as  $\Delta$ . If the numbered points described in the list above are improved, it is indicated in column (\*). Some of the assessments were done under the subjective interpretation of the authors. The index [N] in (\*) denotes if the study compared its results to a numerical flowline model. The derivations were based on the response time being dependent on a ratio of volume (thickness) to a volume (thickness) rate ( $\frac{\Delta V}{\Delta B}$ ) or a comparable scaling approach of length against a velocity ( $\frac{L}{u}$ ).

Study (and Eq.)	description, specialities and applications	(*)
Jo89 $\tau_{V,Jh} = \frac{\Delta V}{\Delta B} = \frac{H^*}{-b_t}$	originally $H^* \hat{=} H_{max}$ . For a block glacier of constant thickness derived in Eq.(5 - 7), only declared as order of magnitude, applied in Haeberli (1995) for Alpine glaciers $> 2$ km length. It is still often used, possibly due to its simplicity and dependency on only two parameters, e.g. in Roe and Baker (2016) with $H^* = H_{mean}$ .	[1] [2] [3] [4]

Study (and Eq.)	description, specialities and applications	(*)
Bahr <i>et al.</i> (1998) Pfeffer <i>et al.</i> (1998) $\tau_{V,a} \sim \frac{[L]}{[\bar{u}]}$ $\sim \left[ \frac{mL^{m-1}}{s\beta} \right]^{\frac{4}{5}} \left[ \frac{1}{S_A} \right]^{\frac{7}{8}}$	scaling approach: for glaciers $m=2$ , hence response time decreases for larger glacier size, if glacier shape and mass balance do not change. But usually smaller glaciers have steeper slopes and thus shorter response times. Their estimate and the one of Jo89 are equal if scaling relation $\frac{\bar{H}}{b_t} \sim [S_A]^{-\frac{5}{8}}$ is applied, which worked for radially symmetric ice caps of numerical model experiments. Here, volume-area scaling and response time are inseparable.	[1]? [2] [3] [4]? [N]
Oerlemans (2001) $\tau_{L,a} \sim c_0 \frac{L}{\bar{u}}$ $= \frac{c}{\beta s \sqrt{1 + 20s\sqrt{L}}}$	response time depends on downward mass transfer, estimated by mean ice velocity ( $\bar{u}$ ) scaled by glacier length. $c$ is calibrated by numerical models. Length response time is applied in e.g. Oerlemans (2005); Leclercq and Oerlemans (2012); Oerlemans (2012) to solve the response equation for glacier length fluctuations.	[1]? [2] [3] [4] [N]
Harrison <i>et al.</i> (2001) $\tau_{V,a} = \frac{H^*}{-b_t - \beta H^*}$	based on Elsberg <i>et al.</i> (2001), applied for South Cascade glacier with $H^* = \Delta V / \Delta S_A$ . In Harrison (2013), for block glacier experiments of constant height ( $H = 10/s$ ), width, and slope a simplified response time of $\tau_V = \frac{2.10}{s^2 L \beta}$ (for near steady state) was estimated. A similar approach was used in Bach <i>et al.</i> (2018) for world-wide glaciers idealised as blocks of constant slope, height, and width and using volume-area & -length scaling. In Harrison (2013), nonlinearities of glacier response are discussed causing $\tau_V$ not to be constant when larger perturbations are applied.	[1] [2] [3] [4] [4] [N]
Raper and Braithwaite (2009) $\tau_{V,a} = \frac{\gamma}{\nu} \cdot \frac{\bar{H}}{-b_t}$	scaling approach: $R \sim S_A^\nu$ ( $R$ : altitude range), $V \sim S_A^\gamma$ , assumed triangular area-altitude distribution symmetrical around ELA. Applied to world-wide glaciers, but works only for mentioned geometry.	[1]? [2] [3] [4]
Roe and O'Neal (2009) $\tau_{V,a} = \frac{w\Delta H \Delta L}{\Delta L s \Gamma \mu S_{A,abl}}$ $= \frac{\Delta V}{\sum_{abl} \Delta \text{melt rate}}$	ratio between anomalous ice volume and anomalous melt rate summed up over ablation area, $\mu$ : melt factor, $\Gamma$ : atmospheric lapse rate. $\hat{=}$ Time taken to melt (or build) anomalous ice volume due to the anomalously warm (or cold) temperature conditions experienced in ablation zone due to an advance (or retreat) of the terminus (length of the glacier's 'memory' of previous climate states), applied also in Roe (2011) and Burke and Roe (2013) to analyse response to climatic persistence.	[1]? [2] [3] [4] [N]
Harrison <i>et al.</i> (2003); Lüthi (2009) $\tau_{V,a} = \frac{1}{\beta(\frac{Z_{abl}}{\gamma H} - 1)}$ $\tau_{S_A,a} = \frac{\eta(1-\eta)}{\beta(\frac{Z_{abl}}{\gamma H} - \eta)}$ 'two-stage-model'	approach of Harrison <i>et al.</i> (2003): Delay between volume and area change introduced by the macroscopic glacier response as critically damped harmonic oscillator accounting for departures from perfect plasticity with $\tau_V < \tau_{S_A}$ . $\tau_V$ controls also amplitude of response. Approach applied on idealised glaciers in Lüthi (2009) with elevation difference in ablation area, $Z_{abl}$ , volume-area scaling exponent, $\gamma \sim 1.4$ . Shape factor $f = \frac{V}{HL}$ and $f_* = \frac{\Delta V}{H \Delta L}$ are used for $\eta = \frac{f_*}{\mu f}$ . Transient response of out-of-equilibrium glaciers investigated.	[1]? [2] [3] [4]? [N]
Roe and Baker (2014) 'three-stage-model'	refined mass redistribution from interior to the terminus in three overlapping stages: mass-balance perturbation drives changes in the interior thickness, which in turn produces changes in the terminus ice flux and finally changes in glacier length (Fig. 2.1).	[1]? [2] [3] [4]? [N]

Most analytical or scaling approaches assume that glacier area or length responds instantly to volume changes, hence neglect the time it takes to redistribute mass by the ice flow (problem [3] in list of Ch. 2.2). Therefore, they are also called 'one-stage-models' in Roe and Baker (2014). The approaches of Harrison *et al.* (2003) and Lüthi (2009), see Table 2.1, can be called 'second-stage-models' as they introduced a delay between volume and area changes. While a mass balance perturbation has a slow but instant impact on a glacier's volume, its length changes only after a certain delay, as the perturbation signal reaches the terminus with a finite velocity. Experiments with rapid climate oscillations showed that the glacier's volume might vary, but its length can stay constant (Lüthi, 2009).

As ice volume is more directly affected by changes in the specific mass balance than length or area, the volume response time is shorter than the area or length response time (e.g Oerlemans, 2001). The sigmoidal delayed evolution of glacier length after a mass balance perturbation and hence the glacier length response time, can only be described in an analytically almost correct way by the three-stage-model of Roe and Baker (2014), further explanations are given in Fig. 2.1.

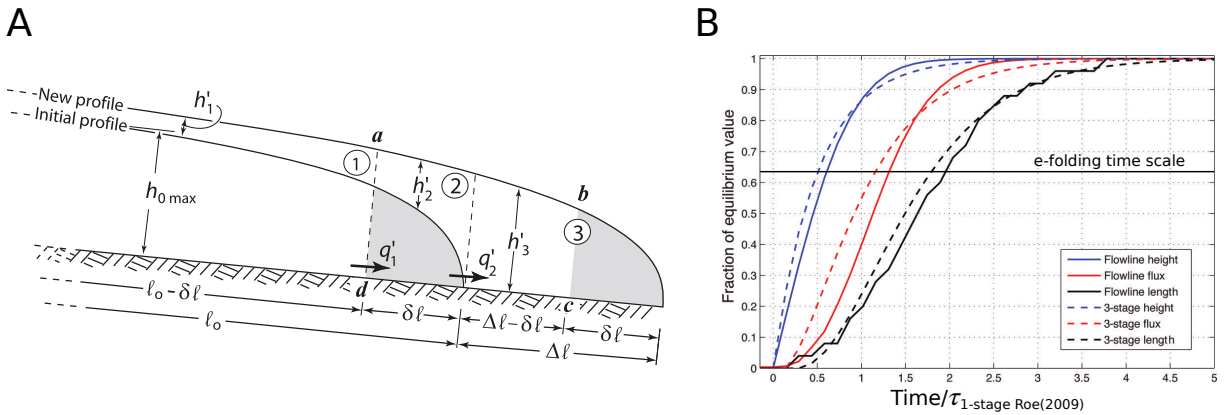


**Fig. 2.1:** (A) Schematic illustration of the transition from an initial equilibrium glacier with length  $l_0$  to a perturbed equilibrium of length  $l_0 + \Delta l$  in three overlapping stages for a positive step change in the mass balance ( $b' > 0$ ) on a longitudinal flow band of unit width. ①: The perturbation results in thickening of the upper glacier. ②: The thickening  $h'_1$  causes an increased flux  $q'_1$  into the terminus region, which then results in an increase of the thickness  $h'_2$  of region ②. ③: This in turn drives an increase in flux  $q'_2$  and an advance of the terminus into region ③ to the length  $l_0 + \Delta l$ . The resulting '3-stage-model' is only valid for small perturbation changes with  $\Delta l \ll l_0$  (Ho19, Fig. 15.11), originally adapted from Roe and Baker (2014). (B) The temporal evolution of height  $h'_1$ , flux  $q'_2$  (past the original terminus) and length changes  $\Delta l$  normalized to the perturbed equilibrium values for the three-stage model of Roe and Baker (2014) and a numerical flowline model. The time is scaled as function of the one-stage response time estimate (Table 2.1, Roe and O'Neal, 2009). Due to the self-similar profile changes and the volume-flux relationship being the same in each segment, there is only one underlying time scale for glacier adjustment:  $\tau_1 = \tau_2 = \tau_3 = \tau_{\text{1-stage}}$ , Roe and O'Neal (2009) /  $\sqrt{3}$ . As each adjustment depends on the previous stage, the height increase can be described by an exponential function, while the length increase is best described by a sigmoidal function, hence  $\tau_{\text{3-stage,length}} \sim \sqrt{3} \tau_{\text{1-stage}}$  (Adapted from Roe and Baker, 2014, Fig. 7)

### 2.3 Details on numerical response time definition of our study

In the following, an explicit definition of the response time for numerical flowline models, as used in the literature, is introduced.

If a glacier is in perfect balance with its prevailing constant climatic state,  $C_0$ , it is in equilibrium with a volume  $V_0$  and length  $L_0$ . When this climatic state is changed stepwise from  $C_0$  to  $C_1$ , the glacier adjusts to a new equilibrium of volume  $V_1$ , and length  $L_1$ . If the introduced perturbation by the climatic step  $|C_0 - C_1|$  is small enough, the volume response is assumed to be that of a perturbed linear system. Under this assumption, the first-order linear response equation can be

solved by

$$V(t) = V_1 + (V_0 - V_1) \cdot \exp(-t/\tau_{\text{asymptotic-vol}}), \quad (8)$$

with  $t \in \mathbb{N}$  in years after the climatic step change occurred. So, for small perturbations, glaciers in equilibrium approach exponentially asymptotically their final steady perturbed equilibrium volume with an initial rapid response that gets progressively damped through time (Jo89; Oerlemans, 2001). This approach is somehow similar to the derivation of e.g. the simplified glacier block response time (Eq. 5 - Eq. 7).

If  $|C_0 - C_1|$  is small, the exponential time constant  $\tau_{\text{asymptotic-vol}}$  is the mathematical description of the response time, also called asymptotic (volume) response time in Jóhannesson (1997) and Leysinger Vieli and Gudmundsson (2004). In subsequent numerical studies, the e-folding response time ( $\tau_V, \tau_L$ ) was introduced as the time a glacier needs to complete a fraction of  $1 - \frac{1}{e}$  (63.2%) of its total volume or length<sup>1</sup> change (Oerlemans, 1997),

$$\tau_V = t \left( V = V_1 - \frac{V_1 - V_0}{e} \right), \quad \tau_L = t \left( L = L_1 - \frac{L_1 - L_0}{e} \right). \quad (9)$$

However, mathematically, this e-folding response time makes only sense for small perturbations. Only if the volume evolution is perfectly exponential, the e-folding volume response time would correspond to the asymptotic response time (exponential time constant:  $\tau_{\text{asymptotic-vol}}$ ). This was described nicely by Jóhannesson (1997) with the e-folding approach being just a 'bypass' that hides the same assumption of an exponential evolution.

After a climatic step change, length changes do not occur steadily, but only after a certain delay when the signal of the perturbation has travelled downward to the terminus (Roe and Baker, 2014). This delayed length response evolution can be better fitted by a sigmoidal function than by an exponential one (Fig. 2.1 B),

$$L(t) = L_1 + \frac{L_0 - L_1}{1 + \exp\left\{\frac{t-t_0}{k}\right\}}, \quad (10)$$

with the fitting parameters  $t_0$  and  $k$ . A time scale similar to the asymptotic volume response time but for length, would be the time  $\tau_{\text{asymptotic-len}}$  when  $1 - \frac{1}{e}$  of the total length change occurs,  $L(t) - L_1 \hat{=} \frac{L_0 - L_1}{e}$ , hence

$$L(\tau_{\text{asymptotic-len}}) = \frac{L_0 - L_1}{e} + L_1 = L_1 + \frac{L_0 - L_1}{1 + \exp\left\{\frac{\tau_{\text{asymptotic-len}} - t_0}{k}\right\}}, \quad (11)$$

$$\Leftrightarrow 1 + \exp\left(\frac{\tau_{\text{asymptotic-len}} - t_0}{k}\right) = e, \quad (12)$$

$$\Leftrightarrow \tau_{\text{asymptotic-len}} = t_0 + \ln(e-1) \cdot k. \quad (13)$$

If the length evolution would fit perfectly to Eq. 10, the time to complete (1-1/e) of the length change,  $\tau_L$ , would correspond to the 'sigmoidal' time constant  $\tau_{\text{asymptotic-len}}$  of Eq. 13.

All approaches are somehow based on the assumption of a small perturbation, still they are used for small and large perturbations (e.g. in Zekollari and Huybrechts, 2015). Although the response is aimed to be independent of the magnitude of climatic perturbation and therefore just an expression depending on the current geometry (Oerlemans, 2001), the response time depends significantly on the applied climatic perturbation for real glacier geometries. This is mainly

<sup>1</sup>The length evolution with OGGM can have small unwanted spikes because of numerical issues. A simple workaround was applied by running a moving filter to only keep the smallest length, more in <https://docs.oggm.org/en/v1.1/> (last access: 8 January 2020)

due to changing geometries of the perturbed state. So, with larger applied perturbations, the mathematical approach of a 'time constant' is not valid anymore and the response time is also not a physical property of the glacier anymore (Oerlemans, 2008). Nevertheless, the mathematical models presuppose and define that the e-folding volume response time is a constant and not a function of time (Bahr *et al.*, 2015).

In our study, we use the same e-folding response time definition for all our applied perturbations, even if it has no clear mathematical fundament. At least for the volume evolution, the assumption of an exponential evolution seemed to be roughly valid for larger perturbations (Zekolliari and Huybrechts, 2015), which was also found and discussed for our study in Ch. 5.3.

Both response time approaches, the asymptotic and the e-folding, assume similarly an exponential volume evolution (Jóhannesson, 1997). Information of how well a used exponential fit describes the volume evolution and hence if the assumption is fulfilled could be obtained by looking at the goodness of fit or just comparing between the asymptotic and e-folding estimates as a starting point. In Jóhannesson (1997), the exponential assumption was valid for climatic perturbations causing changes of the glacier volume amounting to one-half of the current volume.

The e-folding response time is easier to determine, more robust with an equal approach for volume, area or length, and is the only used response time definition for numerical estimates in the literature. Therefore, for our study, the response time is always estimated with the e-folding approach, but there are some comparisons to the asymptotic approach. The length response time is less robust and in the end, the interesting aspect is how fast the mass of a glacier changes with a climatic perturbation, which is more represented by the e-folding volume response time. Consequently, our focus is on the e-folding volume response time,  $\tau$  or  $\tau_V$ , with some comparisons to the length response time,  $\tau_L$ . Whenever we wrote response time without additional information, we thus intended to mean the e-folding volume response time. A discussion about the differences in volume and length response time and between the e-folding and asymptotic approach is done in Ch. 5.3.

## 2.4 Response time estimates of real glaciers in the literature

To our knowledge, all estimates that use a numerical (flowline) model apply the e-folding (mostly volume) response time (Eq. 9). One of the first numerical estimates of the e-folding response time might be the study of Jóhannesson (1991), with a response time of Hofsjökull Ice Cap, Central Iceland, found to lie between 50-100 years with increasing response time with size of perturbation. Flowline models for other Icelandic glaciers predicted a similar response time (Jóhannesson, 1997). An early response time estimate for Hintereisferner was done by Greuell (1992) with  $\tau_V = 78 \pm 10$  yr and  $\tau_L = 94 \pm 15$  yr. In Oerlemans (1997) and similarly in Anderson *et al.* (2008), the response time of Franz-Josef glacier in New Zealand was computed as  $\tau_V = 15$  yr and  $\tau_L = 25$  yr with a numerical flowline model. Other response time estimates of Oerlemans (2001) were for Rhone glacier ( $\tau_V = 36$  yr and  $\tau_L = 58$  yr), Nigardsbreen glacier ( $\tau_V = 42$  yr and  $\tau_L = 68$  yr) and Abramov glacier ( $\tau_V = 71$  yr and  $\tau_L = 92$  yr).

In Haeberli (1995), the equation of Jo89 was applied on Alpine glaciers above two kilometres and a clear hyperbolic decrease in response time with higher surface slopes is visible in their plots. Those estimates lied between 10 and 150 years with most being around 30 to 50 years. The analytical methods were usually calibrated by the few existing numerical flowline models of glaciers (e.g. Oerlemans, 1997, 2001, 2005; Roe and O'Neal, 2009; Roe, 2011; Leclercq and Oerlemans, 2012). Using the calibrated analytical equation of Oerlemans (2001) (see Table 2.1) and applying it on 169 glacier length records revealed analytical response times being mostly between 40-100 years (Oerlemans, 2005). A newly calibrated version of the same formula was used in Leclercq and Oerlemans (2012) by taking the numerical estimates of (length) response time from 14 glaciers (see Leclercq and Oerlemans, 2012, Table 1).

In Oerlemans (2007) & Oerlemans (2012), the response time is estimated from observed changes in glacier lengths by inverse modelling with e.g. Vadret da Morteratsch  $\tau_v = 33$  &  $38$  yr, Vadret da Palü  $\tau_v = 4$  &  $6$  yr, Briksdalsbreen  $\tau_v = 5$  yr, Nigardsbreen  $\tau_v = 35$  yr, Hintereisferner  $\tau_v = 31$  yr and Kesselwandferner  $\tau_v = 2$  yr. Whether this can be interpreted rather as a volume or a length response time is unclear.

In Marzeion *et al.* (2012), a relaxation time scale as a ratio of volume to the solid precipitation amount of the 'equilibrium' glacier, following roughly the scaling approach of  $\tau \sim \Delta V / \Delta B$ , was used to compute length changes. With the corresponding time scale of surface area,  $\tau_{SA(t)} = \tau_L(t) \frac{S_A(t)^2}{L(t)}$ , as calibration factor for area changes, and a volume-area scaling the glacier volume and past and future sea-level change were estimated (similar in e.g. Marzeion *et al.*, 2014b, 2018).

In Oerlemans (2018), the e-folding response time of Monacobreen, Spitsbergen, was numerically estimated to be 250 years. The long time scale was explained by the flat glacier. When they used the approach of Jo89, the response time was estimated to 140 years. This is one of the many examples which shows that the mass-balance-elevation feedback has to be taken into account for flat glaciers. Further examples can be found in Oerlemans (2001).

The above mentioned numerically estimated response times for different glaciers were mainly just for one time point and one climatic forcing. However, the time point decides about the geometry of the initial glacier and the magnitude of perturbation about the transient geometry of the glacier brought into a new equilibrium in the perturbed climate.

A detailed study of the Morteratsch glacier response time for different perturbations and glacier states was done by Zekollari and Huybrechts (2015) with a three-dimensional flow model, where the response time of the shrinking glacier scenarios was considerably lower than of growing scenarios. In a warming climate with a smaller initial Morteratsch glacier, the response time would be shorter, which was explained by an overall steeper Morteratsch glacier. In addition, they investigated the response time for different types of climatic perturbations by varying temperature and precipitation separately. They compared those perturbations to a spatially uniform mass-balance perturbation over the glacier. Temperature is the controlling factor for melting, which occurs mostly in the ablation area, and determines the rain/snow ratio. A temperature change would result in shorter length and volume response times than a uniform negative mass-balance forcing. For a decrease in precipitation, slightly longer response times compared to a uniform negative mass balance forcing were found in Zekollari and Huybrechts (2015). Their possible explanation is that the dominant mass-balance change for a precipitation change is at and above the ELA (Zekollari and Huybrechts, 2015).

Ze20 derived the first regional-scale (e-folding) response time inventory of Alpine glaciers above one kilometre with an extended version of the Global Glacier evolution Model (GloGEM-Flow, see Zekollari *et al.*, 2019). They found mean response times of  $50 \pm 28$  years (one standard deviation), averaging between eight different shrinking and advancing experiments.

Overall, both analytical (Table 2.1), and numerical approaches of the literature do show a dependency of the following parameters on the response time: a steeper glacier, a larger mass balance gradient, a stronger mass balance at the terminus or a larger ice velocity, all result in a shorter response time. It might also seem that the response time decreases with increasing glacier length, but long glaciers have generally beds with smaller slopes (e.g. Oerlemans, 2001). The length response time is longer than the volume response time for numerical flowline models ( $\tau_V < \tau_L$ ), e.g. in Oerlemans (2001) for Nigardsbreen or Zekollari and Huybrechts (2015) for the Morteratsch glacier. This is consistent with the ideas of the 'three-stage-model' of Roe and Baker (2014) (Fig. 2.1). In order that the terminus receives the signal of a perturbation, a certain amount of time is needed, also called sometimes 'initial terminus response time' (Pelto and Hedlund, 2001). For this reason, positive perturbations that cause the glacier to grow have a longer

response time (e.g. Leysinger Vieli and Gudmundsson, 2004; Zekollari and Huybrechts, 2015).

However, as the different analytical and numerical approaches to estimate a response time are different and have other assumptions, they cannot easily be compared among each other. According to Roe and Baker (2014), on a constant slope, the evolution of length response with time is only controlled by one timescale which is a function of the melt factor, lapse rate, and overall geometry. Their timescale  $\tau_{\text{one-stage}}$ , Roe and O'Neal (2009) (see Table 2.1) is fundamentally similar to the response time estimate of Jo89, however it does not correspond to the e-folding length time scale from numerical modelling (and possibly also not to the e-folding volume response time). The sigmoidal length evolution can only be described analytically by introducing a three-stage model. Therefore, the length response time estimated numerically through a flowline model is around twice as long as  $\tau_{\text{one-stage}}$  and the response time from the three-stage analytical model is a factor of  $\sqrt{3} \sim 1.7$  longer than  $\tau_{\text{one-stage}}$  (Fig. 2.1 B). This might be the origin of discrepancies in the literature between timescales computed by different methods. In Roe and Baker (2014), their response time estimate is used to estimate glacier length changes. Hereby, glacier sensitivity to a step change in climate, glacier response to climate trends, and glacier variance driven by stochastic climate fluctuations are proportional to their response time (Roe and Baker, 2014). Hence, correctly identifying the right time scale to use is necessary to estimate glacier sensitivities to climate changes for models that use the response time as calibration parameter (Roe and Baker, 2014).

Consequently, a comparison of analytically and numerically estimated response times is difficult, especially in the case of length evolution, because analytical approaches use assumptions that are not necessary for the flowline model (see list in Ch. 2.2 with the issues [1-3]). In addition, the e-folding response time as estimated by a numerical flowline model is very sensitive to the applied climatic perturbation, model, and setup. Thus, it should only be used as a relative measure (see Ch. 5.2).

In our study we are focusing on the numerically estimated response time, although information about the physics behind it are somehow hidden when no explicit equations are used. It is only since recently that growing computer power, together with improvements in numerical models and data availability of glacier geometry and climate, made it possible to use glacier evolution models at larger scale without having to rely on simplified analytical and scaling approaches.

### 3 Methods

The applied workflow in OGGM with the used parameters and datasets (Ch. 3.1) and the result-oriented approach of estimating response time of real glaciers in a warming climate (Ch. 3.2) is introduced.

#### 3.1 Applied software (OGGM), used parameters, and datasets

The Open Global Glacier Model (v.1.1.2, Maussion *et al.*, 2019b) is applied to simulate the response time of both idealised and real glaciers. In the following, the specific workflow that was used is introduced and those aspects of the model that are most relevant for the interpretation of the response time estimates are described. Hereby we distinguish between the *idealised* glacier experiments with a constructed bed and predefined linear mass balance (Ch. 4.1), and real experiments for the Hintereisferner glacier (Ch. 4.2) as well as for all Alpine glaciers (Ch. 4.3). Most information were extracted out of the reference paper (Maussion *et al.*, 2019a) and the software documentation website <https://docs.oggm.org/en/v1.1/> (last access: 8 January 2019), where more detailed information of the model can be found.

**Flowline:** For the *idealised* experiments, either a rectangular or a trapezoidal bed flowline with an array for the bed height, the surface height and the bed widths along this flowline and the resolution (metres per grid points) are chosen. Hereby, at initiation, the surface height is set to the bed height. Thus, for the idealised experiments, no glacier exists at the initial time point.

For the experiments with *real* glaciers, the model downloads and interpolates glacier outlines from the Randolph Glacier Inventory (RGI v6.0, Pfeffer *et al.*, 2014, here for the Alps region 11) and local topographical data (Shuttle Radar Topography Mission; 90 m Digital Elevation Database SRTM, Jarvis *et al.*, 2008) to the local grid. The acquisition date of the SRTM is the year 2000, however the glacier outlines of the RGI are from 2003 in the Alps. This can result in slight inaccuracies in the volume inversion process. The horizontal resolution of the map topography  $dx = a\sqrt{S_A}$  ( $a = 14 \text{ m km}^{-1}$ ) depends on the glacier area,  $S_A (\text{km}^2)$ , with a constriction of  $10 \text{ m} \leq dx \leq 200 \text{ m}$  (for Hintereisferner  $dx=50 \text{ m}$ ). Flowlines are obtained by using a geometrical routing algorithm (adapted from Kienholz *et al.*, 2014), see Fig. 3.1 a for the flowline estimation of Hintereisferner. Grid points have a equidistant grid spacing that is twice as large as that of the underlying map topography (for Hintereisferner 100 m). The geometrical widths are estimated as the normals of the flowline intersecting the glacier outline or tributary catchment area. The actual altitude-area distribution of the glacier, calculated by the catchment areas, is used to correct the geometrical widths (Fig. 3.1 b).

**Climate:** In the *idealised* case, the climate is prescribed by a linear mass balance model with the equilibrium line altitude (ELA) and the mass balance gradient.

For *real* glacier estimates of this work (Hintereisferner and all Alpine glaciers), temperature and precipitation time series are interpolated to the glacier location from gridded observations using the HISTALP dataset (Auer *et al.*, 2007, <http://www.zamg.ac.at/histalp>, last access: 2 January 2020). We also did a similar approach with the CRU climate dataset (Harris *et al.*, 2014), which is the default one in OGGM, however HISTALP has a better resolution than CRU, see discussion in Ch. 5.1. Unless otherwise stated, all results are based on the HISTALP climate.

The monthly mass balance,  $m_i$ , is computed by an extended version of the temperature index melt model of Marzeion *et al.* (2012) for the elevation  $z$  of each flowlines' grid point:

$$m_i(z) = p_f P_i^{Solid}(z) - \mu^* \max(T_i(z) - T_{Melt}, 0) + \epsilon , \quad (14)$$

with the monthly solid precipitation,  $P_i^{Solid}$ , a precipitation correction factor,  $p_f$  (default in Alps using HISTALP: 1.75), the glaciers temperature sensitivity,  $\mu_*$ , the monthly air temperature,  $T_i$ ,

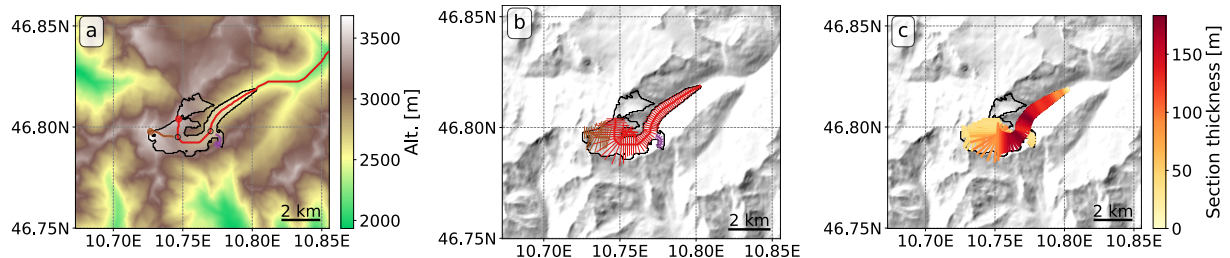


**Fig. 3.1: OGGM workflow using Hintereisferner glacier as example.**

(a) Topography of the glacier, its surroundings with the RGI outline from 2003 (area: 8.036 km<sup>2</sup>), and the computed three flowlines. (b) Glacier width determination (corrected to altitude-area distribution of each catchment area). (c) Ice thickness inversion estimate (volume: 0.58 km<sup>3</sup>) using HISTALP data and glacier-specific calibration of  $p_f = 1.2$ ,  $A = 3A_0$ ,  $\epsilon = -100$ .

the temperature above which ice melt is assumed to occur,  $T_{Melt}$  (default in Alps using HISTALP: -1.75°C), and the residual correction term,  $\epsilon$ . The fraction of solid precipitation to the total precipitation is estimated by the temperature below which precipitation is assumed to be solid,  $T_{solid}$  (default: 0°C), and by the temperature above which precipitation is assumed to be totally liquid,  $T_{Liquid}$  (default: 2°C). 100% solid precipitation is assumed if  $T_i \leq T_{Solid}$ , 0% if  $T_i \geq T_{Liquid}$  and linearly interpolated in between. A default temperature lapse rate of 6.5 K km<sup>-1</sup> is applied to the HISTALP estimates. The temperature sensitivity parameter,  $\mu^*$ , is calibrated for each glacier with the method of Marzeion *et al.* (2012) by using the mass-balance observations provided by the World Glacier Monitoring Service (WGMS, 2017), with 56 observed glaciers in the Alps. The default mass balance related parameter set for the HISTALP glacier was determined with a cross-validation and tested for the 46 Alpine glaciers with more than 5 years of mass-balance observation, see <https://cluster.klima.uni-bremen.de/~github/crossval/> (last access: 8 January 2019).

For the estimates of the *temporally evolving Hintereisferner response time*, the mean constant climate of 23 years is applied using a running mean of ±11 years. The *Alps bulk approach response time* is calculated with the center year  $t_{star}$  and a window size of ±15 years. The reason for this approach is further explained in Ch. 3.2.

**Inversion:** Since the bedrock elevations of *real* glaciers are hidden by the glaciers above, they have to be obtained by subtracting the ice thickness from the glacier surface elevations and by assuming a bedrock that remains unchanged over time (Farinotti *et al.*, 2017). The ice thickness distribution of a glacier is crucial to determine the total volume of the glacier. Despite this importance, direct ice thickness measurements are sparse and ice-thickness inversion methods have to be applied. In OGGM, an ice thickness inversion procedure similar to Farinotti *et al.* (2009) is used. The ice flux along each glacier cross section depends on the average velocity  $u$  and the cross-section area  $S$  with  $q(\text{m}^3 \text{s}^{-1}) = u \cdot S_c$ . If  $u$  and  $q$  can be estimated, the local ice thickness,  $h$ , can be computed by assuming a rectangular, parabolic, or trapezoidal bed shape. In our study of real glaciers, the default settings of a mix between parabolic, trapezoid, and rectangular bed shape were taken. The depth-integrated ice velocity is computed by the shallow-ice approximation (SIA, Hutter, 1981, 1983),

$$u = \frac{2A}{n+2} h \sigma_b^n, \quad (15)$$

with the ice creep parameter  $A$  (default:  $A_0 = 2.4 \cdot 10^{-24} \text{ s}^{-1} \text{ Pa}^{-3}$ ), the Glen's flow law exponent ( $n=3$ ). The basal shear stress,  $\sigma_b$ , is computed by

$$\sigma_b = \rho g h s, \quad (16)$$

assuming an ice density of  $\rho = 900 \text{ kg m}^{-3}$ , a constant gravitational acceleration  $g=9.81 \text{ m s}^{-2}$ , and using the surface slope ratio  $s$  along the flowline. Longitudinal stress gradients are neglected

in the SIA, however their effects on the volume response time are small according to Greuell (1992); Leysinger Vieli and Gudmundsson (2004).

An additional sliding velocity to account for basal sliding can be added using a parametrisation of Oerlemans (1997) relying on Budd *et al.* (1979),

$$u_s = \frac{f_s \sigma_b^n}{h}. \quad (17)$$

If basal sliding is not neglected,  $f_s$  is set to the default value of  $5.7 \cdot 10^{-20} \text{ s}^{-1} \text{ m}^2 \text{ Pa}^{-3}$ . In our study, however, no sliding parametrisation is used for all experiments by setting  $f_s = 0$ .

Due to mass-conservation considerations, the ice flux on a grid point of a flowline corresponds to

$$q = \int_{\Omega} (\dot{m} - \rho \frac{\delta h}{\delta t}) dS_A = \int_{\Omega} \tilde{m} dS_A, \quad (18)$$

where  $\Omega$  is the catchment area upstream of this point,  $\dot{m}$  the actual observed mass balance data along the flowlines, and  $\tilde{m} = \dot{m} - \rho \delta h / \delta t$  the 'apparent mass balance'. However, the temporal change of ice thickness distribution,  $\delta h / \delta t$ , is unknown. Therefore, an equilibrium steady state is assumed ( $\delta h / \delta t = 0$ ) with  $\tilde{m} = \dot{m}$  using the equilibrium mass-balance  $\bar{m}(t_{star})$  with  $\int \bar{m} = 0$  by construction. The ice thickness inversion estimate for the Hintereisferner is shown in Fig. 3.1 c.

The local thickness and hence the total volume are very sensitive to the creep parameter  $A$ . A stiffer glacier (smaller  $A$ ) gets thicker and the computed ice flux is larger compared to a less stiff glacier. Increasing the precipitation factor,  $p_f$ , leads to a larger total precipitation amount and therefore results in a higher mass-balance gradient, a higher ice flux and hence a larger volume. In addition, the bed shape plays an important role, e.g. applying parabolic bed shapes causes the inversion volume to be smaller compared to rectangular bed shapes.

OGGM uses the shallow-ice approximation with default no lateral drag. Adding lateral bed stresses (parametrisation from Adhikari and J. Marshall, 2012) reduces the ice velocity, hence causes an increase in the ice volume. In this study, no lateral drag was added and therefore effects of lateral bed stresses on the response time are not analysed.

**Ice dynamics** are computed, for both ideal and real glaciers, by solving

$$\frac{\delta S_c}{\delta t} = w \bar{m} - \Delta u S_c \quad (19)$$

numerically with a forward finite difference approximation scheme on a staggered grid by using the widths,  $w$ , mass balances,  $\bar{m}$ , depth-integrated velocities,  $u$ , and cross-section areas,  $S_c$ , along the flowline. To ensure numerical stability, the time stepping  $\Delta t$  is chosen such that the Courant-Fridrichs-Lowy (CFL) condition is met with  $\Delta t = \gamma \frac{\Delta x}{\max(u)}$  with  $\gamma$  as the dimensionless Courant number. In the experiments of this work, we set  $\gamma = 0.01$  (*cfl\_condition*), a minimum time step (*mindt*) to zero and the maximum possible time step (*maxdt*) limited to 5 days (with OGGM v.1.1.2). Most solvers, including the default solver in OGGM do not conserve mass for very steep slopes. The more robust solver "MUSCL superbee" of Jarosch *et al.* (2013) uses a second-order flux-limiting spatial discretization scheme that enforces mass conservation. "MUSCL superbee" is also implemented in OGGM, but can only be used for a non-changing bed shape with a single flowline. A short comparison between the response time computed by the default and the "MUSCL Superbee" solver is done in Ch. 4.2.1 and shows no large differences. For all other experiments, the default solver of OGGM is used.

For the *idealised glacier experiments* (Ch. 4.1), the default OGGM parameters are used if not otherwise stated (see Table 4.1).

For the *temporally evolving Hintereisferner response time* (Ch. 4.2), OGGM was calibrated by changing  $A$ ,  $p_f$ , and  $\epsilon$  such that the modelled glacier length evolution from 1862 onwards fits best

the glacier length observations. The best glacier-specific fit for Hintereisferner (minimum absolute error between modelled and observed length observations) was found for  $A=3A_0$ ,  $p_f=1.2$ , and  $\epsilon=-100$  (unpublished method and calibration from Matthias Dusch).

For the *Alpine glacier response time* (Ch. 4.3), the default parameters for Alpine glaciers using HISTALP were taken. With this default set of parameters, a total Alpine glacier volume of  $153 \text{ km}^3$  is estimated by the inversion process (RGI outlines of 2003). As the Alpine glacier volume from the intercomparison study of Farinotti *et al.* (2019) (ensemble of five models) amounts to  $130 \pm 30 \text{ km}^3$ , we tuned the ice creep parameter  $A$  such that the OGGM Alpine volume estimate is also roughly  $130 \text{ km}^3$  ( $A=2.2A_0$  for HISTALP parameters, Fig. A.5). A higher  $A$ -parameter makes the ice less stiff and might be necessary to compensate e.g. the neglected temperature dependency of  $A$  or the sliding during the inversion. However, if the bed sliding velocity estimate parametrisation of Oerlemans (1997) with  $f_s=5.7 \cdot 10^{-20} \text{ s}^{-1} \text{ m}^2 \text{ Pa}^{-3}$  is applied (see Eq. 17), the total Alpine ice volume would be too low for  $A>0.1 \cdot A_0$  (Ch. A.1). Thus, another option would have been to tune  $f_s$ , which is assumed to produce similar response time estimates.

## 3.2 Approach to estimate response times of real glaciers that are in a large disequilibrium with the current climate

The visible glacier changes from real-world observations are the result of a complex continuous dynamical change of the climate. To be able to compare the geometry-climate imbalance between different glaciers but for the same climatic perturbation, the glacier has to be in equilibrium with the initial climate. Otherwise the response signal would be the interference between the actual response to the new perturbation and the integrated past climatic change. Hence, it would depend on the glacier-specific climatic history (Zekollari and Huybrechts, 2015). The static definition of the response time, going from an initial equilibrium state to a perturbed equilibrium state, as described in Ch. 2.3, is especially necessary when comparing results among different glaciers between time and for different magnitudes of climatic perturbation. Those prerequisites make the response time definition very abstract and not 'observable': nowadays glaciers are in a strong disequilibrium with the climate and real-world climatic perturbations, e.g. the occurring climate change of the 20<sup>th</sup> and 21<sup>st</sup> century, cannot be described as a climatic step change.

In numerical flowline models, an equilibrium glacier is obtained by applying a constant climate over several centuries until the volume or length does not change with time anymore. If current state transient glaciers are brought into equilibrium with the current climate (applying the constant mean climate of 31 years), they are much smaller and have a very different mean geometry. Hence, the computed response time of those equilibrium glaciers would correspond to glaciers with totally different characteristics than the transient ones. A way to overcome this problem is to introduce a calibrated (negative) temperature bias that creates a glacier in equilibrium that is similar to the transient glacier but in another (cooler) climatic environment (Zekollari and Huybrechts, 2015).

For the temporally evolving Hintereisferner response time (Ch. 4.2) the temperature bias is calibrated such that the equilibrium glacier has the same length as the modelled transient glacier length. To preserve the length of a glacier between transient and equilibrium glaciers a stronger negative temperature bias has to be applied than to preserve the volume of a glacier. Glaciers can only get into equilibrium with a length that is equal to the transient glacier length, if they have thickened considerably in the ablation area in order that ice masses can be transported and sustained at lower altitudes. Therefore, preserving the length of Hintereisferner will produce an equilibrium glacier that is thicker and hence has more volume than the transient glacier estimate of the model. The other way round, an equilibrium glacier with the same volume as the transient glacier, is shorter. As the glacier volume is not directly observable and also not known in the past, the temperature bias for the equilibrium glaciers is calibrated by preserving the length.

The length evolution of Hintereisferner is the only variable that was observed from 1862–2003 (sporadic dataset from Leclercq *et al.*, 2014), calibrated lengths in Fig. A.4.

For the *analysis of Alpine glaciers* (Ch. 4.3), the response time is calculated for an equilibrium glacier that has a similar area as the RGI outline of 2003. Hence, for the Alps an 'area-preserving' approach is applied because the area is known from observations. To get an equilibrium glacier with the area of the RGI outline of 2003, we used the climate of  $t_{star}$ <sup>2</sup>, which is defined such that the transient glacier of 2003 is in equilibrium. Hence, the geometry of 2003 should be maintained approximately when applying the climate of  $t_{star}$  over a long time period. In addition, the residual  $\epsilon$  in Eq. 14 was set to zero. Even though glaciers are in near-equilibrium with the climate of  $t_{star}$ , we added for each glacier an individually calibrated small temperature bias to ensure that the area of the RGI outline is preserved.

An other option would have been to apply a fitness function that minimizes the average difference in surface elevation and width between transient and equilibrium glacier. This was done in Eis *et al.* (2019) to compare observed and forward modelled glacier states. For the sake of simplicity, we used here the presented simpler area-preserving approach.

---

<sup>2</sup>the year  $t_{star}$  is different for each glacier and a parameter of the mass balance calibration (Ch. 3.1).

## 4 Results and Analysis

Different experiments are described and analysed, from the most idealised glaciers (Ch. 4.1) over the Hintereisferner glacier as a case study (Ch. 4.2) to an estimate of the Alpine glaciers' response time (Ch. 4.3).

### 4.1 Idealised glacier experiments: response time sensitivity

To understand the mechanisms that control the response time, idealised glacier experiments are a perfect departure point. By changing only one parameter at a time and using simplified glacier shapes, we can better understand the individual influence of different parameters.

The climatic setting, i.e. the mass balance, is predefined for all idealised experiments by applying a linear mass balance model. The input parameters for the model are the initial equilibrium line altitude,  $\text{ELA}_0$  (m), and the mass balance gradient,  $\beta$  ( $\text{mm w.e. yr}^{-1} \text{m}^{-1}$ ).

The simplest reference experiment is described in Ch. 4.1.1 and is repeated with slight modifications of the glaciers or climatic properties in Ch. 4.1.2, Ch. 4.1.3, and Ch. 4.1.4. In the most ideal case, the glacier has a constant bed width and a constant bed slope (Ch. 4.1.2). For these experiments, the response time is estimated for glaciers where we modify the mass balance gradient, the overall bed slope ratio and later on also the initial equilibrium line altitude,  $\text{ELA}_0$ , the creep parameter  $A$ , the climatic perturbation of the ELA,  $\Delta\text{ELA}$ , and the bed shape. In Ch. 4.1.3, idealised glacier experiments with a changing bed width in the accumulation area are analysed for several initial equilibrium line altitudes ( $\text{ELA}_0$ ). In Ch. 4.1.4, the response time for a more realistic glacier bed with a changing bed slope and a bedrock depression is estimated for different perturbations ( $\Delta\text{ELA}$ ). At the end of this subsection, a short overview over the findings is given (Ch. 4.1.5).

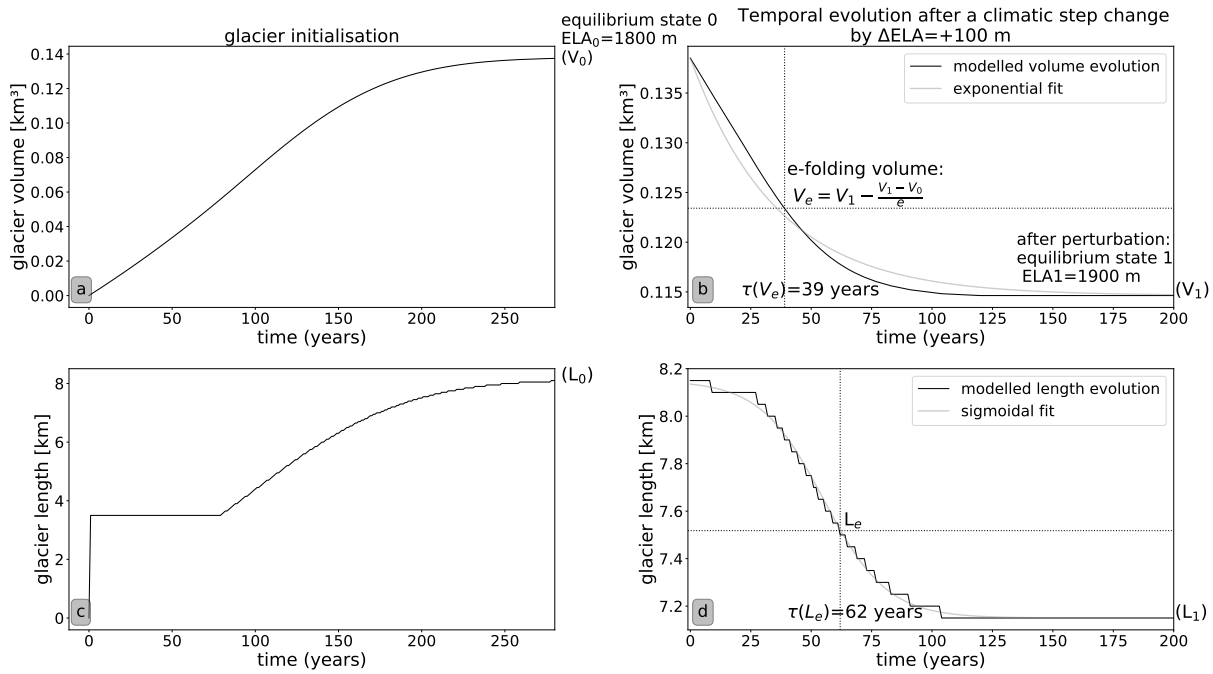
#### 4.1.1 Simplest reference idealised model

Figure 4.1 describes how the e-folding response time can be estimated with given geometric and climatic parameters of an idealised glacier. Used parameters are listed in Table 4.1.

In the idealised experiments, glaciers have to grow first over the predefined bed with the applied parameters until they reach an initial equilibrium state with volume  $V_0$  and length  $L_0$  (Fig. 4.1 a,c). While the volume evolution increases steadily, the glacier length directly increases in the first year from 0 km to 3.5 km, which corresponds to the horizontal distance between top of the glacier and the prescribed initial ELA ( $\text{ELA}_0$ ). After the first year, the model has added mass everywhere above the  $\text{ELA}_0$ . Therefore, the glacier length after one year corresponds to the predefined distance between the top of the glacier and the  $\text{ELA}_0$ . Only when a glacier has grown substantially in thickness, the glacier can transport sufficient mass below  $\text{ELA}_0$ , which explains why a further increase in the glacier's length occurs only after a delay.

When the glacier has reached the initial equilibrium state 0, the model perturbs the climate with a step change in the climate. In this case,  $\text{ELA}_0$  is increased by  $\Delta\text{ELA} = +100 \text{ m}$  to  $\text{ELA}_1$  and volume and length of the glacier shrink until the glacier is again in equilibrium with the perturbed climate (equilibrium state 1). While the temporal evolution of volume after the climatic step change can be explained by an exponential fit (Fig. 4.1 b), the length evolution is better described by a sigmoidal fit (Fig. 4.1 d), as explained in Ch. 2.3.

The length decreases in finite steps and the step size depends on the chosen resolution, here 50 metres per grid point (= $\text{map\_dx}$ ). Increasing  $\text{map\_dx}$  results in a smoother length evolution, however it needs more computational effort. The  $cfl\_condition$ ,  $mindt$  and  $maxdt$  are set in a way that they ensure numerical stability (Table 4.1). The variable  $rate$  defines at which ratio it is assumed that the glacier has reached its equilibrium. The variable  $ystep$  describes how often to check whether the glacier reached equilibrium (here every 10 years). A short analysis of response time sensitivity to resolution and to  $ystep$  is in the appendix (Ch. A.1).



**Fig. 4.1:** Model initialisation with (a) volume and (c) length evolution until the glacier is in equilibrium with the applied climate (equilibrium state 0). A climatic step change is applied at time point 0 in (b, d) from an  $\text{ELA}_0=1800 \text{ m}$  to  $\text{ELA}_1=1900 \text{ m}$ . The temporal evolution into the new perturbed equilibrium state 1 is depicted for (b) volume and (d) length. In (b, d) the e-folding response time (i.e. the time when the volume or length have shrunk to  $X_e = X_1 - (X_1 - X_0)/e$ , as defined previously in Ch. 2.3) is marked with a vertical line. Model setup parameters are shown in Table 4.1.

**Table 4.1:** Model setup parameters for the idealised reference glacier experiment plotted in Fig. 4.1. If not described otherwise, the default values from OGGM v.1.1.2 were used.

parameters for:		
resolution	$\text{nx}= 200$ grid points	$\text{map_dx}= 50 \text{ metres/grid point}$
geometry	bed top: 2500 m	min. bed bottom: 500 m
	constant bed width: 150 m	rectangular bed shape
	constant bed slope ratio: $\frac{\Delta \text{bed altitude}}{\text{nx} \cdot \text{map_dx}} = 0.2$	
ice dynamics (Eq. 15, Eq. 16)	creep parameter: $A=A_0=2.4 \cdot 10^{-24} \text{ s}^{-1} \text{Pa}^{-3}$	$n=3$
	$\rho=900 \text{ kg m}^{-3}$ , $g=9.81 \text{ m s}^{-2}$	
numerics	$cfl\_condition= 0.01$	$\text{mindt}= 0$ , $\text{maxdt}= 5$
	$rate= 0.001$	$\text{ystep}= 10 \text{ years}$
climate	$\text{ELA}= 1800 \text{ m}$	constant mass balance gradient: $3 \text{ mm w.e. yr}^{-1} \text{ m}^{-1}$
climatic perturbation	$\Delta\text{ELA}=\text{ELA}_1-\text{ELA}_0=+100 \text{ m}$	

### 4.1.2 Constant bed width

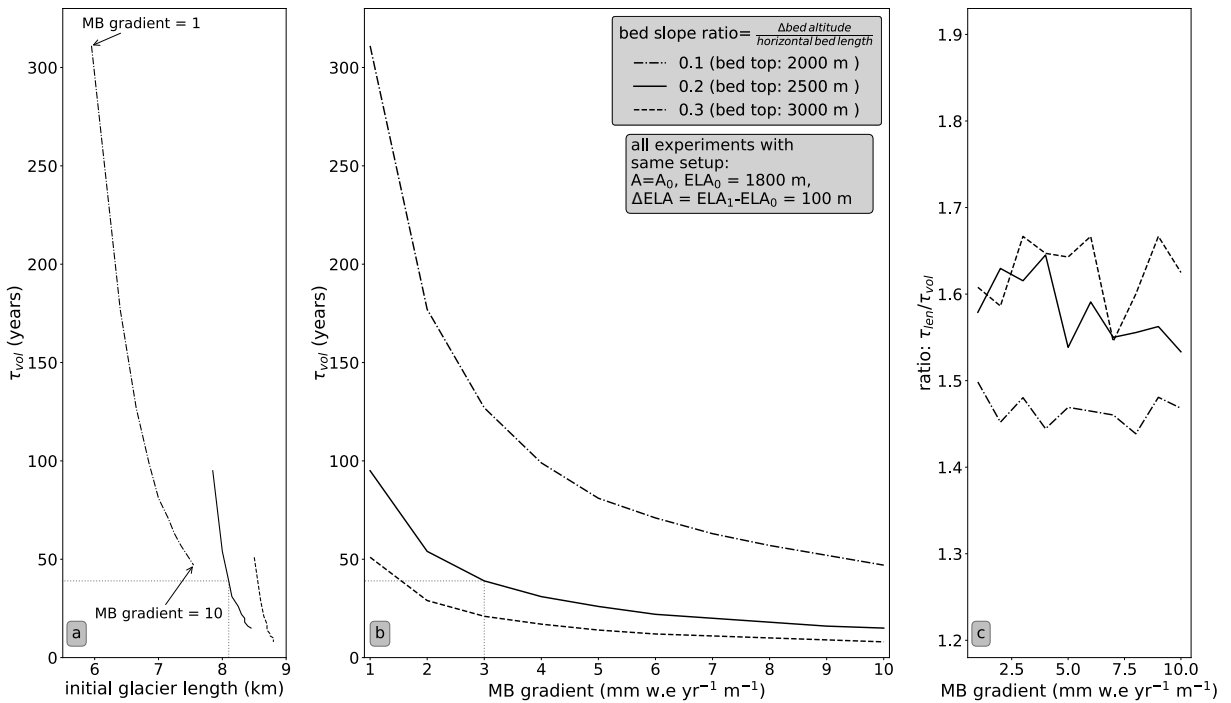


**Fig. 4.2:** Idealised glacier experiment estimates of the e-folding volume response time against (a) the initial glacier length and (b) the mass balance gradient for a changing linear mass balance gradient and three different constant bed slope ratios. All other used parameters are kept equal to the reference glacier, which corresponds to the values from the intersection of the dotted grey line (Ch. 4.1.1). In (c), the ratio between e-folding length against volume response time is plotted.

The initial equilibrium glacier length, the response time, and the ratio between length and volume response time were estimated for idealised glaciers with different mean bed slope ratios (0.1, 0.2, 0.3) and various mass balance gradients ( $1-10 \text{ mm w.e. yr}^{-1} \text{m}^{-1}$ ). All other parameters were kept equal to those from the reference glacier (Table 4.1). Hence, among others, all used idealised glaciers had a constant bed width. The response time estimate of the reference glacier of Ch. 4.1.1 is marked in Fig. 4.2 at the intersection of the vertical and horizontal grey dotted line with a bed slope ratio of 0.2 and a mass balance gradient of  $3 \text{ mm w.e. yr}^{-1} \text{m}^{-1}$ .

In this specific setup, longer idealised glaciers have rather shorter response times (Fig. 4.2 a). To understand that, we have to look at the different geometric and climatic characteristics that have 'formed' these glaciers. The steeper the glacier and the larger the mass balance gradient, the shorter is the initial glacier. Hence, the physical drivers of response time changes in this experiment seem to be the bed slope and the mass balance gradient changes. The flatter the glacier, the more sensitive is the response time to the mass balance gradient. While the response time is above 300 years for a mass balance gradient of  $\beta=1 \text{ mm w.e. yr}^{-1} \text{m}^{-1}$ , it is only around 50 years for  $\beta=10 \text{ mm w.e. yr}^{-1} \text{m}^{-1}$  for a slope ratio of 0.1. Overall, the response time is more sensitive to the bed slope for small mass balance gradients.

A closer look into the setup might explain the changes in the response time. Hereby, references are made to the scaling approach of Jo89 (Eq. 4) where a more negative mass balance at the terminus and a smaller ice thickness scale (here the mean) are associated with shorter response times. Further, estimates are compared to the formula of Oerlemans (2001) (Table 2.1) where the glacier (length) adjustment speed is related to a length scale and a characteristic ice velocity.

First, we discuss the mechanisms that produce longer equilibrium glaciers. A steeper glacier has higher ice velocities and an increased mass flux from the accumulation into the ablation

area (Oerlemans, 2001). Thus, steeper glaciers in equilibrium are longer (for this setup). The thickening or thinning of a glacier is amplified by the mass-balance-elevation feedback, i.e. the positive feedback mechanisms of a normal increase in the mass-balance with elevation (Ho19). The larger the mass balance gradient, the more important this feedback gets. Consequently, for higher mass balance gradients, a glacier grows much thicker in the accumulation area and the thus induced higher mass transfer into the ablation area produces larger ice velocities and also a longer glacier in equilibrium.

In this idealised simple experiment, the mass balance rate at the terminus,  $b_t$ , can be directly estimated with geometrical considerations,

$$-b_t = \beta \cdot (\text{bed top altitude} - \text{ELA}_0 - s \cdot L_0) . \quad (20)$$

Hereby, we use the mass balance gradient,  $\beta$ , and the altitude difference between top and terminus,  $s \cdot L_0$ , with the bed slope ratio,  $s$ , and initial glacier length,  $L_0$ . Hence, due to the setup of a constant  $\text{ELA}_0$ , a constant glacier bed top altitude, a constant slope, and the assumption of linear mass balance increase with height, a longer initial glacier is produced by a higher bed slope ratio and/or a larger mass balance gradient. As a result, the slope and the mass balance gradient are direct and indirect (via initial glacier length) drivers of the mass balance at the terminus (Eq. 20) and thus influence the response time as well.

The decrease in response time with increasing bed slope and/or larger mass balance gradients is also visible when applying analytical formulas on the setup and can be explained e.g. by larger ice velocities, a more negative mass balance at the terminus, and the mass-balance-elevation feedback.

The volume responds faster than the glacier length with a ratio of around 1.5 to 1.6 between length and volume response time (Fig. 4.2 c). While the volume of a glacier starts to react immediately to a climatic step change, the length only changes after a certain amount of time (Fig. 4.1 b, d), which was also called initial terminus response by Pelto and Hedlund (2001). Further, the length/volume response time ratio seems to be rather independent of the applied mass balance gradient. According to Oerlemans (2008), the delay of  $\tau_L$  can depend, however, on the used grid resolution. In our study, increasing the resolution from 50 metres per grid point to 10 metres per grid point on an equally long glacier did not produce significant variations of  $\tau_{len}/\tau_{vol}$ , see appendix Ch. A.1.

The experiments shown in Fig. 4.2 were repeated with changing additional parameters, but still keeping a constant bed width (Fig. 4.3).

Another climatic property of a glacier is the **equilibrium line altitude (ELA)**. By increasing the initial ELA ( $\text{ELA}_0$ ) of an idealised equilibrium glacier with a constant slope (Fig. 4.3 a1), the newly formed glacier in equilibrium is shorter and hence its response time longer. As described above, this can be explained by the less negative mass balance at the terminus (Eq. 20). The effect is largest for small slopes where the decrease in the altitude difference from terminus to top has more direct and indirect (via length) influence on the mass balance at the terminus. Two glaciers have similar response times, if e.g. the higher  $\text{ELA}_0$  of the one glacier is balanced out by a lower mass balance gradient of the other glacier. Hence, a glacier with a constant slope ratio of 0.2 and a mass balance gradient of  $2 \text{ mm w.e. yr}^{-1} \text{ m}^{-1}$  has the same response time as a glacier with a mass balance gradient of  $3 \text{ mm w.e. yr}^{-1} \text{ m}^{-1}$  and a 200 m higher  $\text{ELA}_0$ . There is no clear relationship between  $\text{ELA}_0$  and ratio of length to volume response time visible (Fig. 4.3 a2).

The **strength and 'direction' of the climatic perturbation** is described by the change of ELA between the initial equilibrium state 0 (here always  $\text{ELA}_0 = 1800 \text{ m}$ ) and perturbed equilibrium state 1 with  $\Delta \text{ELA} = \text{ELA}_1 - \text{ELA}_0$ . Overall, the shrinking ( $\Delta \text{ELA} > 0$ ) and growing experiments ( $\Delta \text{ELA} < 0$ ) show a common trend: The larger the perturbation, the shorter is the response time. However, in this simplified setup, the effect is negligible for glaciers with rather steep slopes ( $\geq 0.2$ ). Still, for a small slope ratio (0.1) and a mass balance gradient of  $3 \text{ mm w.e. yr}^{-1} \text{ m}^{-1}$  a

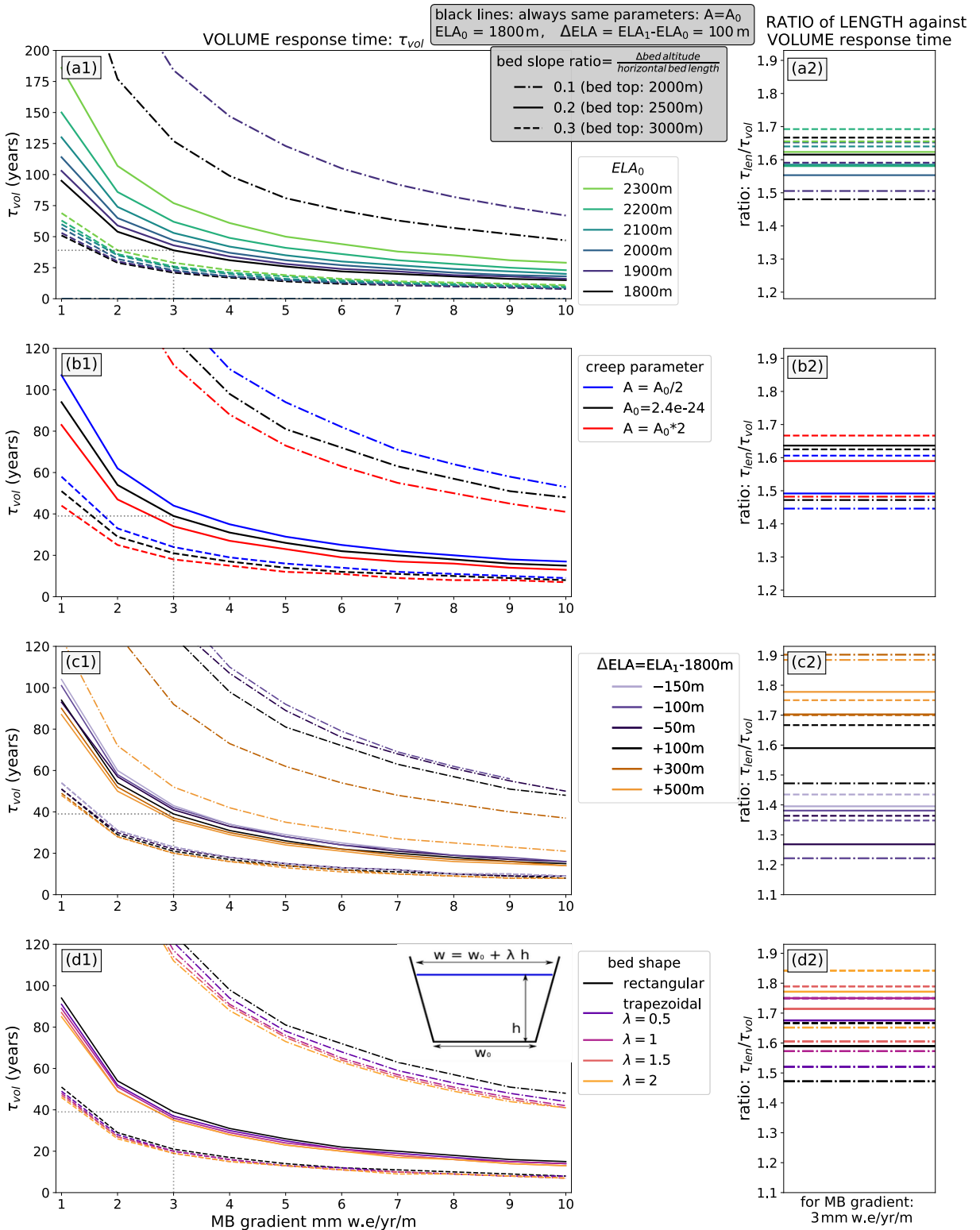


**Fig. 4.3: E-folding response time of idealised glaciers with constant width and constant mass balance gradient.** Same experiments as in Fig. 4.2 (black lines), but showing additional influences by (a) the initial equilibrium line altitude, (b) the ice creep parameter  $A$ , (c) the climatic perturbation  $\Delta ELA$  and (d) the glacier's bed shape. All other parameters are kept equal to the reference glacier, which corresponds to the values from the intersection of the dotted grey line (Ch. 4.1.1). On the right side, the ratio of length to volume response times for an example mass balance gradient of  $3\text{mm w.e. yr}^{-1}\text{ m}^{-1}$  is given.

strong increase in the perturbation from  $\Delta\text{ELA} = +100 \text{ m}$  to  $\Delta\text{ELA} = +300 \text{ m}$  results in a 30 year shorter response time. This response time dependence on the ELA perturbation value might be also to some extent a result of the mass-balance-elevation feedback. It gets most evident when comparing an experiment with the same absolute climatic perturbation of  $|100| \text{ m}$ , but in the one case a shrinking glacier with  $\Delta\text{ELA} = +100 \text{ m}$  and in the other case a growing glacier with  $\Delta\text{ELA} = -100 \text{ m}$ . Glaciers that adjust into a colder climate respond slower compared to those adjusting into a warmer climate. A possible explanation is that the glacier has to thicken first before an enhanced mass flux forces the glacier to grow into lower altitudes. In lower altitudes, the counteracting stronger melting driven by the mass-balance-elevation feedback has to be balanced by a higher mass turnover which needs time. With these considerations we can also understand why the ratio of length to volume response time ( $\tau_{\text{len}}/\tau_{\text{vol}}$ ) is smaller for growing glaciers (1.2-1.4) compared to shrinking glacier experiments (1.5-1.9), see Fig. 4.3 c3.

The strict definition of the e-folding response time is independent of the climatic perturbation, because it is described as a time constant and built on the assumption of a linear response, see Ch. 2.3 and further discussion in Ch. 5.3.

The **bed shape** for all idealised experiments so far was chosen to be rectangular. Simulating idealised glaciers with a trapezoidal bed shape, hence a larger width at the glacier surface with  $w_{\text{surface}} = w_{\text{bedrock}} + \lambda \cdot h$  (glacier thickness  $h$ ,  $\lambda > 0$ ), leads to equilibrium glaciers that have slightly shorter response times (Fig. 4.3 d1). The larger the bed width difference between bedrock and surface of the glacier, the smaller is the response time. However, the largest difference in response time between rectangular and a trapezoidal bed shape with  $\lambda = 2$  is only 10 years for a glacier with a slope ratio of 0.1. Enhanced by the mass-balance-elevation feedback, a more trapezoidal bed shape glacier is thicker. Hence, the mass transfer along the glacier is strengthened by larger ice velocities, which might explain slightly shorter response times of trapezoidal bed shape glaciers compared to those with a rectangular bed shape. For more trapezoidal bed shape glaciers, there is also a stronger lag between length and volume response time (Fig. 4.3 d2).

The **ice creep parameter**  $A$  of the Glen's flow law (Eq. 1) relates shear stress to the deformation rate and is a model parameter in Eq. 15 with a default value of  $A_0 = 2.4 \cdot 10^{-24} \text{ s}^{-1} \text{ Pa}^{-3}$ . The  $A$ -parameter is mostly kept constant in time and between different glaciers for bulk-approaches in OGGM. The choice of the  $A$ -parameter is relevant for the determination of the response time. A smaller  $A$ -parameter causes the glacier to be stiffer and therefore it grows thicker and slightly longer in its equilibrium. We found that applying a smaller  $A$ -parameter forms a glacier that has a longer response time (Fig. 4.3 b1). Decreasing the  $A$ -parameter by a factor of two seems to have similar effects as increasing the  $\text{ELA}_0$  by plus 200 metres for slopes equal or above 0.2 (Fig. 4.3 b1,a1).

For the other experiments so far where we modified mean slope, mass balance gradient, bed shape, or  $\text{ELA}_0$  on a constant-slope glacier, a longer initial equilibrium glacier resulted in shorter response times. However, decreasing the  $A$ -parameter, decreases directly the ice velocity per definition as well (Eq. 15). Therefore, in contrast to the other experiments, in this setup the longer equilibrium glacier induced by the stiffer ice results in a longer response time,  $A \xrightarrow{(L_0 \uparrow)} \tau \uparrow$ . The effect of the decreased  $A$ -parameter on the ice velocity is hereby more important than the effect of the increased ice thickness of the initial glacier. In addition, for stiffer glaciers ( $A < A_0$ ), the ratio between length and volume response time diminishes slightly.

### 4.1.3 Changing bed widths

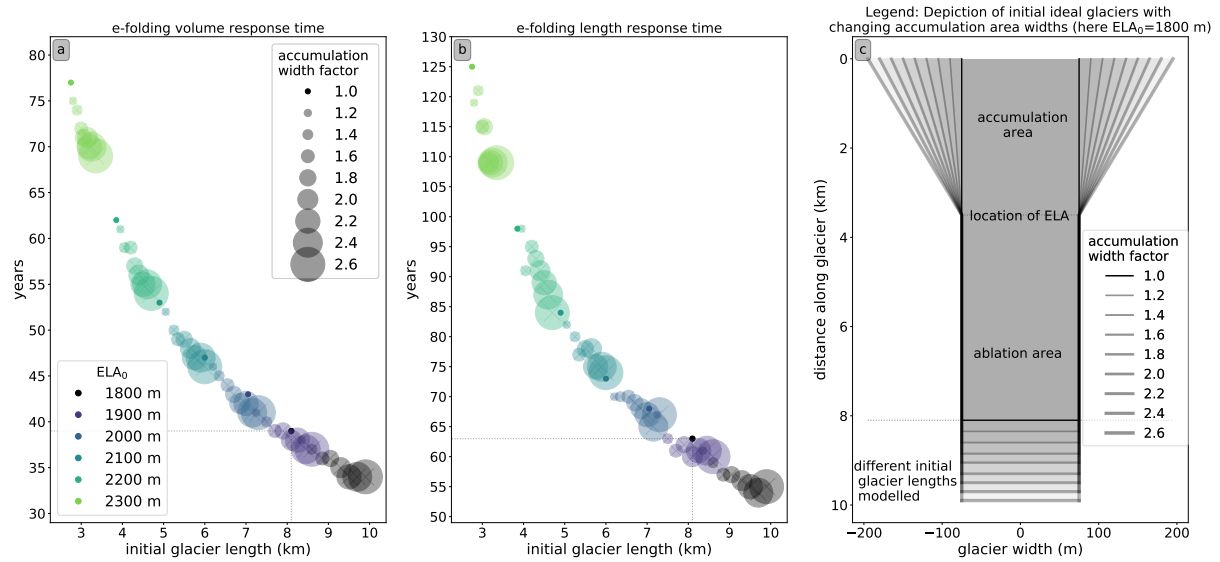


**Fig. 4.4: Effects of changing glacier bed hypsometry and/or initial ELA ( $\text{ELA}_0$ ) on the equilibrium glacier length and the resulting e-folding response time of (a) volume and (b) length.** All other parameters are kept equal to the reference glacier, which corresponds to the values from the intersection of the dotted grey line (Ch. 4.1.1). In (c), the legend for the glaciers' hypsometry ( $\text{ELA}_0=1800 \text{ m}$ ) is depicted for different accumulation area widths with the resulting equilibrium glacier lengths.

Two glaciers with different constant widths but with overall similar other properties in the geometry and the climate they are exposed to would have the same response time, because the relative volume change would occur in the same speed. However, the hypsometry, i.e. the altitude-area distribution of the glacier, plays an important role for the response time. Equilibrium glaciers with different widths in the accumulation area were used for the next experiments (Fig. 4.4). The glacier bed width has been set to increase linearly from the ELA up to the top of the glacier. This corresponds better to the geometry of most valley glaciers (e.g. Roe and O’Neal, 2009). In this setup, building glaciers that are wider in their upper part results in larger accumulation and ablation areas, and longer equilibrium glaciers (Fig. 4.4c). Consequently, both a lower  $\text{ELA}_0$  or a wider accumulation area (expressed by a larger accumulation width factor in Fig. 4.4a), form longer glaciers with shorter response times, due to the enhanced mass transfer along the glacier. The length response time (Fig. 4.4b) is longer than the volume response time by a factor of around 1.6, which is similar to the other experiments.

### 4.1.4 Changing bed slopes with a constant bed width

The slope seems to be one of the most important parameters that control the response time of idealised glaciers. However, on real glacier beds, bed (and surface) slopes vary substantially with height. Often, glaciers are steeper in their upper parts, which was found for Alpine glaciers (Ch. 4.3.2) and is also described in Oerlemans (2001). Therefore, the following experiments investigate the influence of idealised glaciers with a non-constant bed slope (Fig. 4.5).

- A In **experiment A** of Fig. 4.5, glaciers are formed on a bed with a slope ratio of 0.2 on the first 5 km and a slope of 0.08 behind that. If the initial ELA ( $\text{ELA}_0$ ) is set high enough, the grown initial equilibrium glaciers are shorter than 5 km and their bed slope is constant with a value of 0.2 (Fig. 4.5 A.4). Hence, we have a similar situation as already analysed with Fig. 4.3 a1. The volume response time decreases with increasing length from around 77 to 43 years for all experiments with perturbations of  $\Delta\text{ELA} \geq 50 \text{ m}$ . As described before,

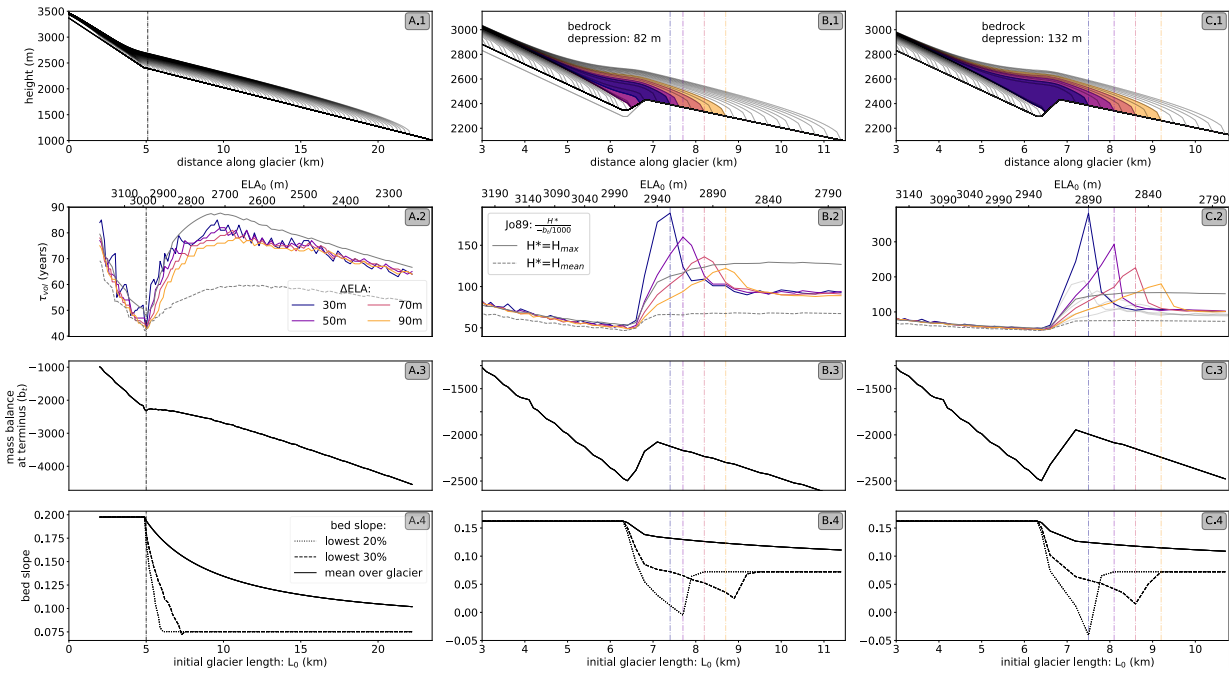


**Fig. 4.5: Influences of bed slope changes along the glacier flowline on the volume response time for glaciers with different initial ELA.** A constant width with a rectangular bed shape,  $\text{mapdx}=100$  m, a mass balance gradient of  $4 \text{ mm w.e. yr}^{-1} \text{ m}^{-1}$  and the default  $A$ -parameter are used for four different climatic perturbations,  $\Delta\text{ELA} \in \{30, 50, 70, 90\} \text{ m}$ . In (A.2, B.2, C.2), the e-folding volume response time together with the analytical estimate of Jo89 (Eq. 4 with initial equilibrium glacier state maximum ice thickness  $H_{\max}$  and mass balance at the terminus  $b_t$ ) are plotted. In (A.1, B.1, C.1), the chosen bed profiles and their initial equilibrium state glaciers are depicted. In (B, C), those glacier states with maximum response time values are marked as vertical lines. In (B.1, C.1), the corresponding part that has melted when reaching the perturbed equilibrium of these glacier states is shaded with the color of the applied perturbation.

the response time decrease can be explained by the larger mass transfer which is indicated by the increasing mass balance at the terminus<sup>3</sup> (see Fig. 4.5 A.3 for  $L_0 < 5 \text{ km}$ ). For small perturbations ( $\Delta\text{ELA} \leq 30 \text{ m}$ ), the response time fluctuates with increasing glacier length, which is possibly related to numerical grid approximations.

For  $L_0 \geq 5 \text{ km}$  the glaciers' bed slope is less steep, resulting in an increase of the volume response with glacier length. This is different to most other experiments described so far.

The smaller slope and also the larger thickness of the lower glacier part (Fig. 4.5 A.1) result in a glacier that is exposed to a less negative mass balance at the terminus compared to a glacier with constant slope (mass-balance-elevation feedback). We can see this in the only marginally decreasing mass balance at the terminus for  $5 \text{ km} \leq L_0 \leq 10 \text{ km}$  in Fig. 4.5 A.3. Increased ice thicknesses and smaller ice velocities, induced by the flatter glacier, might explain the enhanced response time with longer glaciers (for  $5 \text{ km} \leq L_0 \leq 10 \text{ km}$ ). With this setup, the response time sensitivity to the climatic perturbation is much larger for glaciers with in mean 5.9 years decrease between  $\Delta\text{ELA}=50 \text{ m}$  and  $\Delta\text{ELA}=90 \text{ m}$ , compared to 1.5 years for shorter glaciers. A possible reason is that for larger perturbations the perturbed glacier is steeper. Hence, the glacier response from the flatter initial equilibrium glacier to a steeper state is faster.

If the glacier is very long (above 10 km), the influence of the upper steeper slope gets

<sup>3</sup>The mass balance at the terminus is defined here as the mass balance at the bed height of the last grid point. Using the surface height of the last grid point would produce oscillating values due to the different ice thicknesses of the last grid points.

smaller. Therefore, the response time decreases again for longer glaciers, which is induced by the same effect as for glaciers with a constant slope. In addition, for very long glaciers the bed slope of the perturbed glacier varies less for different magnitudes of climatic perturbation. This explains why the response time does not change much for different  $\Delta\text{ELA}$ .

- B Bedrock depressions can exist for real-world glaciers or might be produced artificially during the ice thickness inversion process of OGGM. The effect of a bedrock depression on a glacier melting into it is analysed in experiment B with a bedrock depression depth of 82 m (Fig. 4.5 B.1). This corresponds roughly to a bedrock depression that is produced for the Hintereisferner through the inversion process. For this idealised case, glaciers that melt into a bedrock depression (depicted by coloured shading) have very long response times. Due to the bedrock depression and the mass-balance elevation feedback, the initial mass balance at the terminus is less negative for slightly longer glaciers (here between glacier lengths of 6.2 km–7 km in Fig. 4.5 B.3, mass-balance-elevation feedback). This is a possible indication for the enhanced response times.

The smaller the climatic perturbation, the longer is the response time for a glacier melting into the bedrock depression and the smaller is the initial glacier length 'window' where a long response time is modelled. For large perturbations, the bedrock depression has a weaker influence with a peak of 122 years for  $\Delta\text{ELA}=90$  m compared to 189 years for  $\Delta\text{ELA}=30$  m. This can be explained by the larger part of the glacier that melts away for larger perturbations. Hereby, only a fraction of the underlying bed of the melted glacier is the bedrock depression.

A possible parameter that would describe whether a glacier is melting into such a bedrock depression, would be e.g. the bed slope of only the lower parts of the initial glacier. The smaller the perturbation, the smaller should be the bed slope quantile to look at to detect such irregularities in the bed. In Fig. 4.5 B.4, it is visible that for  $\Delta\text{ELA}=50$  m the lowest 20% of the bed slope have a very low value indicating that the glacier terminus is near to a bedrock depression.

- C Experiment C (Fig. 4.5 C), is equal to experiment B but with a 1.6 times deeper bedrock depression of 132 m, see grey plotted line for comparison in Fig. 4.5 B.1. A larger bedrock depression results in longer peak response times with 382 years for  $\Delta\text{ELA}=30$  m, which corresponds to an increase by a factor of 2, see light grey plotted response time of Fig. 4.5 B.2 in Fig. 4.5 C.2. The mass balance increase due to the bedrock depression is around 1.6 times larger. This is expected from the 1.6 times deeper bedrock depression and explains the longer response times in experiment C.

For deep enough bedrock depressions, bed slope ratios of the lowest 20% quantiles of elevation of a glacier can be even negative (Fig. 4.5 C.4) which is then a clear indication for a bedrock depression.

In the following, we compare the e-folding volume response time estimates to those from the analytical approach of Jo89 (Eq. 4) which is a ratio of the maximum (or mean) ice thickness to the mass balance at the terminus (see Fig. 4.5 A.2,B.2,C.2): While Jo89 qualitatively agrees to the e-folding estimates for simple bed slope changes (see Fig. 4.5 A.2), it does not reproduce the "peak" response times in case of bedrock depressions (Fig. 4.5 B.2,C.2). Jo89 estimates are longer if a glacier has a bedrock depression. However, the Jo89 response time estimates are not shorter if the glacier does not retreat into the bedrock depression. It also has to be noted that the numerical model was still needed to get the information about the mass balance at the terminus and of the ice thickness that were inserted into the formula of Jo89.

A similar qualitative behaviour of experiments A, B, C of Fig. 4.5 occurs for length response time estimates (not plotted) with a ratio of mean e-folding length to volume response time of

$\tau_L/\tau_V = 1.5 \pm 0.1$  (with one standard deviation). The estimate through the asymptotic approach (Ch. 2.3) shows also a similar behaviour. The mean ratio between asymptotic and e-folding volume response time is  $\tau_{V,\text{asymptotic}}/\tau_{V,\text{e-folding}} = 0.95 \pm 0.03$  and the mean ratio between asymptotic and e-folding length response time is  $\tau_{L,\text{asymptotic}}/\tau_{L,\text{e-folding}} = 1.12 \pm 0.08$ .

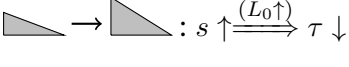
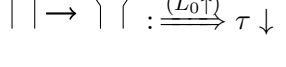
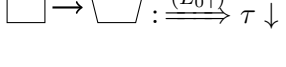
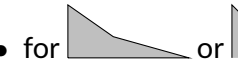
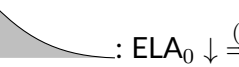
#### 4.1.5 Lessons from the idealised glacier experiments

In Table 4.2, the outcome of the different idealised experiments is presented by showing the qualitative trends in the response time when varying a single model parameter. The most important unambiguous drivers of the response time are the slope and its changes along the glacier as well as the mass balance gradient. ELA<sub>0</sub> and glacier size (length ( $L_0$ ), area, volume) do not show a clear relation with response time. We summarize the most important findings here:

- Most parameter changes that produced initial glacier length increases resulted in the end in a shorter response time ( $L_0 \uparrow \rightarrow \tau \downarrow$ ). However, this is not the case for the ice creep parameter  $A$ , where a stiffer glacier with all other parameters kept the same is longer in its equilibrium and has a longer response time ( $L_0 \uparrow \rightarrow \tau \uparrow$ ). In addition, especially for a more complex bed, e.g. on a glacier with a flat tongue and a steep accumulation area, an ELA<sub>0</sub> decrease results in a longer equilibrium glacier and a longer response time ( $L_0 \uparrow \rightarrow \tau \uparrow$ ). Therefore, idealised glaciers of very different length can have similar response times and there is no clear correlation between initial glacier size (length, area, volume) and response time.
- Furthermore, 'predicting' the response time with parameters that describe only the initial equilibrium state might get problematic when comparing the response time of the same initial glacier but for different climatic perturbations. Possibly the arrival state (perturbed equilibrium) of the glacier is even more determinant for the response time than the starting state (initial equilibrium).
- We have also seen that the response time seems to be very sensitive to bed slope changes. This can have large consequences since a bedrock depression can only be 'detected' by the lowest quantiles of a glacier's bed slope. This has to be considered when computing response times for many glaciers with unknown bedrock properties. In addition, the horizontal resolution of the glacier can be important if a certain bedrock depression occurs in the model.
- The response time estimate by the analytical formula of Jo89 shows similar qualitative behaviour in the response time trend for changing glacier setups on a glacier with a changing slope but without bedrock depressions (Fig. 4.5 A). However, the "peak" response times for glaciers melting into a bedrock depression are not reproduced in the same way (see Fig. 4.5 B). Further, the mass balance at the terminus and the ice thickness were numerically computed, as they cannot be observed for an initial equilibrium glacier. Hence the computed Jo89 estimate of our study is also no real analytical estimate anymore and comparisons should be done with care.
- Especially for the volume estimates, the differences between the e-folding and asymptotic approach are negligible, indicating a nearly exponential change in the volume with time, see Ch. 2.3 and further discussion in Ch. 5.3. The length response time is always longer than the volume response time and the ratio  $\tau_L/\tau_V$  varies between 1.1 and 1.9 depending on the geometric and climatic characteristics of the glacier.

In the discussion part, our idealised glacier experiments are compared to the literature and to the other experiments of our study (Ch. 5.2).

**Table 4.2: Summary of studied dependencies of the response time ( $\tau$ ) for idealised glaciers if a single parameter of the model is changed.** If not stated otherwise, the changed parameter is compared to the reference ideal glacier of Ch. 4.1.1. The presented variations in the setup influence how fast mass is transferred along the glacier. This changes also parameters as the mass balance at the terminus,  $b_t$ , the maximum ice thickness,  $H_{max}$ , and the ice velocity,  $u$ . An important driver is the mass-balance-elevation feedback.

Geometry	Climate
<ul style="list-style-type: none"> <li>slope (<math>s = \frac{\Delta \text{height}}{\Delta \text{horizontal distance}}</math>)              <math>\rightarrow</math> : <math>s \uparrow \xrightleftharpoons{(L_0\uparrow)} \tau \downarrow</math>             a steeper glacier results in a shorter response time (if bed slope is constant over the glacier) [Fig. 4.2]         </li> </ul>	<ul style="list-style-type: none"> <li><math>\beta</math> : (mm w.e. <math>\text{yr}^{-1} \text{m}^{-1}</math>) mass balance gradient             <math>\beta \uparrow \xrightleftharpoons{(L_0\uparrow)} \tau \downarrow</math>             a higher mass balance gradient decreases the response time (for a constant increase of mass balance with height) [Fig. 4.2]         </li> </ul>
<ul style="list-style-type: none"> <li>hypsometry              <math>\rightarrow</math> : <math>\xrightleftharpoons{(L_0\uparrow)} \tau \downarrow</math>             a wider accumulation area results in a shorter response time [Fig. 4.4]         </li> </ul>	<ul style="list-style-type: none"> <li><math>\text{ELA}_0</math>: (m) initial equilibrium line altitude             <math>\text{ELA}_0 \downarrow \xrightleftharpoons{(L_0\uparrow)} \tau \downarrow</math> (only if constant bed slope)                       decreasing <math>\text{ELA}_0</math> decreases the response time [Fig. 4.3 a1]         </li> </ul>
<ul style="list-style-type: none"> <li>bed shape              <math>\rightarrow</math> : <math>\xrightleftharpoons{(L_0\uparrow)} \tau \downarrow</math>             changing from rectangular to trapezoidal bed shape decreases the response time [Fig. 4.3 d1]         </li> </ul>	<ul style="list-style-type: none"> <li><math>\Delta \text{ELA}</math>: (m) climatic perturbation             <math>\Delta \text{ELA} \uparrow \xrightleftharpoons{(L_0\rightarrow)} \tau \searrow</math>   <math>\tau_{\text{growing}}, \Delta \text{ELA} &lt; 0 &gt; \tau_{\text{shrinking}}, \Delta \text{ELA} &gt; 0</math>             with a stronger climatic perturbation, the response time is slightly shorter [Fig. 4.3 c1]         </li> </ul>
<b>more complex:</b> <b>specific bed geometry &amp; changing <math>\text{ELA}_0</math></b> <ul style="list-style-type: none"> <li>for  or  : <math>\text{ELA}_0 \downarrow \xrightleftharpoons{(L_0\uparrow)} \tau \uparrow</math>            if the ablation area is much flatter than the accumulation area, response time increases for decreasing <math>\text{ELA}_0</math> [Fig. 4.5 A, Fig. 4.6]         </li> <li>bedrock depression:  <math>\xrightleftharpoons{(L_0\uparrow)} \tau \uparrow</math> glacier melting into a bedrock depression have much longer response times [Fig. 4.5 B,C]</li> </ul>	<b>Ice dynamic parameter</b> <ul style="list-style-type: none"> <li><math>A</math>: ice creep parameter  <math>A_0 = 2.4 \cdot 10^{-24} (\text{s}^{-1} \text{Pa}^{-3})</math>            see Eq. 1 &amp; applied on SIA Eq. 15             <math>A \downarrow \xrightleftharpoons{(L_0\uparrow)} \tau \uparrow</math>             a 'stiffer' glacier has a longer response time [Fig. 4.3 b1]         </li> </ul>

## 4.2 Response time for different Hintereisferner glacier states

In the previous chapter, we analysed the response time for idealised experiments. Here, we performed experiments that capture real-world glaciers ("realistic" glaciers). For this purpose, we computed first the response time evolution on a well-studied glacier, the Hintereisferner. It is a reference glacier of the WGMS (2017), which means that the glacier fluctuations are mainly driven by climatic changes and not caused by artificial snow, heavy debris cover, or ice calving. Further, it has a long time of mass balance measurements based on the glaciological method, since the year 1952/1953. The Hintereisferner is also chosen because it has not a very complex shape and is known to the authors by several mass balance campaigns. In addition, the Hintereisferner has a long observational record of its lengths, which is useful to calibrate the model, as described in Ch. 3.1. Hintereisferner is a northeast-orientated valley glacier in the Ötztal Alps (Austria) with an area of 8.036 km<sup>2</sup> (RGI from 2003) and a length of 6.9 km (2003), a maximum height of 3939 m a.s.l. and a minimum height of 2490 m a.s.l. (WGMS, 2017).

In OGGM, ice dynamics of the Hintereisferner are computed by using three flowlines, as depicted in Fig. 3.1 a,b. The mass-balance calibration and inversion process is computed with the HISTALP climate dataset and the Hintereisferner-specific OGGM parameter calibration of Matthias Dusch,  $A=3A_0$ ,  $p_f=1.2$ ,  $\epsilon=-100$ . In doing so the model is adjusted to the existing glacier length observations (Ch. 3.1).

A simple experiment to better understand influences of the complex Hintereisferner bed geometry on the response time for different glacier lengths is done in Ch. 4.2.1. Hereby different possible equilibrium glaciers with the main flowline bed geometry of Hintereisferner but using a constant width, the calibrated  $A$ -parameter and a linear mass balance model are analysed. Then, in Ch. 4.2.2, an attempt is made to estimate the response time evolution of the Hintereisferner including the HISTALP climate dataset with the Hintereisferner-specific calibration, all three flowlines, changing widths, and by using length-preserving equilibrium states (see Ch. 2.3 & 3.2).

### 4.2.1 Idealised Hintereisferner with one flowline, linear mass balance, rectangular bed shape, and a constant width for different initial ELA

The following preliminary experiment aims to fill the gap between the very simple idealised experiments in Ch. 4.1 and the quite complex temporal response time evolution of Hintereisferner in the following Ch. 4.2.2. The main flowline bed profile of Hintereisferner (Fig. 4.6 a) was estimated via the inversion process. Therefore, 250 grid points were added outside the glacier boundary in order that the glacier can grow in a lot of different geometric states. To simplify the experiment, a constant bed width of 300 m and a rectangular bed shape are chosen. Similar to the ideal experiments (Ch. 4.1), a constant and linear mass balance was applied for different initial ELAs ( $ELA_0$ ) (from 2480 m to 3300 m, every 2.5 m) together with a constant mass balance gradient of 4 mm w.e. yr<sup>-1</sup> m<sup>-1</sup>. These settings are similar to the mass balance estimates using the HISTALP data of 2003. By applying the different  $ELA_0$ , the initial glacier length of the main flowline of the 'constant width Hintereisferner' varies from 20 km to 1 km and the mean bed slope ratio changes accordingly (from 0.1 to 0.4, Fig. 4.6 b,d). Hence, this experiment may yield information about the response time sensitivity of possible idealised geometries of Hintereisferner.

An overall tendency of the response time is visible for the simplified Hintereisferner-like glaciers with just one main flowline, constant width, and exposed to a constant mass-balance. The lower the  $ELA_0$ , hence the longer the initial glacier, the higher is the response time. This can be explained by the effect that a longer Hintereisferner-like glacier has rather a flatter bed (and surface) slope, especially in the lower parts of the glacier (Fig. 4.6 d). With increasing length, the mass balance decreases at the terminus (Fig. 4.6 b), and the glacier thickness increases (Fig. 4.6 a). The same tendency towards longer response times for a longer (and flatter) glacier was already

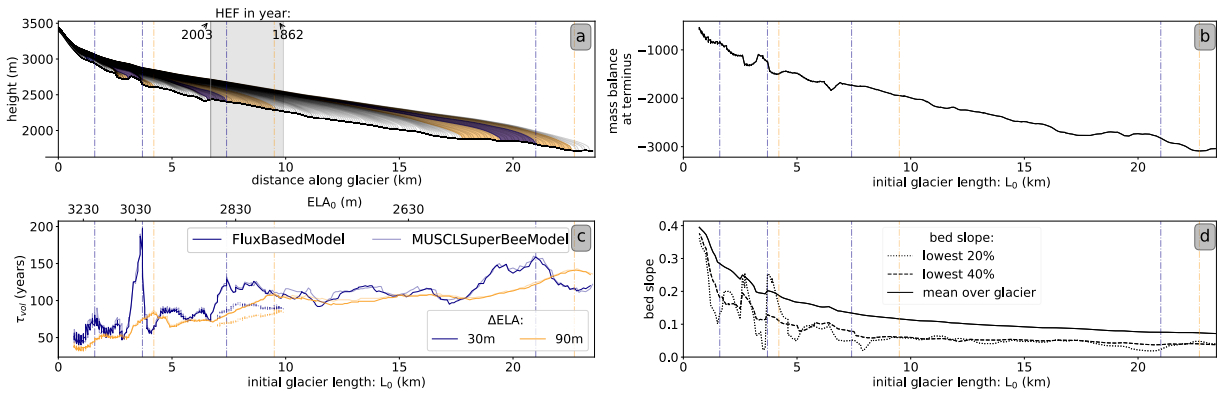


**Fig. 4.6: Response time of the idealised Hintereisferner-like glaciers for different initial ELAs**

( $\text{ELA}_0$ : 2480 m to 3300 m) with a constant mass balance gradient of  $4 \text{ mm w.e. yr}^{-1} \text{ m}^{-1}$  and  $A=3 A_0$ . Only the main flowline, a constant width, and a rectangular bed shape are applied. In (a), the used bed geometry is shown, together with the initial equilibrium glacier states (grey lines). In (b), the mass balance at the terminus and in (d), the corresponding initial bed slopes are plotted. In (c), the resulting response time for an ELA increase of  $\Delta\text{ELA}$  of 30 m and 90 m are plotted for both, the default *FluxBasedModel* and the more robust *MUSCLSuperBeeModel*. For peak response times, the corresponding initial glacier state is marked with vertical lines. In (a), the melted part in the perturbed equilibrium is coloured. In (c), for comparison, results of the most realistic but much more complex estimate of the response time evolution (1862–2003, see Ch. 4.2.2) are plotted as dots with, in (a), the corresponding initial glacier state lengths shaded in grey.

discussed in the more idealised experiment of (Fig. 4.5 A, for lengths between 5 and 10 km). However, it is the other way round for very long glaciers in Fig. 4.5. This is not clearly visible on the more complex bed geometry Hintereisferner-like case of (Fig. 4.6 a). An explanation might be that the complex bed geometry exhibits a rather exponentially decreasing mean bed slope in contrast to the idealised bed with a bend (Fig. 4.5 a).

The response time seems to be very sensitive to bedrock depressions or inhomogeneities, especially for small perturbations ( $\Delta\text{ELA}=30 \text{ m}$ ), which was already analysed in the more idealised experiment B & C of Fig. 4.5. The initial equilibrium glacier states that yield high response times seem to coincide with those glacier states that melt into a bedrock depression, e.g. the one at around 7 km (Fig. 4.6 a,c). This is also apparent by changes in the bed slope of the lowest 20% of elevation of the glacier (Fig. 4.6 d) and slight variations of the mass balance at the terminus (Fig. 4.6 b).

For stronger perturbations, the response time is mostly shorter and, in addition, a less extreme peak in the response time is simulated if the glacier retreats into the bedrock depression. Moreover, the maximum response time occurs for a longer glacier. Further, in this case, the peak is smoothed, as a large part of the glacier melts where only a small part of the underlying bed includes the bedrock depression, which is again very similar to the experiments described in Ch. 4.1.4.

The response time estimates of the default OGGM ice-dynamic *FluxBasedModel* are similar to those from the more robust mass-conserving *MUSCLSuperBeeModel* (Fig. 4.6 C). Only for very long glaciers, some differences are visible, which makes sense because the larger the glacier, the more probable are numerical instabilities for the *FluxBasedModel*. As the *MUSCLSuperBeeModel* cannot be applied to glaciers with varying widths and bed shapes, it is assumed that errors that result from violating mass conservation on very steep slopes are small for the other experiments.

#### 4.2.2 Attempt to capture the Hintereisferner response time temporal evolution

To estimate how the response time of Hintereisferner has changed with time, the used model OGGM was first calibrated ( $p_f$ ,  $A$  and  $\epsilon$ ) to describe best the observed length evolution (see

Fig. 4.8) using the HISTALP database (done by Matthias Dusch, see Ch. 2.3 & 3.2). The lengths of the transient Hintereisferner states are extracted from that calibration.

The transient glacier state of Hintereisferner for 2003 with a volume of  $0.58 \text{ km}^3$  (Fig. 3.1) is much larger than the corresponding nearly-vanished glacier in equilibrium (Fig. 4.7 d). To model a Hintereisferner in equilibrium with the same length as the transient Hintereisferner in 2003, a negative temperature bias of  $-1.5^\circ\text{C}$  has to be applied (Fig. 4.7 e). Already in 1862, Hintereisferner is in a large disequilibrium between its geometry and the climate (compare Fig. 4.7 a,b). When looking at the temporal evolution of the temperature bias that is necessary to preserve the glacier length for an equilibrium glacier (see appendix Fig. A.4), it is visible that Hintereisferner seems to recover from the climate-geometry imbalance, as the necessary temperature bias is in absolute number smallest in 1913, which coincides with the calibration parameter  $t_{star}$  of the OGGM model for Hintereisferner. Although the calibrated length of Hintereisferner decreases monotonously with time (Fig. 4.8), the mass balance (here mean of 23 years) varies without a clear trend until roughly 1980 (Fig. A.3). The rather cold climate with more solid precipitation around 1913 according to the HISTALP climate dataset (Fig. A.3) indicates why the modelled transient Hintereisferner was nearest to equilibrium at that time. Therefore, the smallest temperature bias had to be applied (Fig. A.4). The applied temperature bias that is necessary to build a glacier in equilibrium that has the same length coincides with the variations in the mass balance. For example, in the colder period around the year 1970, the Hintereisferner was nearest to equilibrium in the near past. In that period we could say Hintereisferner has caught up again slightly with the climate. From 1970 till 2003, the lag between the climate and the glacier's geometry increased more and more, which is indicated by the necessary monotonously increasing temperature bias to preserve the length of the glacier. This coincides with the time period of highest temperatures, least solid precipitation and therefore smallest mass balances as well (Fig. A.3).

The little ice age, which ended in the middle of the 19<sup>th</sup> century, might explain why the Hintereisferner is too large for the warmer climate from 1850 onwards (e.g. Marzeion *et al.*, 2014a). The disequilibrium of the current glacier state, however, is a mixture of both, natural variability and anthropogenic warming. This is confirmed for the Hintereisferner by ensemble statistics of a geometric glacier length model, executed by Herla *et al.* (2017). The signal of increased warming in the last 20 years of the mean climate is also visible in Fig. A.3 a.

Applying initial temperature biases to preserve the length of Hintereisferner for the initial equilibrium smoothes out the variability of the temporal evolution in the climate. This makes the interpretation of the following presented temporal evolution of the response time difficult and any generalisations should be done with care. Another aspect is that bringing the Hintereisferner into equilibrium by applying a constant artificial climate (mean of 23 years) over several centuries might not be the right scale to analyse the disequilibrium of a glacier. The anomalous warm climate of e.g. around 1862 would not have occurred over several centuries in the row. Therefore, the strong retreat of an equilibrium glacier with a climate as presented in Fig. 4.7a does not represent the disequilibrium on longer scales. Applying a mean climate of 50 years could smooth out the natural variability stronger and might be more appropriate in this context. However, here we are applying a length-preserving temperature bias, individually calibrated for each centred year climate. Thus, the applied initial climate is somehow dictated by the length of the glacier. The choice of the amount of years to use for the mean climate only changes the necessary temperature bias that will be applied but not the actual response time evolution.

How fast the simulated equilibrium Hintereisferner states respond to a climatic step change increase of  $\Delta T=+0.195^\circ\text{C}$  ( $\cong \Delta \text{ELA}=30 \text{ m}$ ) from 1862 to 2003 is depicted by the volume and length response time plotted in Fig. 4.8. Overall the e-folding volume response time varies between 97 and 74 years in between 1862 and 2003. Until 1920, no considerable changes occur, except for one peak in 1876 which coincides with a minimum in the mass balance gradient of the

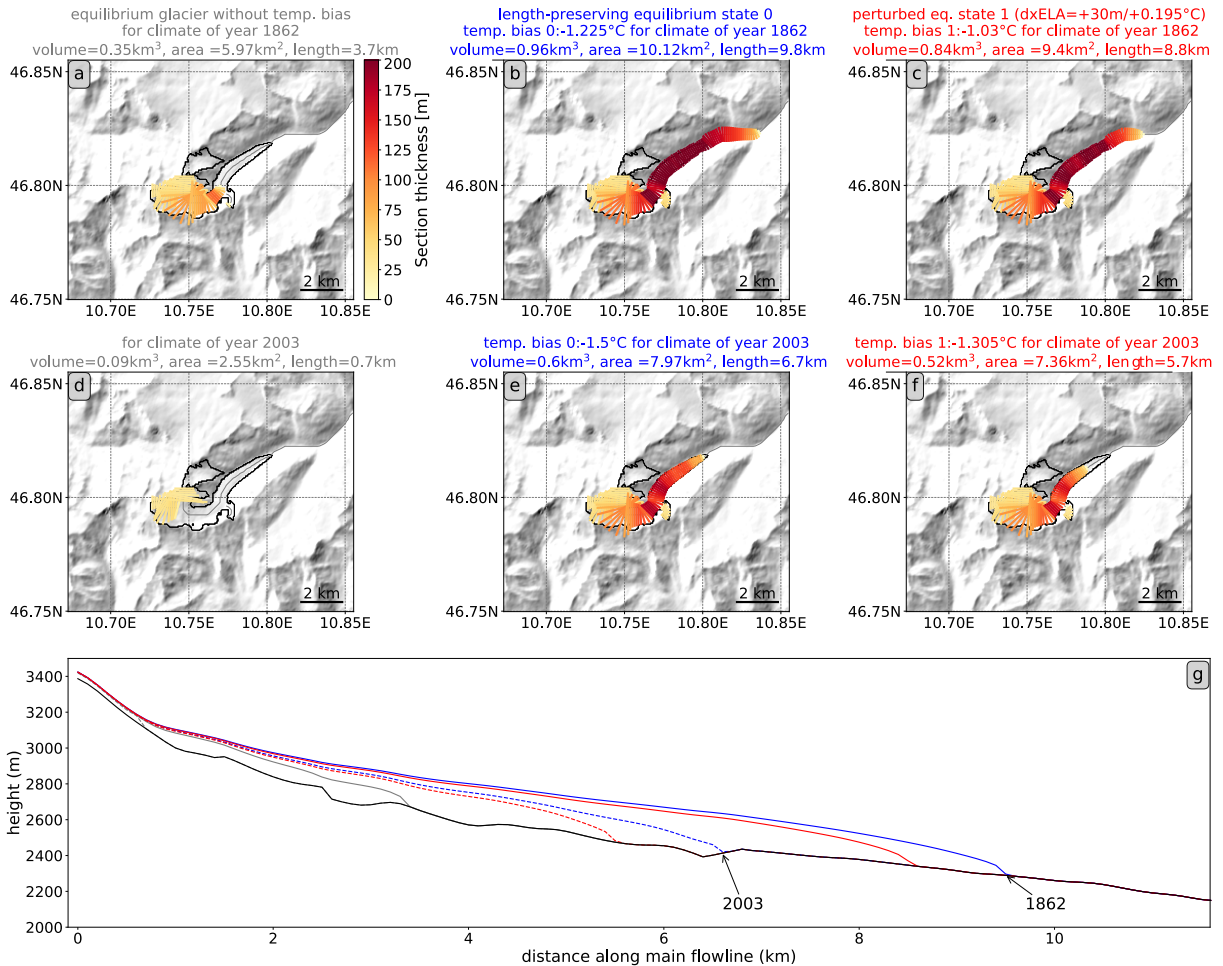


**Fig. 4.7:** Ice thickness of Hintereisferner (HEF) glacier states using the mean climate of (a, b, c)  $1862 \pm 11$  years and of (d, e, f)  $2003 \pm 11$  years, plotted for (a, d) an equilibrium HEF without temperature bias and for (b, e) an equilibrium HEF that has the same length as the transient HEF by applying a negative temperature bias. In (c, f), the perturbed HEF equilibrium state is plotted where the climate of (b, e) was changed by applying a temperature bias of  $\Delta T = +0.195^\circ\text{C}$  ( $\equiv \Delta \text{ELA} = 30$  m). In (g), the altitudinal profile of the main flowline is shown together with the surface heights of the different Hintereisferner states and the bed height from the inversion process. The HEF-specific model parameters and the lengths for the transient HEF were calibrated using observed glacier lengths.

ablation area<sup>4</sup> as well as with a maximum of the mass balance at the terminus. The smaller mass balance gradient together with a higher mass balance at the terminus could explain the slight increase in response time around 1873, similar to the idealised experiments (Ch. 4.1.2). From 1920 on the response time increases, which coincides also with a decrease in the mass balance gradient. However, while the mass balance gradient starts to increase around 1935, together with a decrease in the mass balance at the terminus, the response time still becomes slightly larger reaching its peak in 1953. This is different to the ideal case experiments and the analytical estimate of Jo89. Other drivers of the response time, the weighted surface or bed slope<sup>5</sup>, indicate that the retreating Hintereisferner gets steeper in the mean, i.e. visible in Fig. 4.7 g. This would also result in a rather faster responding glacier according to the ideal experiments.

The reason for the peak response time occurring around 1953 and the decrease only afterwards could be the following: Before 1953, the bedrock depression of around 80 m located at

<sup>4</sup>In contrast to the idealised experiments, the mass balance gradient is here defined by a linear regression of the mass balance profile in the ablation area only.

<sup>5</sup>For the real glacier experiments the area-weighted slope of all flowlines is used as the width along the flowlines' changes.

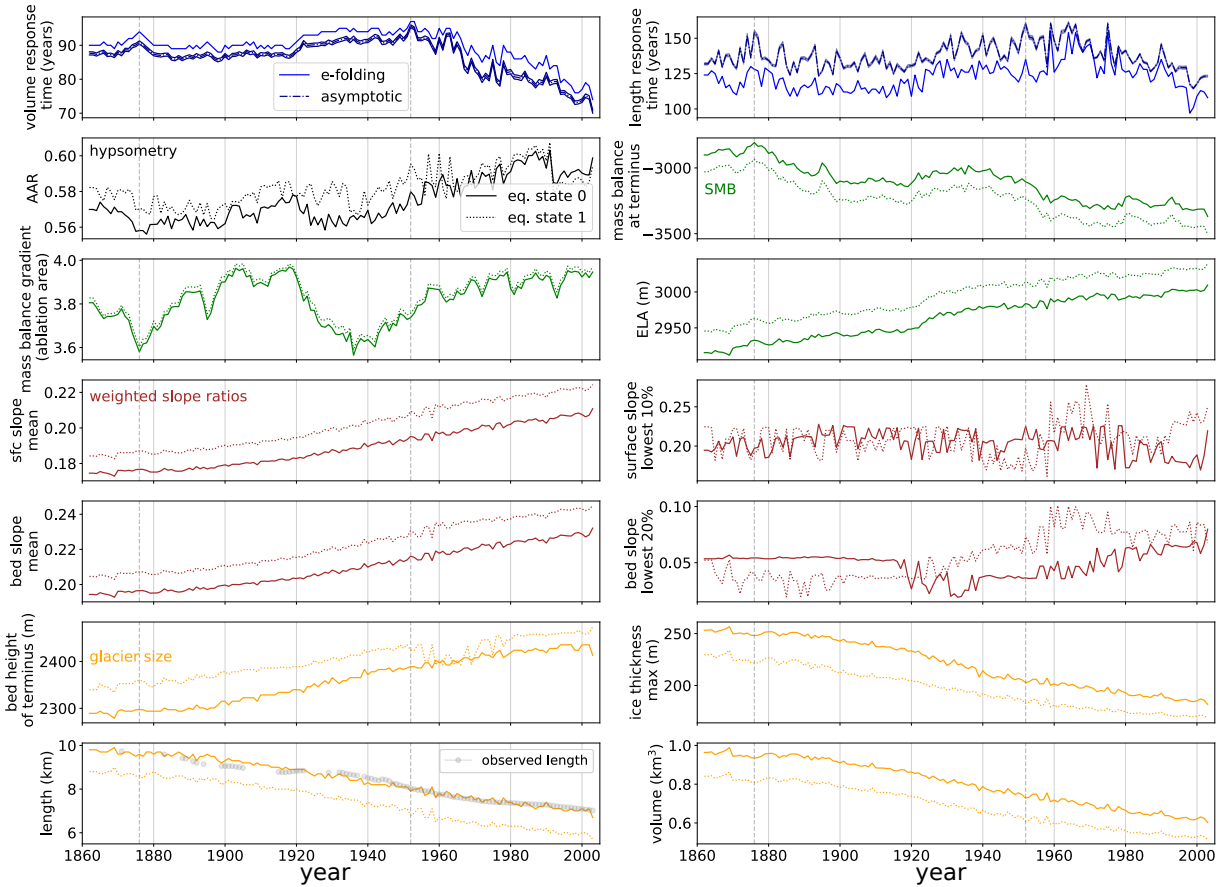


**Fig. 4.8: Temporal evolution for length-preserving equilibrium Hintereisferner (HEF) states from 1862 to 2003.** The evolution of the volume and length response time estimates are plotted for the e-folding (default) and the asymptotic approach. The evolving hypsometry, surface mass balance (SMB), weighted slope ratios and glacier size are plotted beneath for the length-preserved equilibrium state 0 and perturbed equilibrium state 1. In this case, the climatic perturbation between equilibrium state 0 and equilibrium state 1 is  $\Delta\text{ELA}=+30 \text{ m}$  ( $\Delta T=+0.195^\circ\text{C}$ ). The HEF-specific model parameters and the lengths for the transient HEF were calibrated using observed glacier lengths.

kilometres 6.4 to 6.8 along the glacier is covered by the glacier for both, initial and perturbed glacier. Around 1953, the perturbed glacier starts to melt into the bedrock depression. The indicator for that is the start of a decreasing bed height at the terminus from 1953 on. Therefore, as simulated for the more idealised Hintereisferner (see Fig. 4.6, vertical violet line at 7.5 km), the longer response time might result from the existence of this bedrock depression. For the last 40 years, the model computed a decreasing response time. This depicts the overall tendency of the shrinking Hintereisferner due to the increase in the mean bed and surface slope.

Volume and length of the modelled equilibrium Hintereisferner states were steadily decreasing together with the increase of the ELA from 1862 to 2003. The e-folding response time, however, increased slightly at first and then decreased since 1953. Thus, we cannot identify a clear relation between the Hintereisferner glacier size and response time. In the case of a perturbation of  $\Delta\text{ELA}=+90 \text{ m}$ , there exists a correlation between ELA, length, or volume and response time but this might not have a causal direct relationship. The physical reason for the steadily decreasing response time from 1862 to 2003 for a high perturbation on Hintereisferner (Fig. 4.9) is rather the steepening of the glacier that happens when the glacier decreases in size (see idealised experiment Fig. 4.5  $5 \text{ km} < L_0 < 10 \text{ km}$ ).

A possible relationship between the accumulation area ratio (AAR) and the response time is not clearly visible for the estimates on different Hintereisferner states.

The temporal evolution of response time is plotted also in the figure of the response time

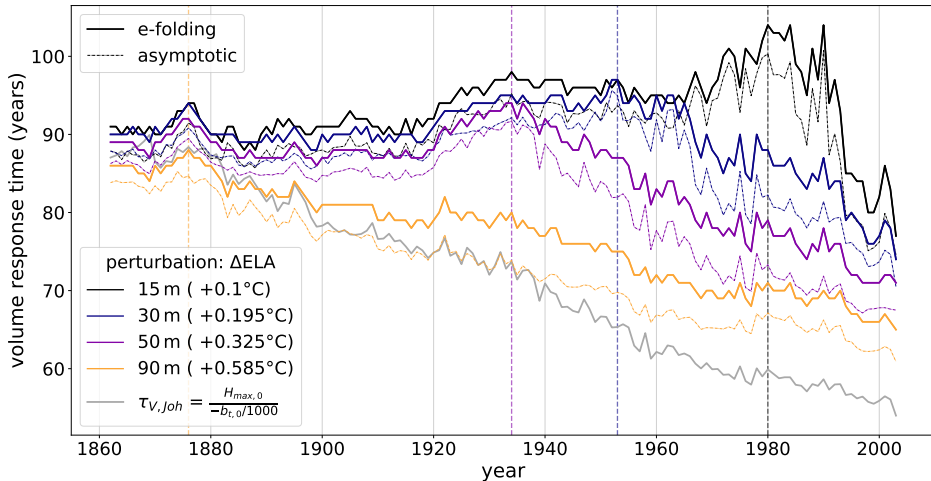


**Fig. 4.9: Volume response time evolution of Hintereisferner for different climatic perturbations between  $\Delta T=+0.1^\circ\text{C}$  and  $\Delta T=+0.585^\circ\text{C}$  for the e-folding and the asymptotic response time approach. The corresponding maximum for each temperature perturbation are marked as vertical lines. The analytical response time estimate of Jo89 (Eq. 4) was added using the initial equilibrium glacier state maximum ice thickness  $H_{max}$  and mass balance at the terminus  $b_t$ .**

estimates for the more idealised Hintereisferner (Fig. 4.6 c, dotted points). The shape is comparative, although the response time estimates of the more idealised Hintereisferner are much longer and seem to vary more. There are several factors that explain these differences: In the more complex estimate, the mass balance is estimated with the HISTALP dataset. Hereby, the temperature (with the calibrated temperature bias) and precipitation parameter are taken as input together with the calibration parameters (Eq. 14). For the more idealised Hintereisferner, mass balance is prescribed by the applied ELA and mass balance gradient. That means that the more complex estimate that corresponds better to reality uses a mass balance profile which does not change linearly with height. Hence, the mass balance change with altitude is greater and more linear in the ablation area than in the accumulation area. At higher elevation, however, snow fall might decrease with elevation (Ho19). This is also the reason why for the 'real' experiments only the mass balance gradient of the ablation area was estimated. In addition, the more complex real experiments use three flowlines, a mixed bed shape and a changing width. All these aspects together might explain why the idealised Hintereisferner experiment is more sensitive to the bedrock depression.

For an ELA increase of +30 m, the e-folding volume response time is on average only three years longer than the asymptotic volume response time (Eq. 8). Thus, their estimates have similar values in that case. The length response time is very noisy which might be produced by the OGGM model where glacier length changes only in steps. The e-folding length response time varies between 155 and 97 years and starting with the centred year 1953 rather a decreasing trend is visible, similar to the volume response time. The e-folding length response time is, for  $\Delta\text{ELA}=30\text{ m}$ , 15 years shorter than the asymptotic length response time (Eq. 10 & Eq. 13) indicating that the length evolution does not fit perfectly to the sigmoidal curve, further discussion in Ch. 5.3.

In Fig. 4.8, the climate was perturbed by an increase of  $\Delta T=+0.195^\circ\text{C}$ , hence by raising the ELA 30 m. Fig. 4.9 shows the same experiment for four different perturbations with ELA increases of 15 m to 90 m ( $\Delta T=+0.1^\circ\text{C}$  to  $\Delta T=+0.585^\circ\text{C}$ ). Throughout the temporal evolution, a clear tendency towards shorter response times for larger climatic step change temperature increases is visible, for both e-folding and asymptotic approach. The faster response might be

explained by the perturbed Hintereisferner retreating into steeper areas for larger perturbations (Fig. 4.7 g). To a much smaller degree, the slightly increasing mass balance gradient of the perturbed climate for higher perturbations (not plotted, median of  $3.84 \text{ mm w.e. yr}^{-1} \text{ m}^{-1}$  for  $\Delta T=+0.1^\circ\text{C}$  to  $3.9 \text{ mm w.e. yr}^{-1} \text{ m}^{-1}$  for  $\Delta T=+0.585^\circ\text{C}$ ) might affect the response time. Consequently, it is

$$\Delta \text{ELA} \uparrow \rightarrow \text{steeper perturbed glacier slope (and mass balance gradient } \uparrow) \rightarrow \tau \downarrow .$$

This effect was already visible for the more idealised Hintereisferner experiment shown in Fig. 4.6. It also occurs in the study of Zekollari and Huybrechts (2015) for the Morteratsch glacier using a 3D-flow model. In the study, they conclude that in a warming climate, the response time of Morteratsch glacier decreases because the glacier steepens. Moreover, in their model, warming results in additional surface melt, which enhances the glacier flow by increased basal sliding. This is not accounted for in our used flowline model setup of OGGM as basal sliding is not included and the  $A$ -parameter is set constant, hence independent of temperature.

The maximum response time in 1953 for  $\Delta \text{ELA}=+30 \text{ m}$  occurs later and more pronounced for  $\Delta \text{ELA}=+15 \text{ m}$  (Fig. 4.9). This maximum occurs earlier or is "smoothed out" for larger perturbations  $\Delta \text{ELA}=\{+50 \text{ m}, +90 \text{ m}\}$ . As the peak is in different years for different perturbations, it cannot be explained by the climatic condition or geometry from the initial state glacier, which is the same for all perturbations. These variations have to originate from the different amount of melting into different perturbed equilibrium states. Probably the bedrock depression could be the reason for the shift in the response time peak for smaller perturbations.

The approach of Jo89 has been computed as well by dividing the maximum ice thickness  $H_{max,0}$  by the mass balance at the terminus  $b_t$  of the initial equilibrium glacier (Eq. 4). It coincides quite well with the numerically estimated e-folding volume response time for a long Hintereisferner (from 1862 to 1900). The response time estimate of Jo89 decreases over the entire period but stronger than the numerical estimate of the largest perturbation. The underestimated response time of Jo89 for smaller Hintereisferner states starting with the year 1900 might come from the limitations listed in Ch. 2.2. These are in this case mainly the neglected mass-balance-elevation feedback and an assumed idealised geometry. Why it coincides best with the e-folding volume response time estimates for long Hintereisferner states is unclear. Although the derivation of Jo89 is based on the assumption of a small perturbation, the response time is most similar to the e-folding response time for large perturbations on the Hintereisferner. The response time increase in the first place and the only delayed decrease for applied smaller perturbations is not reproduced when applying the formula of Jo89. If the driver of these short-term response time variations was the bedrock depression, it would mean that the approach of Jo89 does not take that into account and would explain the best fit to the estimate of the largest perturbation. This was the case for the idealised experiments where the Jo89 estimates did not reproduce the "peak" response times for glaciers melting into a bedrock depression (Fig. 4.5 B,C). In any case, comparing between analytical or scaling approaches and e-folding numerical response time estimates should be done with care, because they might use different assumptions. As mentioned for the idealised experiments, the mass balance at the terminus and the maximum ice thickness of the initial equilibrium Hintereisferner were calculated numerically. Therefore, the computed Jo89 estimate is not anymore purely a scaling approach.

To conclude, the response time evolves with time as the shape and size of Hintereisferner states change. For the largest perturbation, short time variations in the response time seem to be smallest, possibly because local phenomena as bedrock depressions are smoothed out. Overall, the response time of a single glacier seems to change for different states in the last century and is also highly dependent on the applied perturbation. Therefore, it can be said that there exists no well-defined single constant response time for a glacier, as described in Benn and Evans (2014). An important message of this experiment might be, that it is difficult to compare response times

among glaciers if not the same perturbation is applied and that for small perturbations bedrock depressions might have an influence on the response time.

The analysis of response time of different sizes on a single glacier bed shape, cannot be generalized to other glaciers and bed shapes. In the case of Hintereisferner, the slope on its average and especially the lower parts of it (e.g. the amount of the 10% or 20% lowest bed or surface slope) seem to play an important role for changes in the response time of Hintereisferner. Nevertheless, the actual interaction of the lowest slope quantiles of elevation of the glacier with the response time is complex and difficult to use for a 'prediction'. Most of the variables are also highly correlated with each other and a clear signal of a causal relationship of a single variable cannot be extracted.

In addition, the bedrock depression of the modelled Hintereisferner on km 6.4 to 6.8 at a height of around 2500 m a.s.l. might just result from the volume inversion process. If it is an artefact of the model, these are uncertainties in the response time that have to be taken into account. Still, observations of the bed height profile of Hintereisferner were done in 1997 by measuring the ice thickness with a ground penetrating radar (Span and Fischer, 2005). In their estimate of the bed height, there is a bedrock depression between 2500 and 2550 m a.s.l., but it is less deep (< 50 m) than the estimate with the volume inversion process of OGGM (around 82 m). Generally, bedrock depressions are common for mountain glaciers and are formed by erosion processes, i.e. they are the source of current and future proglacial lakes (Otto, 2019).

Moreover, the temporal evolution of response time estimated in this study is just a theoretical construct and its application to real-world problems is difficult. The Hintereisferner states were always brought into equilibrium with a changing temperature bias. Hence, no direct information whether the climate-geometry disequilibrium has changed over time can be extracted. Consequently, the output should be better interpreted as response time changes of equilibrium glaciers with lengths fitting to the observations between 1862 and 2003.

A possible signal of the climate-geometry disequilibrium might be visible from the temperature bias that was applied beforehand to preserve the length (compare Fig. A.3 and Fig. A.4). On those periods where it was colder than in the mean, the necessary negative temperature bias to preserve the length, which decreases here monotonously, is higher. Therefore, the glacier was more in equilibrium for those periods with a higher mass balance. Hence, we could say that around 1913 and around 1970 the glaciers' geometry had been caught up the most with the climate, and the climate-geometry disequilibrium was smallest. However, this is only valid when using the short-term occurring favourable climate for glacier growth as constant climate over several centuries. Therefore, we cannot deduce a statement of how the disequilibrium between climate and geometry of Hintereisferner has changed in reality from our estimates.

For this experiment, we have only used small parts of the available observational data of Hintereisferner and the results are constraint by the use of the shallow-ice approximation. In addition, surface mass balance measurements of the Hintereisferner before 2000 included the Langtaufererjochferner (e.g. Geist and Stotter, 2007), which is not described as a separate flow-line in the out-of-the box OGGM model, although this could have been corrected manually. We used this simplified approach with a global glacier model to later apply similar methods on many glaciers at the same time.

### 4.3 Response time of Alpine glaciers

We estimated the response time of Alpine glaciers using the HISTALP climate dataset and its calibrated mass balance parameter set. Hereby, the melting temperature is set to  $T_{\text{melt}} = -1.75^{\circ}\text{C}$ , the temperature lapse rate to  $6.5 \text{ K km}^{-1}$ , the precipitation factor to  $p_f = 1.75$ , and the liquid precipitation temperature to  $T_{\text{liquid}} = 2^{\circ}\text{C}$  (Eq. 14). No lateral drag and no sliding was added. Before using these parameters, the  $A$ -parameter was tuned to  $A=2.2A_0$  in order that the total glacier volume after the inversion corresponds to the Alpine glacier volume of the consensus estimate of Farinotti *et al.* (2019) (Fig. A.5).

To calculate the response time of glaciers with the current geometry (from 2003), we used equilibrium glaciers that have a similar area as the one from the RGI (Ch. 3.2). The climate at the year ' $t_{\text{star}}$ ' (mean constant climate with center year  $t_{\text{star}}$  of 31 years) represents a theoretical equilibrium climate for each individual glacier, hence a climate where the glacier of the inversion process (from 2003) is approximately in equilibrium. To match better the area of the equilibrium glacier to the transient glacier from the inversion process, an additional calibrated temperature bias was added to the  $t_{\text{star}}$  climate for each glacier individually. This initially applied temperature bias varies between  $-0.28^{\circ}\text{C}$  and  $+0.21^{\circ}\text{C}$  with in median  $+0.001^{\circ}\text{C}$  (Fig. 4.10 e). While the area of the glaciers in initial equilibrium was calibrated to be similar to the RGI ( $<1\%$  deviation), the total volume of all Alpine glaciers in equilibrium is larger ( $V_{\text{eq}} = 147 \text{ km}^3$ ) than the transient calibrated volume ( $V_{\text{inv}} = 130 \text{ km}^3$ ) (Fig. 4.10 a,c). To bring a glacier into equilibrium with the same volume as the transient glacier, a warmer climate than the one applied with  $t_{\text{star}}$  plus the additional temperature bias would be necessary. This is because preserving volume would result in a shorter glacier with less area and length than the transient glacier but being overall thicker than the transient glacier. In order to maintain a specific length or area, a glacier has to be thick enough in the accumulation area. Only then, the mass can be redistributed towards the tongue. Therefore, preserving length or area of a transient glacier in equilibrium needs more negative temperature biases, hence a climate which is more favourable for glacier growth (Ze20; Zekollari and Huybrechts, 2015). As the area of individual (Alpine) glaciers is better known than the volume, we used here the described area-preserving approach.

There are 3927 Alpine glaciers in the RGI, but for some it was not possible to estimate a response time, probably because they were already too small in their transient state. Thus in total, we estimated the response time of 3863 Alpine glaciers using the HISTALP climate dataset and the above described area-preserving initial equilibrium estimate for four different shrinking scenarios with a temperature increase of  $\Delta T = \{+0.1^{\circ}\text{C}, +0.25^{\circ}\text{C}, +0.5^{\circ}\text{C}, +1^{\circ}\text{C}\}$ .

In the following, we analyse first the total Alpine glacier volume and area response time as well as the distribution of the individual glaciers' response time (Ch. 4.3.1). Then, glaciers are clustered in how their response time changes for different climatic perturbations (Ch. 4.3.2). In addition, the most important geometric or climatic parameters that control the response time are analysed and a rough predictive model is estimated (Ch. 4.3.3).

#### 4.3.1 Total volume & area response time of the entire Alpine glacier ice mass and distribution of response time estimates for individual glaciers

The e-folding response time of the entire Alpine glacier volume varies between 100 years for a climatic perturbation of  $\Delta T = +0.1^{\circ}\text{C}$  and 48 years for  $\Delta T = +1.0^{\circ}\text{C}$  with the response time of the total glacier area being respectively 32 and 20 years longer (Fig. 4.10). The relative total glacier volume decrease is 10% for  $\Delta T = +0.1^{\circ}\text{C}$  and 65% for  $\Delta T = +1.0^{\circ}\text{C}$ . The relative corresponding area decrease is smaller with 8% for  $\Delta T = +0.1^{\circ}\text{C}$  and 58% for  $\Delta T = +1.0^{\circ}\text{C}$ . There is a linear trend of decreasing response time for increasing change between initial equilibrium state 0 and perturbed equilibrium state 1. Per percent increase in the total Alpine glacier volume decrease, the volume response time decreases 1.0 years. Per percent increase in area decrease, the area re-

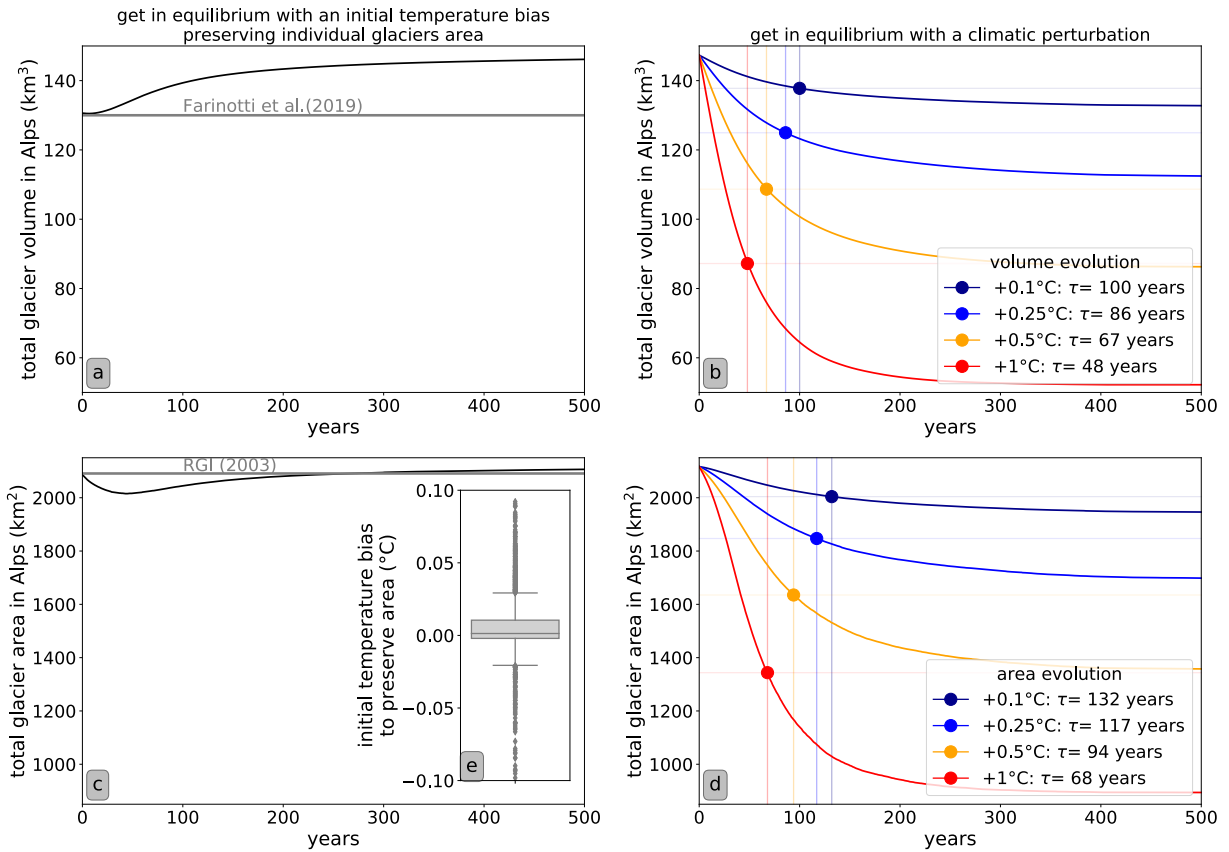


**Fig. 4.10: Temporal evolution of (a, b) modelled summed up volume and (c, d) area of all Alpine glaciers.** In (a, c), the process of getting glaciers into an equilibrium is shown, where the transient glacier area (RGI outline of 2003) is preserved by applying a constant mean climate with centred year  $t_{star}$  and an additional temperature bias, see (e). In (a, c), year 0 corresponds to the sum of the transient glacier states and year 500 to the initial equilibrium states 0. The response time estimates are computed by applying a climatic step change with temperature perturbations between  $\Delta T=+0.1^{\circ}\text{C}$  and  $\Delta T=+1^{\circ}\text{C}$  on the initial equilibrium state 0. In (b, d), the corresponding temporal summed up volume and area evolution of all Alpine glaciers are shown with the initial equilibrium states 0 at year 0 and the perturbed equilibrium states 1 at year 500. In (b, d), volume and area e-folding response times of the entire Alpine ice masses of the glaciers are marked.

sponse time decreases 1.3 years. However, only four perturbations were applied, meaning that these values and the linearity are only rough estimates.

When we compare the volume response time of the entire volume of all Alpine glaciers of our study to the estimates of Ze20, we see some discrepancies. The response times of the entire ice volume for the four shrinking scenarios ( $\Delta T=+0.5^{\circ}\text{C}$  and  $\Delta T=+1^{\circ}\text{C}$  for two time periods) of Ze20 are between 36 and 42 years, which is shorter than the estimates of our study. In addition, the sensitivity of response time changes with volume change is much lower (0.24 years decrease per % increase in  $\Delta V$ ) in the study of Ze20. As the setups, the used model, climate and glaciers are not the same, those discrepancies are expected. A more in-depth comparison is found in Ch. 5.1.

The response time between individual Alpine glaciers can vary between 886 years and 1 year when applying a perturbation of  $\Delta T=+0.1^{\circ}\text{C}$ , and between 172 and 2 years for  $\Delta T=+1.0^{\circ}\text{C}$ . The response time decreases with increasing  $\Delta T$  with median values of 74 [72, 76]<sup>6</sup> years for  $\Delta T=+0.1^{\circ}\text{C}$ , 53 [52, 54] years for  $\Delta T=+0.25^{\circ}\text{C}$ , 35 [35, 36] years for  $\Delta T=+0.5^{\circ}\text{C}$  and 20 [20, 20] years for  $\Delta T=+1.0^{\circ}\text{C}$  (Fig. 4.11a). Mean values are higher than the medians especially for low  $\Delta T$  with in mean 96 [93, 98] years for  $\Delta T=+0.1^{\circ}\text{C}$ . The strongly right-skewed distribution for

<sup>6</sup>95% confidence interval with a bootstrapping method

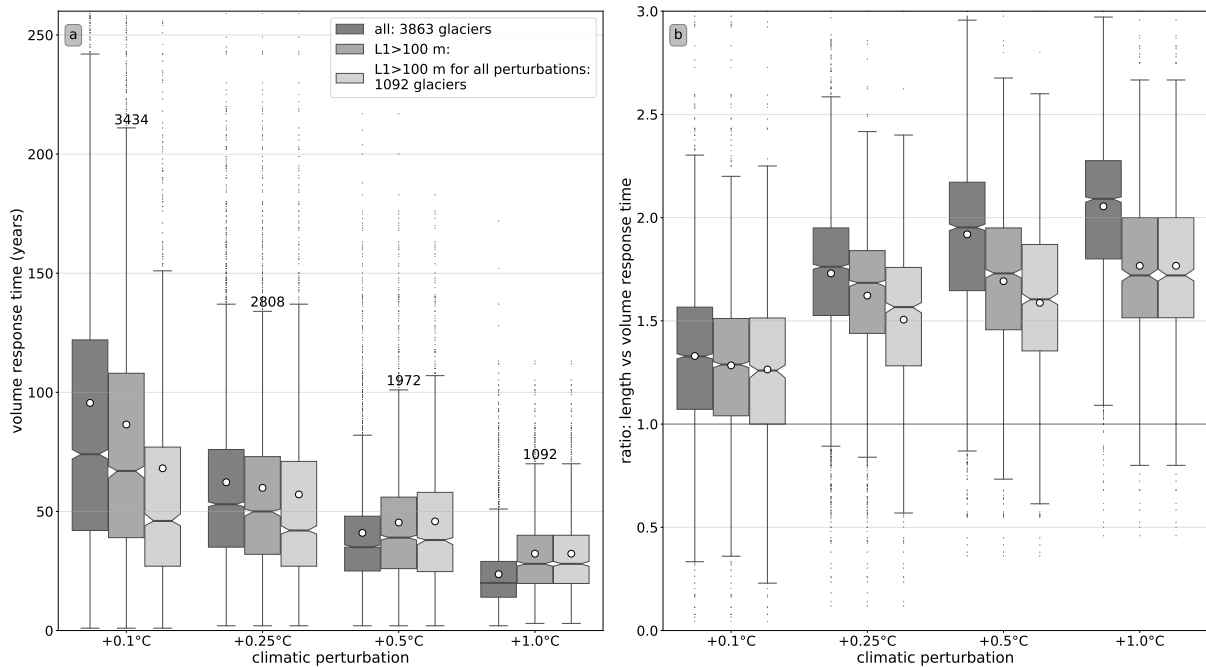


**Fig. 4.11: Distribution of individual (a) e-folding volume response times and (b) ratios of length to volume response times for Alpine glaciers when applying different perturbations.** It is distinguished between all glaciers, those that still exist in the perturbed equilibrium (length  $L_1 > 100$  m) with the amount of glaciers indicated and those 1092 glaciers that still exist for  $\Delta T = +1^\circ\text{C}$ . The notches correspond to the 95% confidence interval of the medians using a bootstrapping method. The mean values are plotted as circles. A comparison to the asymptotic approach is in Fig. A.6.

a low  $\Delta T$  results from the effect that there are some few glaciers that have extremely long response times, e.g. the 5% glaciers with longest response time have  $\tau \geq 237$  years for  $\Delta T = +0.1^\circ\text{C}$ .

The variability of response time between the individual glaciers can be measured by looking at the interquartile range, hence the values between the 25%- and 75%-quantiles indicated by the boxplots in Fig. 4.11 a. While for  $\Delta T = +0.1^\circ\text{C}$  50% of the glaciers have a response time between 42 and 121 years, for  $\Delta T = +1^\circ\text{C}$  50% of the glaciers' response time is between 14 and 29 years. Hence, the variability in between the glaciers' individual response time decreases for larger  $\Delta T$ , where most glaciers seem to respond in a relatively similar speed.

When only those glaciers are analysed that still exist when they reach the perturbed equilibrium state (length  $L_1 > 100$  m), variations between the different  $\Delta T$  get less important. This is most pronounced if only the 1092 glaciers are taken that still exist in the perturbed equilibrium state of the largest perturbation, with in median 46 [44, 49] years for  $\Delta T = +0.1^\circ\text{C}$  and 28 [27, 29] years for  $\Delta T = +1.0^\circ\text{C}$ . Thus, by choosing only larger glaciers, less variations in the response time occur for different  $\Delta T$ .

The ratio of length to volume response time increases with larger  $\Delta T$  (Fig. 4.11 b). While the median ratio of Alpine glaciers is 1.33 [1.32, 1.34] for  $\Delta T = +0.1^\circ\text{C}$ , it is 2.09 [2.07, 2.10] for  $\Delta T = +1.0^\circ\text{C}$ . When looking only at the 1092 glaciers that still exist for  $\Delta T = +1^\circ\text{C}$ , the length response time is closer to the volume response time. This rather longer length response time compared to the volume response time was also found in the idealised experiments of Ch. 4.1 and in the temporal response time evolution of Hintereisferner (Ch. 4.2.2). It is discussed in Ch. 5.3 together with a comparison to the asymptotic approach.

### 4.3.2 K-Means clustering for changes in the response time between the different temperature perturbations

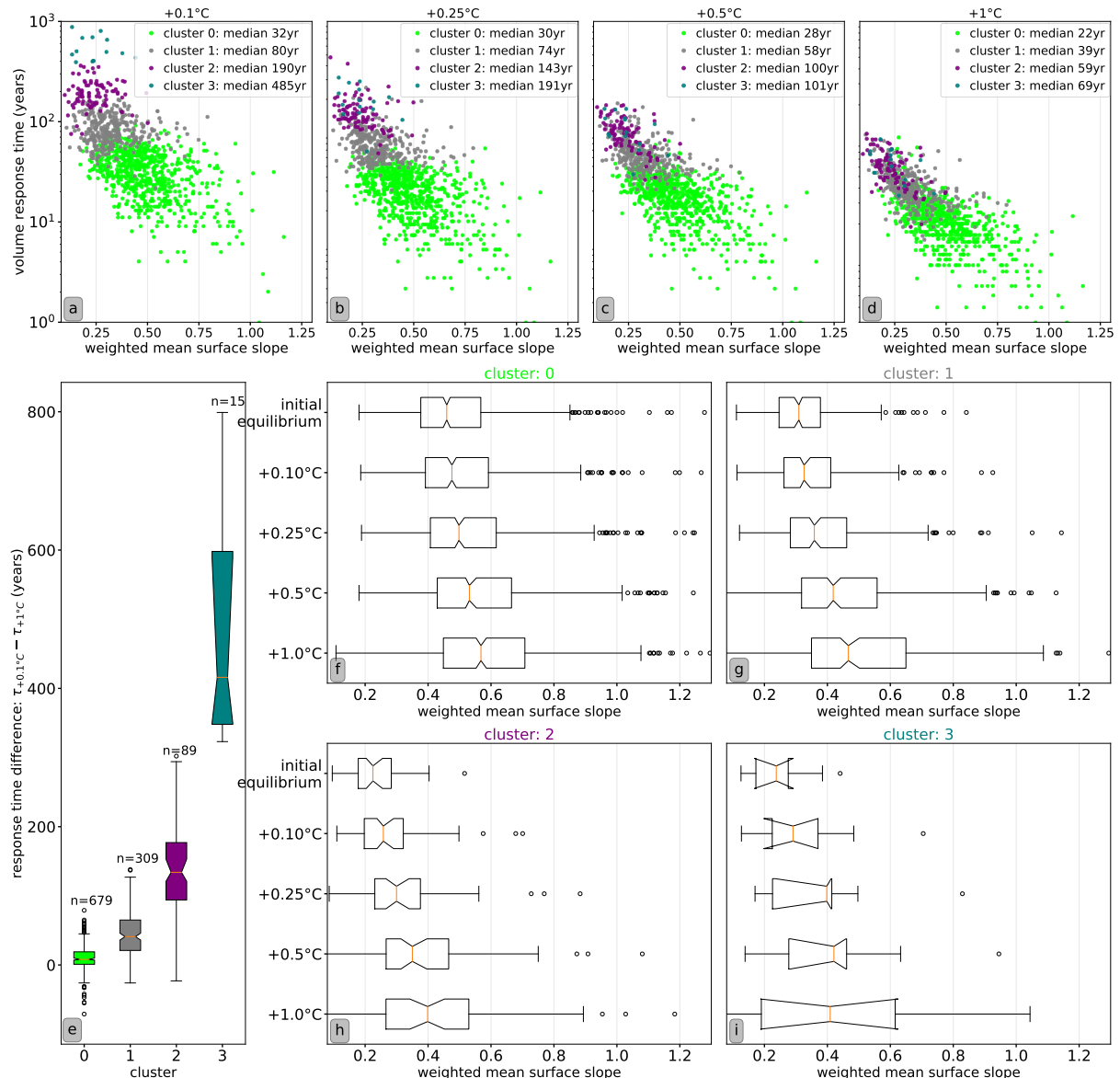


**Fig. 4.12:** K-Means clustering of 1092 Alpine glaciers that are above a length of 100 m in the perturbed equilibrium state of the largest step change temperature increase ( $\Delta T = +1^\circ\text{C}$ ). Glaciers are grouped in four clusters of 679, 309, 89, and 15 glaciers after their behavior in the change of response time with different  $\Delta T$ . In (a-d), response time for different  $\Delta T$  is shown for each glacier color-coded with the respective cluster. In (e), response time differences between lowest and highest  $\Delta T$  are plotted for each cluster. In (f-i), the distribution of the initial and the perturbed equilibrium state glaciers' mean area-weighted surface slope is shown for each cluster. The volume of those 1092 glaciers is 92% of the total Alpine glacier volume with cluster 0 corresponding to 34%, cluster 1 to 42%, cluster 2 to 14% and cluster 3 to 2% of the total Alpine glacier volume.

Some glaciers seem to respond much faster for a higher temperature perturbation. Therefore, it is interesting to classify glaciers into groups that show a similar behaviour. For this purpose the K-means clustering algorithm (e.g. Wilks, 2011), was used, which clusters data in this case after similarities of response time changes in between the four different temperature perturbations ( $\Delta T$ ). For a better analysis of the geometric properties (e.g. surface slope) of the perturbed equilibrium state glaciers, only those glaciers that are above 100 m in the perturbed equilibrium

for  $\Delta T=+1.0^\circ\text{C}$  were chosen, which corresponds to 1092 glaciers and 92% of the total Alpine glacier volume (in the initial equilibrium). A data array of 4 values from the different  $\Delta T$  for each of the 1092 glaciers was fed into the algorithm by using the python-package *sklearn* (Pedregosa *et al.*, 2011).

Most of the glaciers are in cluster 0 with 679 of 1092 glaciers and they differ only weakly between the response time estimates of different  $\Delta T$ : in cluster 0, the median response time decreases from 31 years for  $\Delta T=+0.1^\circ\text{C}$  to 22 years for  $\Delta T=+1.0^\circ\text{C}$  (Fig. 4.12 a-d). Glaciers that are in the other clusters have much longer response times for lower  $\Delta T$ , especially those 15 glaciers from cluster 3, with a median response time difference of 416 [346, 589] years between lowest and highest  $\Delta T$  (Fig. 4.12 e). Those glaciers that had very long response times for low  $\Delta T$  have the largest decrease in the response time for high  $\Delta T$  (compare cluster 3 in Fig. 4.12 a-d), but their initial volume corresponds only to 2% of the total Alpine glacier volume.

Overall, the response time decreases with stronger applied perturbations for 85% of those 1092 Alpine glaciers. When we look at mean surface slope changes between glaciers of the initial equilibrium state and the different perturbed equilibrium states, a clear trend of increasing surface slope for higher  $\Delta T$  is visible for all clusters (Fig. 4.12 f-i). Looking only at the initial equilibrium state slopes (see Fig. 4.13 o), rather shorter response times are associated for glaciers with steeper slopes. Hence, as most individual glaciers are steeper in their perturbed equilibrium state for a higher  $\Delta T$ , the steeper perturbed glacier might be the explanation for a shorter response time of a glacier if a higher  $\Delta T$  is applied. This was also found for those idealised glacier experiments that were built with a steeper upper part (Ch. 4.1.4) and for the Hintereisferner (Ch. 4.2) that is flatter at its tongue.

With this in mind, a possible explanation why some glaciers have very different response times for different perturbations could be the hypothesis that those glaciers have also very different mean slopes comparing perturbed equilibrium states of low to high perturbations. To support or oppose this hypothesis the distribution of mean surface slopes for the different perturbed equilibrium states and each cluster are analysed in the following (Fig. 4.12 f-i).

The cluster with minor changes in the response time between the perturbations, cluster 0, has already rather high mean surface slope ratios in the initial state with in median 0.46 [0.45, 0.47]. For the perturbed state, this increases to 0.47 [0.47, 0.49] for  $\Delta T=+0.1^\circ\text{C}$  and to 0.57 [0.55, 0.59] for  $\Delta T=+1.0^\circ\text{C}$  (Fig. 4.12 f). The glaciers of e.g. cluster 2 are in their initial equilibrium much flatter with in median 0.22 [0.20, 0.24] as surface slope ratios. In the perturbed state, this increases to 0.25 [0.23, 0.29] for  $\Delta T=+0.1^\circ\text{C}$  and to 0.39 [0.34, 0.43] for  $\Delta T=+1.0^\circ\text{C}$  (Fig. 4.12 h). Both clusters, 0 and 2, have therefore a comparative amount of slope ratio difference between low and high perturbation. Hence, the net slope change does not explain directly the behaviour of the different glaciers' response time changes with  $\Delta T$  of the two clusters.

However, the response time seems to decrease not linearly but rather hyperbolic ( $\frac{1}{x}$ ) or logarithmic with respect to the slope (see Fig. 4.13o in the case of initial equilibrium slopes). Thus, the same amount of slope increase on a flat glacier decreases stronger the response time than on a already steep glacier. Consequently, a change of the perturbed slope ratio between  $\Delta T=+0.1^\circ\text{C}$  and  $\Delta T=+1.0^\circ\text{C}$  for initially flatter glaciers, as e.g. those of cluster 2, might have also a larger impact on the response time compared to those in cluster 0 that are already steep in their initial equilibrium state.

To conclude, different changes of the surface slope between the initial and perturbed glaciers might explain the different behaviour of glaciers when they are exposed to distinct perturbations.

Applying higher positive temperature perturbations causes not only the glaciers to be steeper in their perturbed equilibrium state but is also related to a higher mass balance gradient. In the case of those 1092 Alpine glaciers, the median mass balance gradient of  $4.88 \text{ mm w.e. yr}^{-1} \text{ m}^{-1}$  in the initial equilibrium increases to  $4.9 \text{ mm w.e. yr}^{-1} \text{ m}^{-1}$  for  $\Delta T=+0.1^\circ\text{C}$  and to  $5.1 \text{ mm w.e. yr}^{-1} \text{ m}^{-1}$  for  $\Delta T=+1.0^\circ\text{C}$ . An increase in the mass balance gradient generally decreases the response time

of a glacier, e.g. found for idealised glaciers in Fig. 4.2.

Therefore, it might be that both, steeper glaciers and higher mass balance gradients of the perturbed equilibrium states for larger  $\Delta T$ , are generally associated with glaciers that have shorter response times for larger applied positive temperature perturbations.

To see what kind of glaciers are in which cluster some example glaciers are named below with their change in response time between  $\Delta T=+0.1^\circ\text{C}$  and  $\Delta T=+1.0^\circ\text{C}$ . In cluster 0, one of the more well known glaciers is the Belvédère glacier in the Piedmont, Italy ( $\tau_{+0.1^\circ\text{C}}=41$  years,  $\tau_{+1^\circ\text{C}}=30$  years). In cluster 1 there are e.g. the Hintereisferner ( $\tau_{+0.1^\circ\text{C}}=78$  years,  $\tau_{+1^\circ\text{C}}=52$  years) and the Vernagtferner ( $\tau_{+0.1^\circ\text{C}}=87$  years,  $\tau_{+1^\circ\text{C}}=112$  years) inside, an example glacier of cluster 2 is the Kesselwandferner ( $\tau_{+0.1^\circ\text{C}}=163$  years,  $\tau_{+1^\circ\text{C}}=60$  years), all from the Ötztal Alps, Austria.

The Vernagtferner is one of the few glaciers with a rather increasing response time for larger perturbations. Although the mean slope,  $s$ , of the perturbed equilibrium state of Vernagtferner increases slightly for higher perturbations ( $\Delta T=+0.1^\circ\text{C}$ :  $s=0.11$ ,  $\Delta T=+1^\circ\text{C}$ :  $s=0.23$ ), the slope of the lowest 40% of elevation of the glacier decreases for higher perturbations ( $\Delta T=+0.1^\circ\text{C}$ :  $s_{40\%}=0.18$ ,  $\Delta T=+1^\circ\text{C}$ :  $s_{40\%}=0.13$ ). The overall small slope and the decrease in the lower part might be a signal why the response time of the Vernagtferner becomes longer for higher  $\Delta T$ . A bedrock depression, which was analysed in the idealised experiments in Fig. 4.5 B.1, B.2 and Fig. 4.6, could be the cause. Possibly the initial equilibrium state of Vernagtferner does melt only then into such a bedrock depression when the largest temperature increase is applied, which would explain the longer response time for  $\Delta T=+1^\circ\text{C}$ , and would be in accordance with the flat slope of the lowest 40% of elevation of the glacier. However, this is only a speculation and was not further analysed.

A possibility to improve the clustering would be to manually distinguish between glaciers that have shorter response times for increasing perturbations and those that have longer response times and analyse the differences between those groups.

#### 4.3.3 Most important geometric and climatic parameters that control the response time and a rough predictive model

We will now focus on the glacier-specific geometric or climatic conditions that control the e-folding volume response time and develop simple predictive response time models distinguishing between the applied climatic perturbations. In this subchapter, we analyse the response time and the initial climatic and geometric characteristics of 3813 out of 3863 Alpine glaciers where a response time was estimated<sup>7</sup>. A selection of different parameters and their relationships is plotted in Fig. 4.13 differing between the two applied perturbations  $\Delta T=+0.25^\circ\text{C}$  and  $\Delta T=+1.0^\circ\text{C}$ . In the same time, we investigate first qualitatively which parameters were most important when using three predictors from a multiple linear regression with a forward selection scheme<sup>8</sup>.

Generally, the effect of glacier size (volume, area and length) on the response time is very weak, which was also found in the idealised experiments (Ch. 4.1.5) and in the Alpine glacier response time estimate of Ze20.

Only for  $\Delta T=+1.0^\circ\text{C}$ , a slight signal of increasing response time for larger glaciers (Fig. 4.13 a) and for glaciers with a larger height difference (Fig. 4.13 f, elevation range) is visible. This is consistent with the signal of glaciers with lower terminus heights having rather longer response times (Fig. 4.13 d). The variable explaining most of the variance for  $\Delta T=+1.0^\circ\text{C}$  is the mean ice thickness of the glacier (Fig. 4.13 g) with a  $R^2$  of 0.47. The three most important parameters in a multiple linear regression are the mean ice thickness (linear relationship), the mass balance gradient in

<sup>7</sup>For some glaciers a response time was computed but some important characteristics could not be estimated, they were too small. Therefore these glaciers were omitted.

<sup>8</sup>Predictors were chosen by the Bayesian Information Criterion (BIC) forward selection scheme (Wilks, 2011).

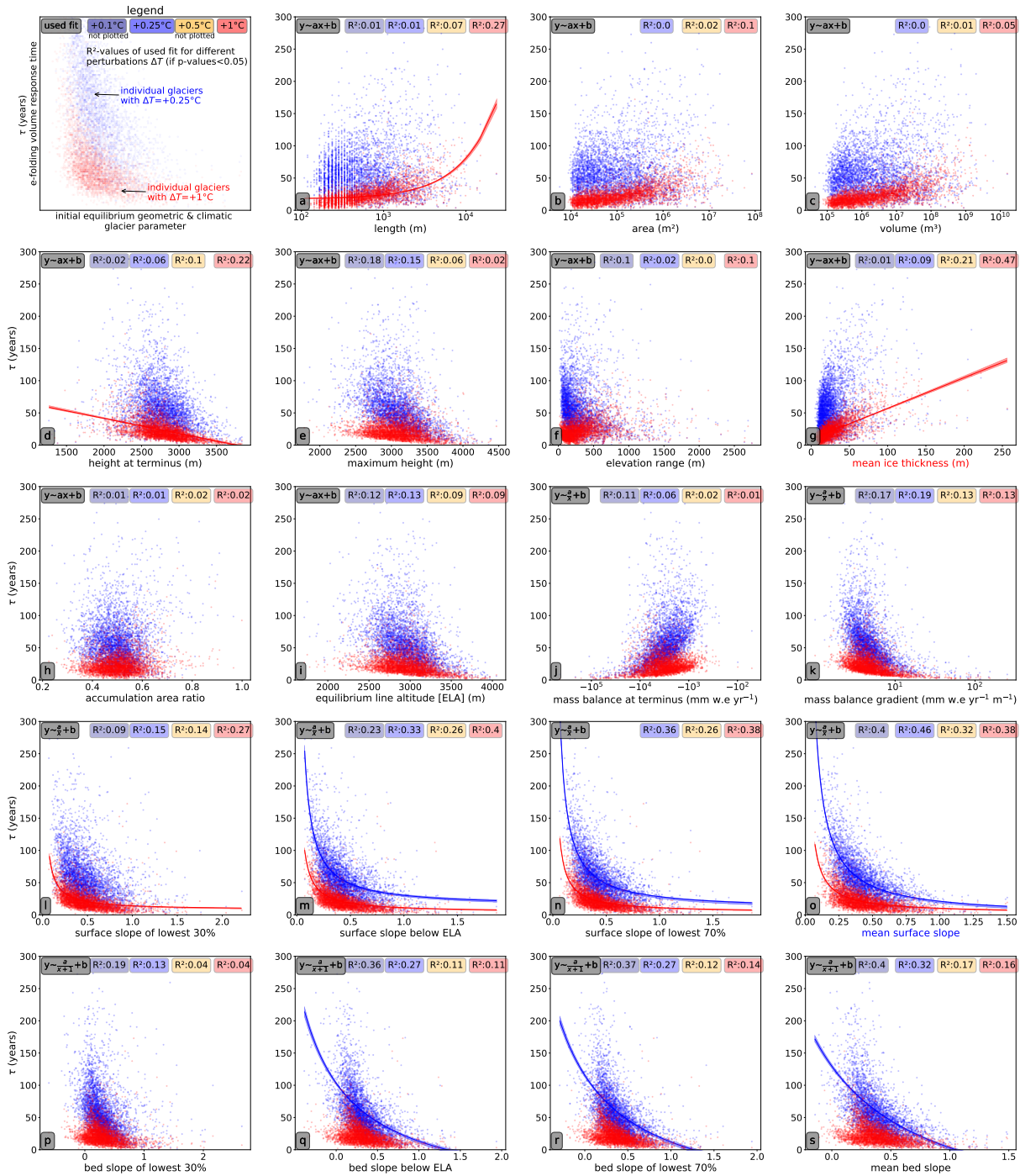


**Fig. 4.13: Relationship between a selection of different initial equilibrium state geometric and climatic parameters of Alpine glaciers and e-folding volume response time  $\tau$ , plotted for two perturbations ( $\Delta T=+0.25^\circ C$  and  $\Delta T=+1.0^\circ C$ ). Parameters are properties of (a-g) glacier size and location, (h) hypsometry, (i-k) surface mass balance, (l-o) area-weighted surface slope ratios, and (p-s) area-weighted bed slope ratios. We applied those fitting formulas that fitted best by visual assessment. Hereby, the noted  $R^2$ -values were computed by the applied fitting formulas. If  $R^2>0.2$  and  $p\text{-values}<0.05$ , the fit is plotted with its 95% confidence interval (only for  $\Delta T=+0.25^\circ C$  and  $\Delta T=+1.0^\circ C$ ). In total, the dots correspond to 3813 glaciers, but only those glaciers with  $\tau<300$  years are shown. The mean area-weighted surface slope (using  $y \sim \frac{a}{x} + b$ ) explains most variance for  $\Delta T=\{+0.1^\circ C, +0.25^\circ C, +0.5^\circ C\}$ . For  $\Delta T=+1^\circ C$ , it is the mean ice thickness (using  $y \sim ax + b$ ).  $a$  and  $b$  are the fitting parameters.**

the ablation area ( $y \sim \frac{1}{x+1}$ ), and the mean area-weighted surface slope ( $y \sim \frac{1}{x}$ ) (Fig. 4.14, legend). These relations are qualitatively in line with the experiments of idealised glaciers (Table 4.2) and

with analytical or scaling approaches: e.g. the ice thickness is also in the numerator of Jo89, the mass balance gradient in the denominator of Lüthi (2009), and the slope in the denominator of Roe and O'Neal (2009) (Table 2.1). The reason why mean ice thickness is controlling response time for high  $\Delta T$  but not for smaller  $\Delta T$  is not clear. A possible indication could be that for small  $\Delta T$ , response time is more variable between glaciers (Fig. 4.11 a). This variance cannot be described well by the mean ice thickness.

A slightly different perspective of the most important predictors is gained when looking at response times applying **temperature perturbations below +1.0°C**. In this case, the most important parameter from the linear regression is the mean area-weighted surface slope when applying a hyperbolic fit of  $\frac{1}{x}$  (Fig. 4.13 o) with a  $R^2=0.4$  for  $\Delta T=+0.1^\circ\text{C}$ , a  $R^2=0.46$  for  $\Delta T=+0.25^\circ\text{C}$ , and a  $R^2=0.32$  for  $\Delta T=+0.5^\circ\text{C}$ . Hence, there is a negative correlation with steeper glaciers having rather a shorter response time. A hyperbolic fit seemed to suit better and might be more appropriate than a linear fit as it does not get negative for the existing mean surface slopes, which would occur in a linear or quadratic fit.

A similar but weaker relationship is visible for the area-weighted bed slope ratios (Fig. 4.13 p-s). For the bed slope, a hyperbolic fit with  $\frac{1}{x+1}$  was used to prevent that  $x$  gets zero or negative, because the bed slope ratios of the different quantiles are  $> -1$  but sometimes  $< 0$ . The area-weighted bed slope ratio is negative for some glaciers indicating that they lie possibly over an entire bedrock depression. When looking at the area-weighted bed slope of the lowest 30% of elevation of each glacier (Fig. 4.13 p), we do not see a direct indication of longer response times for glaciers melting into a bedrock depression (this was found in idealised experiments, Fig. 4.5 B). Still, the trend of increasing response time for smaller bed slope ratios (of lowest 30% or the total mean) is most important for the lowest perturbations  $\Delta T=\{+0.1^\circ\text{C}, +0.25^\circ\text{C}\}$ . As for smaller  $\Delta T$ , a smaller part of the glacier melts, it might make sense that the bed slope of the lowest quantiles of elevation of a glacier explains more variance for smaller  $\Delta T$ .

The parameter that is important throughout all applied perturbations and for all fits is the mass balance gradient of the ablation area (Fig. 4.14, legend). It is the most important climatic parameter that is controlling the response time, as it describes the altitudinal mass balance distribution over a glacier and therefore influences the mass transfer through the glacier. Although the direct correlation between response time and mass balance gradient is rather weak, it seems to be important in combination with e.g. the mean surface slope.

Additional important parameters from the multiple linear regression are the elevation range (logarithmic for  $\Delta T=+0.1^\circ\text{C}$  and  $\frac{1}{x}$  for  $\Delta T=+0.5^\circ\text{C}$ ) and the area-weighted bed slope of the lowest 30% of elevation of a glacier ( $\frac{1}{x+1}$  for  $\Delta T=+0.25^\circ\text{C}$ ). The elevation range depends itself on the glacier length and slope and was also found as an important parameter in the Alpine glacier estimate of Ze20. The area-weighted bed slope of the lowest 30% of elevation of a glacier might describe when a glacier melts into a bedrock depression (see idealised experiments with Fig. 4.5) and could therefore play a role to predict the response time of glaciers.

Besides the multilinear regression, we used a random forest regression<sup>9</sup> with all predictors (56) or only the three or five most important<sup>10</sup> ones. A *random forest* is a non-parametric unbiased recursive partitioning method based on random decision trees and is capable of performing both, regression and classification tasks (Breiman, 2001). There are different implementations of the random forest regression which use other default settings. In the *scikit-learn* package, randomness is incorporated by training each tree in the 'forest' by a random subset of the data points with replacement, i.e., bootstrap aggregating (bagging). This reduces overfitting. The prediction

<sup>9</sup>with the default settings of the python package: *scikit-learn* (v. 0.21.3, Pedregosa et al., 2011), user-guide under <https://scikit-learn.org/stable/modules/ensemble.html#forests-of-randomized-trees> (last access: 29 January 2020), and `n_estimators=1000` (number of trees in the forest)

<sup>10</sup>The feature importance of the used default settings is the mean decrease in impurity, which describes the average relative rank of a feature used as a decision node in a tree and is also called Gini importance.

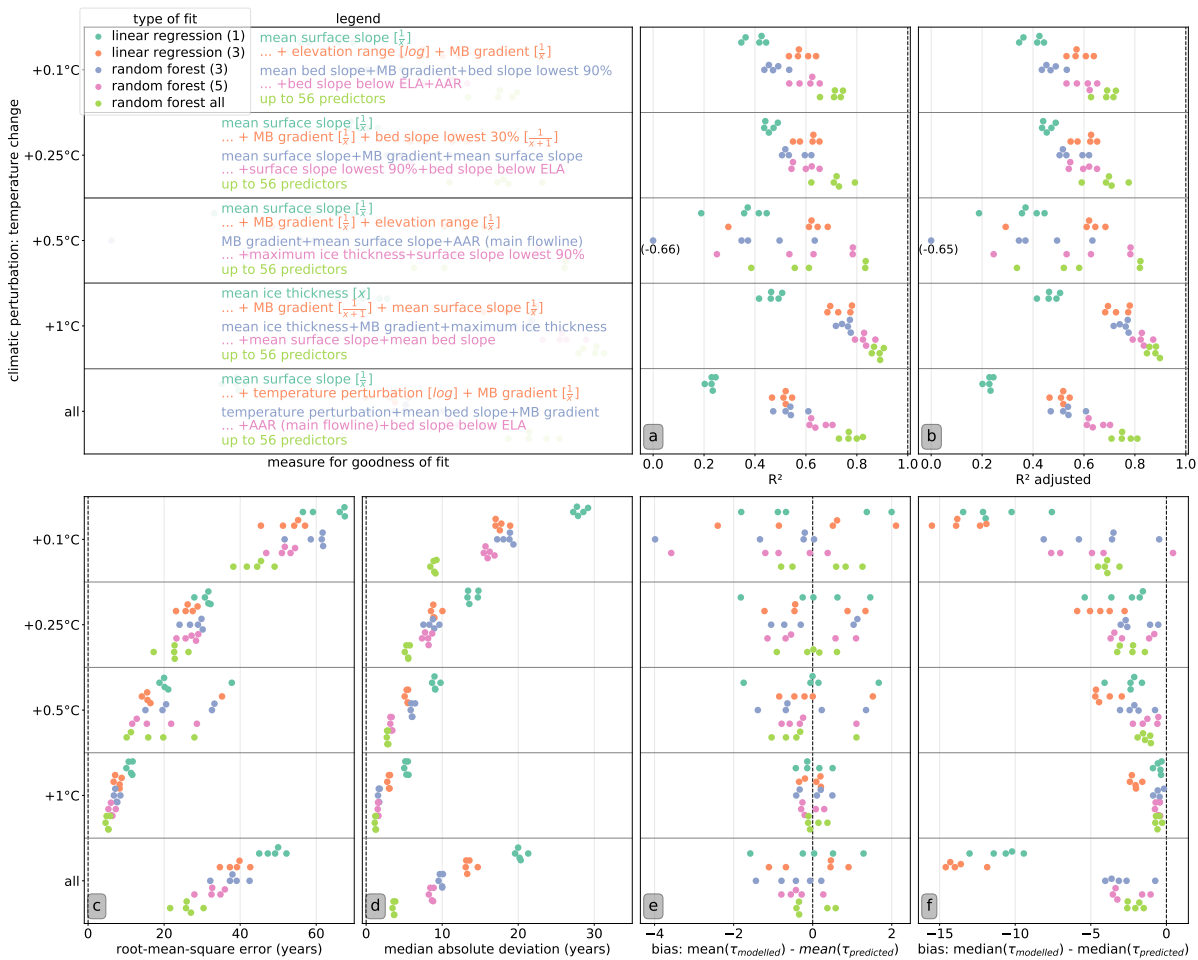


**Fig. 4.14: Cross-validation of the e-folding volume response time predictions for Alpine glaciers with different fits.** Alpine glaciers were separated into five random subsets, using each subset once as test dataset and the remaining 80% as training dataset. The linear regression with the one and three predictor(s) explaining most of the variance (see legend) were used to estimate the goodness of fit for each climatic perturbation separately and all perturbations together. The different applied functions are indicated in the legend as brackets behind the predictors ( $y \sim x$ ,  $y \sim \frac{1}{x}$ ,  $y \sim \frac{1}{x+1}$ ,  $y \sim \log(x)$ ). In addition, random forest regressions were done using the three and five most important predictors (using the Gini importance measure) or up to 56 predictors. In (a-f), the measure of goodness of fit for each dataset (separated by  $\Delta T$  or all together) and fit type is plotted with five dots corresponding to each evaluation of a different subset. The dashed lines indicate the optimal value. All slopes are 'area-weighted' and the mass balance gradient of the ablation area is 'MB gradient'.

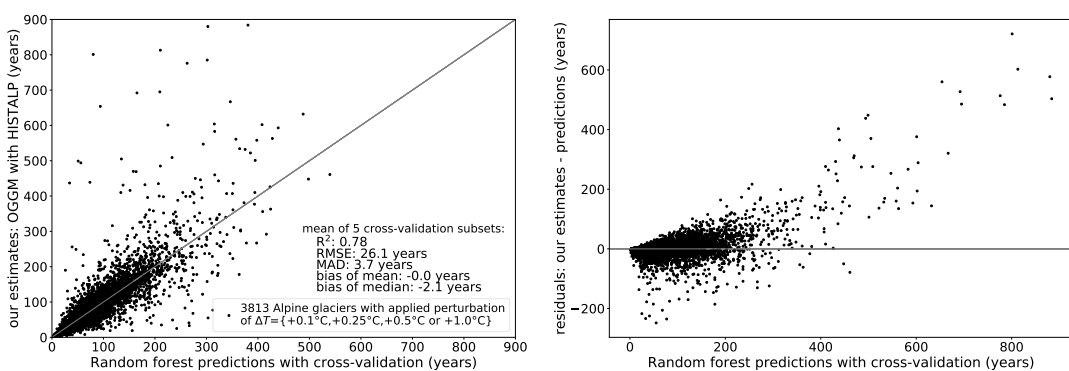


**Fig. 4.15: Scatterplot of random forest regression with up to 56 predictors valid for all four temperature perturbations versus our Alpine response time estimates from the five-fold cross-validation.** The measures of goodness of fit are the mean values from the cross-validation (see Fig. 4.14).

is then a majority vote of all trees (Pedregosa *et al.*, 2011). In our study, the random forest regression is used as a complementary analysis to compare its goodness of fit to the simple estimate of a linear regression with one or three predictors.

In both cases, for (multiple) linear regression and random forest, the quantitative analysis of the goodness of fit (Fig. 4.14 a-f) were obtained by using a five-fold cross validation (Wilks, 2011). Thus, all Alpine glaciers were separated into five randomly chosen subsets. Four of the five subsets are chosen as a training dataset and the remaining last one as the testing dataset. This is repeated five times, in order that each subset is once the testing dataset. Therefore, five different regression equations and goodness of fits were obtained for each of the fitting schemes.

The random forest most important parameters in Fig. 4.14 (legend) are those that were most often chosen as most important. These selected random forest 'most important parameters' should not be interpreted as the only important predictors. We use strongly correlated parameters, e.g. surface slope and bed quantiles. Therefore, any of the correlated parameters might be chosen without a specific preference and the others have automatically a lower importance due to the selected feature importance measure. Consequently, we are not discussing in-depth the chosen most important predictors.

Qualitatively, the mass balance gradient seems to be important for all temperature changes, which was also found with the multilinear regression. For  $\Delta T=+0.1^\circ\text{C}$  three of the five most important parameters of the random forest are bed slope related (mean, of lowest 90% of elevation of glacier and below ELA). This could be an indicator for a possible influence of small-scale changes as bedrock depressions on the response time, that are most sensitive for small perturbations according to the idealised experiments (Fig. 4.5 B).

The parameters controlling most the response time when looking at all perturbations together instead of each separately is a combination of the slope, the temperature perturbation itself and the mass balance gradient (for both multiple linear regression and random forest regression). As analysed already in Ch. 4.3.2, most glaciers have shorter response times for larger temperature perturbations. Hence, it makes sense that the temperature perturbation is an important parameter when looking at all scenarios together, although the physical reason might be the steeper perturbed equilibrium state of a glacier for larger perturbations (Fig. 4.12 f-i).

Using up to 56 predictors and the random forest regression results in the best predictive skill for all measures of goodness of fit on all perturbations separately and all together when applying the cross-validation (Fig. 4.14 a-f). It uses the greatest amount of information, between 20 and 40 predictors contribute to the decision trees. Hence, it is also the most complex model, which can account for nonlinearities and for interactions between the different predictors.

For the random forest regression that uses up to 56 predictors and that is valid for all four applied temperature perturbations, the goodness of fit is also shown visually in the scatterplot of Fig. 4.15. While short response times can be predicted relatively good, response times longer than around 250 years are underestimated by the random forest regression.

Still, the random forest regression with only the five "best" predictors is not much worse than allowing more predictors, at least for larger temperature perturbations (see Fig. 4.14 a-f).

When we compare the different runs of the cross-validation, a large spread between the subsets is visible when looking at the  $R^2$  for  $\Delta T=+0.5^\circ\text{C}$ , especially using only the three "best" predictors of the random forest regression (Fig. 4.14 a). The verification of one subset even produced a negative  $R^2$ , which means that the predictions are worse than using the mean of the test dataset as prediction and indicates an overfitting by noise variables. Due to the even low  $R^2$  for the random forest regression with many predictors for some test subsets with  $\Delta T=+0.5^\circ\text{C}$ , we might conclude that it is more difficult to predict response times for such a perturbation. Possibly it might be necessary to insert other characteristics of the geometry and climate as predictors,

or some more advanced predictive models should be applied. If we repeat this cross-validation many times with different randomly chosen subsets, we could see whether this negative or low  $R^2$  is a fluke due to that specific subset or not.

The  $R^2$  adjusted is the  $R^2$ -value penalizing those models with more predictors (Wilks, 2011). As we are using not more than 56 predictors on a test dataset of around 760 glaciers, no real differences between  $R^2$  and  $R^2$  adjusted are visible (Fig. 4.14 a,b).

Overall it seems that for all goodness-of-fits the predictive models work better for larger perturbations (except  $\Delta T=+0.5^\circ\text{C}$ ). As the used predictors are all geometric or climatic parameters of the initial equilibrium, they characterize best the initial glacier state. Thus, it would make sense if the predictability decreased with higher  $\Delta T$  because they bring glaciers into perturbed states of very different geometry. However, it is the other way round, possibly because variability in the individual glaciers' response time decreases for larger  $\Delta T$  (Fig. 4.11 a).

The root-mean-square error (RMSE) is much larger than the median absolute deviation (MAD) and the decrease of RMSE with higher  $\Delta T$  is also stronger compared to MAD (Fig. 4.14 c,d). This is due to very few glaciers having very long response times for low  $\Delta T$  that could not be predicted well by the models and inflated the RMSE. While the RMSE varies between the chosen cross-validation subsets for  $\Delta T=+0.5^\circ\text{C}$ , the MAD is similar for all subsets. This indicates a poor predictability of the regression models for those glaciers with very long response times for small  $\Delta T$  (see Fig. 4.15).

The differences between modelled (results of the e-folding response time) and predicted mean is around zero (Fig. 4.14 e). However, the median bias is quite negative (Fig. 4.14 f), especially for low  $\Delta T$  and for the multilinear regression. As this simplified regression model minimizes the sum of the squared errors, it gives more weight to outliers, which are glaciers with long response times. Hence, predictions for most glaciers are estimated too long compared to the actually modelled e-folding volume response times. A more robust method against outliers would be to instead use a least absolute deviation regression (see Wilks, 2011).

In addition, the response time distribution is right-skewed, specifically for small  $\Delta T$  (Fig. 4.11 a). Therefore, a more statistically correct way would have been to first transform the data such that they are more normally distributed, i.e. apply a logarithm on the response time. This would also result in strictly only positive predicted response times, which is physically more reasonable. For  $\Delta T=+0.1^\circ\text{C}$ , the applied linear regression without any transformation has no constant variance of the residuals, although this is an assumption to do further statistical analysis (Wilks, 2011). For example, the residual variance depends on the slope of the glacier, if the slope is used as predictor for  $\Delta T=+0.1^\circ\text{C}$ : For flat glaciers, the actual response time differs largely from glacier to glacier and hence from the predicted value as well, while for steeper glaciers there is much less variance in the residuals (not plotted). Furthermore, multiple regressors are not linearly independent and some, e.g. the slopes or different measure of glacier size, correlate strongly between each other.

The random forest regression is non-parametric and by itself more robust as it does not need any assumption of a distribution (Pedregosa *et al.*, 2011), which is one of the reasons why the random forest regression has a smaller median bias.

To conclude, the regression parameters and variables depend on the applied temperature perturbation with the area-weighted surface slope being most important for smaller  $\Delta T$  ( $\leq +0.5^\circ\text{C}$ ) and the mean ice thickness for the largest  $\Delta T$  ( $= 1.0^\circ\text{C}$ ). It might be more practicable to develop a prediction model that includes the applied temperature perturbations, which seems to work quite well, when using a random forest regression (see Fig. 4.15). The factors that control the response time most are, in this case, the applied temperature perturbation itself, a slope parameter, and the mass balance gradient.

A possibility to improve the model would be to add additional geometric characteristics of

the perturbed equilibrium glacier. However, we normally do not know any characteristics of the perturbed glacier. Therefore, the applied  $\Delta T$  is the only parameter that describes how strongly the glacier changes under that climatic step change. In addition, the slope quantiles of the highest 20/30/40/50% of elevation of the initial glacier could be used in the prediction models because they represent better the integrative changing shape from the initial to the perturbed glacier.

Further improvements could be done by the choice of the regression model and its settings. The applied setup for the random forest regression could be tuned by changing the default parameters of the *scikit-learn* package. Moreover, a more robust variable importance measure could be applied. The variable importance measure that has been used here (the default one of *scikit-learn*) is the Gini importance. It is not reliable when potential predictor variables vary in their scale of measurement or their number of categories (Strobl *et al.*, 2007). A permutation feature importance or a drop column feature importance measure could solve this issue. However, it comes with a high computational cost, as the model has to be retrained after dropping each feature one after the other, and it overestimates severely the importance of correlated predictor variables (Strobl *et al.*, 2009). The possibly best way would be to use the R package *party* with the random forest implementation *cforest* that is based on unbiased trees, despite the high computational cost. With that implementation, it is possible to compute a conditional variable importance that correctly deals with correlated parameters, as we have them in our study (Strobl *et al.*, 2008).

Other methods as general additive models where the impact of the predictive variables is described by possibly non-linear smooth functions and additional interactions between the variables could be applied as well to get a better prediction.

Consequently, this first attempt was a short outlook of the general relationships and to seek out possibilities for future studies as well as to identify limitations of predicting response time. As there are a lot of uncertainties in the estimation of the response time itself, e.g. the geometric and climatic input, and obscurities in its definition and use, further discussed in Ch. 5, it does not make sense to propose at this stage a perfect model which would suffer from these ambiguities.

## 5 General discussion

An in-depth comparison to the other existing Alpine glacier response time estimate of Ze20 is done (Ch. 5.1) and to other literature in general (Ch. 5.2). In addition, the differences of the e-folding volume response time to the e-folding length response time and to the asymptotic approach are analysed (Ch. 5.3). Moreover, uncertainties, limitations and possible improvements are presented (Ch. 5.4).

### 5.1 In-depth comparison to Ze20

In Ze20, the first response time inventory of Alpine glaciers with a physically-based model has been derived. Therefore, it is of specific interest to investigate similarities and differences between that study and our results. In Ch. 4.3.1, the total volume response time of Alpine ice masses was already compared to the one of Ze20 and was found to be shorter than the estimates of our study. Discrepancies are expected as the used models, mass balance calibration, climatic input and overall setup of the experiments are very different. In Ze20, response times of only those 792 glaciers that are longer than one kilometre at inventory date (2003) were computed. For a better comparison, we will later use also only transient glacier lengths above one kilometre (after volume inversion), which are in OGGM and with the HISTALP calibrations 947 out of 3863 Alpine glaciers. In addition, in Ze20, the response time and the glacier-specific characteristics are estimated as the mean & median. However in our study, we focus on only shrinking scenarios with perturbations of  $\Delta T=+0.1^{\circ}\text{C}$  to  $\Delta T=+1^{\circ}\text{C}$ . Moreover, we use such an initial climate where glaciers in equilibrium have a similar area as the transient glaciers at RGI inventory date (2003). Thus, directly comparing the estimates between Ze20 and our study is difficult.

In our study, the mean response time for Alpine glaciers above one kilometre averaged over all temperature perturbations is 60 [57, 63] years, with the median being considerably lower with 47 [45, 51] years. As Ze20 used perturbations of  $\Delta T=+0.5^{\circ}\text{C}$  and  $\Delta T=+1.0^{\circ}\text{C}$ , it makes more sense to look at the mean & median of the mean of those two perturbations of our study, which results in a corresponding mean of 46 [44, 47] years and median of 40 [38, 42] years. Hereby, 50% of the glaciers have a response time between 28 and 58 years.

The estimates of Ze20, i.e. average of shrinking & growing experiments, are similar with in mean 50 [48, 52] years and in median 43 [39, 46] years, and with 50 % of the glaciers having a response time between 27 and 70 years. However, when only taking the average of the shrinking glacier experiments of Ze20, the response times are considerably shorter with in mean 32 [30, 33] years, in median 29 [28, 30] years, and 50 % of glaciers between 22 and 38 years (personal communication with Harry Zekollari). Without the influence of growing glacier experiments with typically longer response times, e.g. found in idealised experiments (Fig. 4.3 c1) as well as in Ze20, it makes sense that the average response time of each individual glacier diminishes.

To conclude, the shrinking experiment response time estimates with  $\Delta T=\{+0.5^{\circ}\text{C}, +1^{\circ}\text{C}\}$  of our study using OGGM with the HISTALP climate dataset are rather longer than the respective experiments of Ze20 using GloGEMflow (Zekollari et al., 2019) (Fig. 5.1, left). GloGEMflow takes its climatic input from the ENSEMBLES daily gridded observational dataset (E-OBS vs 17.0 Haylock et al., 2008).

We estimated also the response time of 3804 Alpine glaciers using OGGM and the CRU climate dataset (Harris et al., 2014) with the default calibration parameters (Fig. 5.1, left). The differences in the median response time between the estimates of Ze20 and OGGM CRU or OGGM HISTALP estimates are smaller than those estimates of the same model but different climate datasets (CRU and HISTALP). The median absolute deviation (MAD) and the bias of mean are also larger between the OGGM estimates (Fig. 5.2 a) than between Ze20 and CRU (Fig. 5.2 b) or HISTALP (Fig. 5.2 a). However, our response time estimates (OGGM with HISTALP) are much longer than estimates of Ze20 for some glaciers, which results in a high RMSE between the

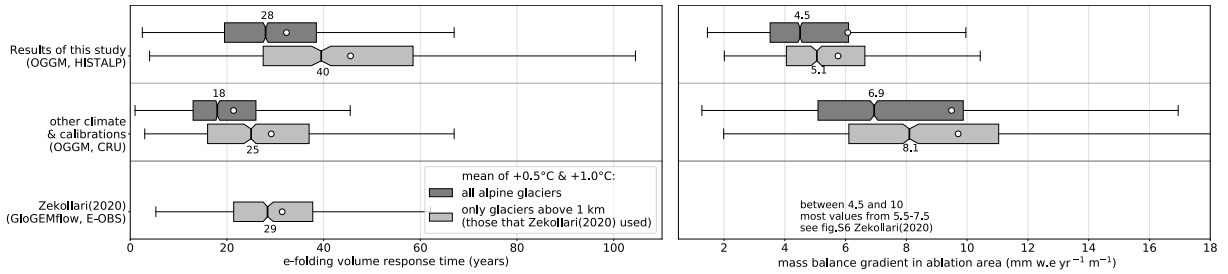


**Fig. 5.1: (left): Comparison of different mean e-folding volume response time estimates of Alpine glaciers with temperature perturbations of  $\Delta T=+0.5^{\circ}\text{C}$  and  $\Delta T=+1^{\circ}\text{C}$  (shrinking scenarios). It is distinguished between (most) Alpine glaciers (HISTALP: 3863, CRU: 3804) or only those 792 glaciers that were used in Ze20 (Zekollari et al., 2020, Alpine transient glacier length  $>1\text{ km}$ ). (right): same for the (ablation) mass balance gradient of the initial equilibrium glaciers.** Discrepancies come from different model setups, input data and calibrations. Numbers indicate the median values and means are plotted as circles. For the response time estimates with the CRU climate dataset the default calibration parameters of  $p_f=2.5$ ,  $T_{\text{melt}}=-1^{\circ}\text{C}$  with  $A=3.6A_0$  for the Alps were used instead of the HISTALP calibration parameters  $p_f=1.75$ ,  $T_{\text{melt}}=-1.75^{\circ}\text{C}$  with  $A=2.2A_0$  (see Eq. 14 and Fig. A.5 for the  $A$ -parameter tuning).

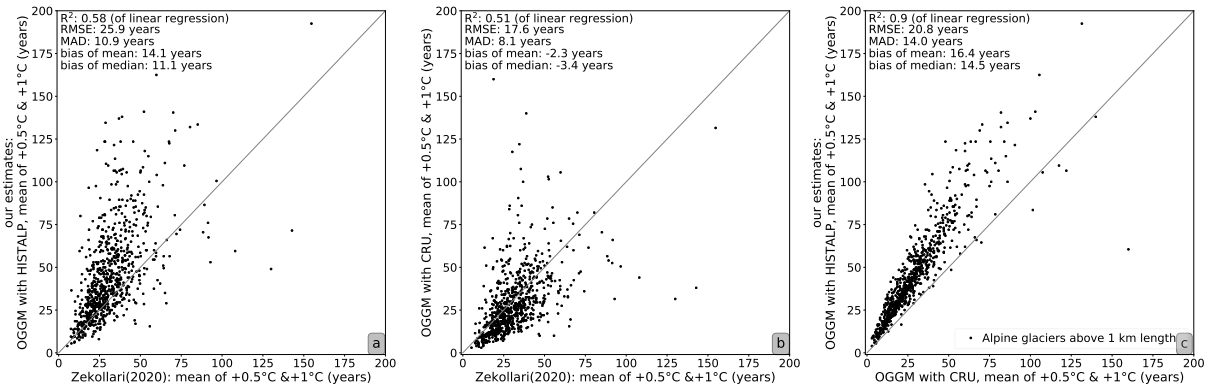


**Fig. 5.2: Comparison of different mean e-folding volume response time estimates of Alpine glaciers above 1 km length (those that Ze20 used).** The same estimates as in Fig. 5.1 are shown. The indicated  $R^2$ -values are the square of the linear Pearson correlation coefficient (Wilks, 2011),  $p\text{-value}<1\text{e}-4$ .

two estimates (see Fig. 5.2 a). Moreover, the spread between the response times of glaciers is larger for OGGM HISTALP estimates than for Ze20 (visible in boxplots of Fig. 5.1 left). In addition, the linear correlation is much better between the two estimates of the OGGM model ( $R^2=0.9$ , Fig. 5.2 c) than those compared to Ze20 ( $R^2<0.6$ , Fig. 5.2 a,b). To conclude, response time estimates differ in median less between Ze20 and OGGM estimates, but they correlate better between OGGM estimates of different climatic datasets (and calibration parameters).

One of the parameters that is significantly different between CRU and HISTALP estimates is the mass balance gradient in the ablation area, which is much larger in the CRU dataset compared to HISTALP (Fig. 5.1, right). This could be a possible explanation for the shorter estimated response times on the CRU dataset, as glaciers with a larger mass balance gradient respond generally faster (see e.g. Table 2.1 or Fig. 4.2). The distribution of the mean (shrinking and growing experiments) mass balance gradient of Ze20 is plotted in Fig. S6 in Ze20 with most values being roughly around  $5.5-7.5\text{ mm w.e. yr}^{-1}\text{ m}^{-1}$ . The rather shorter response time of Ze20 for the shrinking experiments might also come from the rather higher mass balance gradient compared to our results with the HISTALP climate dataset.

Other estimates of the mass balance gradients of all Alpine glaciers are rare. In Raper and Braithwaite (2009), mass balance gradients of Alpine glaciers are around  $4.3\pm0.8\text{ mm w.e. yr}^{-1}\text{ m}^{-1}$  (one standard deviation) when using a degree-day model. In Bach et al. (2018), the mass balance gradient for Central Europe Alpine glaciers was estimated to be  $9\pm2\text{ mm w.e. yr}^{-1}\text{ m}^{-1}$  applying

a multiple linear regression calibrated by observed measurements. The reason why we used the HISTALP dataset for the analysis in the Alps in our study instead of CRU is that HISTALP has a better resolution and exists for a longer time period, which was important for the temporal evolution of the response time on Hintereisferner (Ch. 4.2.2).

Although the discrepancies between Ze20 and our results might arise only from different applied climate datasets, they might also be associated to general differences of the models. In OGGM, multiple connected flowlines are used to compute the depth-integrated flux of ice (Maussion et al., 2019a), while the model which is used in Ze20, GloGEMflow (Zekollari et al., 2019), does not explicitly account for glacier branches and tributaries. In addition, in Ze20, they calibrate their Alpine glacier model with geodetic mass balance estimates where repeated mapping of glacier surface elevations is used to estimate the volume balance (Cogley et al., 2011). Whereas OGGM relies only on direct mass-balance observations as geodetic mass balance estimates are yet not included into the model. Therefore, it is also expected that the ice thickness estimates and with that the bed topographies and the ice-flow dynamic calibrations are different between the models.

An other important aspect is that we used in our study an area-preserving approach, where each transient glacier is individually exposed to such a climate that the equilibrium glacier has a similar area than the transient glacier (Ch. 3.2). In Ze20 however, equilibrium glaciers were formed by exposing them all to the climate of 1972-2001 and 1989-2018 with a negative temperature bias of  $-0.5^{\circ}\text{C}$  or  $-1^{\circ}\text{C}$ . Hence, in Ze20, glaciers might be much larger or much smaller in the initial equilibrium than they are actually in their transient state. Further, their initial equilibrium is different for each scenario but the perturbed state is equal for each scenario. In our study, it is the other way round. To understand the reasons for only model differences, a more in depth-study would be necessary where the setups in the response time estimate and applied datasets are more comparable.

In Ze20, a rule of thumb relationship was introduced to estimate roughly the response time of an (Alpine) glacier using the average surface slope of the lowest 80% of elevation of the glacier and the glacier's elevation range, both from the initial equilibrium state. We applied this relationship to the initial glacier characteristics estimated by OGGM and compared the 'predicted' response times to those obtained numerically with OGGM (Fig. 5.3).

As the rule of thumb of Ze20 was fitted by the average of four shrinking and four growing experiments, it does not include the amount of temperature perturbation that was applied. Using the mean of all perturbations of our study for glaciers above one kilometre length gives a  $R^2$  of 0.33 between the rule of thumb of Ze20 and our study. For the average over all perturbations, the mean estimate from the rule of thumb is near to the mean from our study. However in median, glaciers have 16 years longer response times in OGGM with the HISTALP calibrations compared to the rule of thumb (Fig. 5.3 a). The rule of thumb works worst when comparing it to our estimates with  $\Delta T=+1.0^{\circ}\text{C}$ , where we obtained a negative  $R^2$  and a median bias of -30 years (Fig. 5.3). An undesirable effect of the linear fit is also that some glaciers are predicted to have negative response times.

We did not expect a good fit of the rule of thumb of Ze20 to our estimates for several reasons: The rule of thumb was derived by using another definition, i.e. mean of the shrinking and growing scenarios' response time, than we used. Further, the response time estimates of Ze20 are rather shorter than our estimates, even when only looking at their shrinking experiments with  $\Delta T=\{+0.5^{\circ}\text{C}, +1^{\circ}\text{C}\}$  (Fig. 5.1). Therefore, the rule of thumb works better with their estimates ( $R^2=0.58$  in Ze20).

In addition, the rule of thumb was estimated by using the entire dataset, i.e. all glaciers above one kilometre. With a cross-validation (as done for the estimates of Fig. 4.14), they would have got a smaller  $R^2$ . Hence, the rule of thumb was made to fit to their specific dataset and their

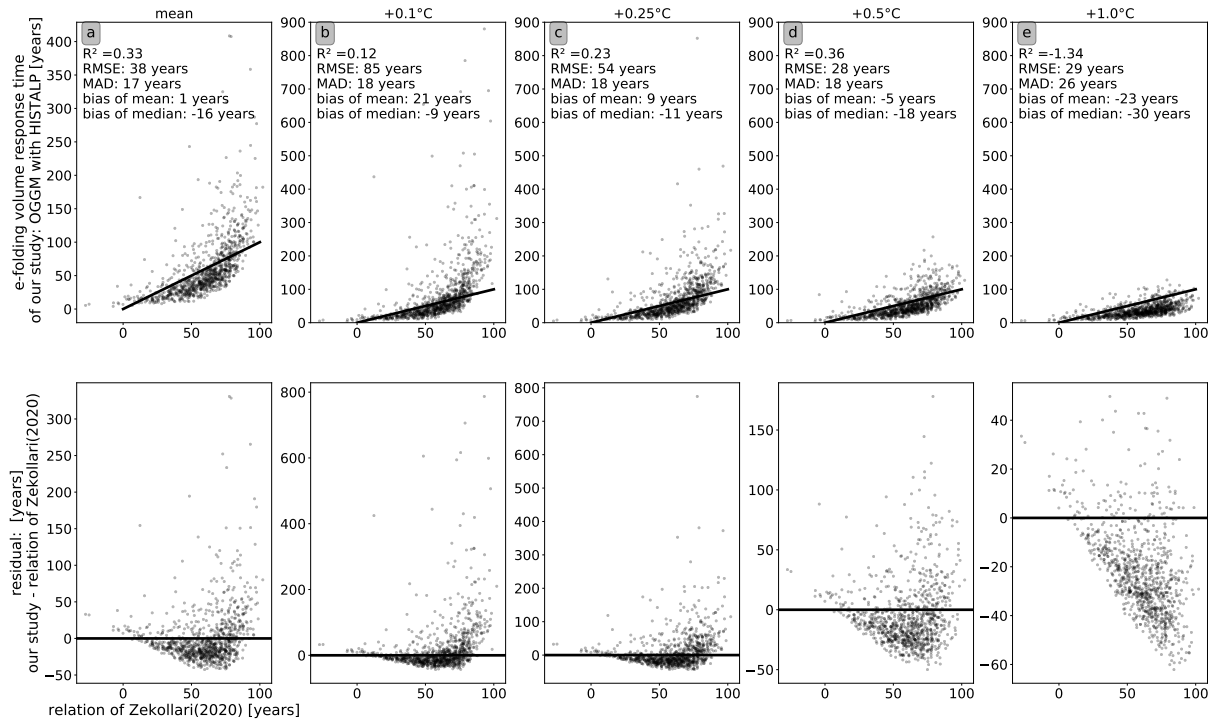


**Fig. 5.3: Comparison of the rule of thumb relation from Ze20 (Zekollari et al., 2020)**

( $\tau = 121 - 1.24 \cdot s_{80\%} - 0.028 \cdot \Delta z$  with  $s_{80\%}$ , average surface slope in % of the lowest 80 % of elevation of the glacier, and  $\Delta z$  (m), the glacier's elevation range), **to the modelled e-folding response time estimates of our study with OGGM (with HISTALP climate)**. To stay consistent with Ze20, only glaciers that are longer than one kilometre (transient glacier length after volume inversion) are used. This corresponds in our study to 947 out of 3863 glaciers. In (a), response time estimates are plotted for each glacier as mean of all four perturbations and in (b-e) for each perturbation separately. Dots that are on the black line correspond to a perfect fit. The  $R^2$  between the modelled values and estimates from the rule of thumb of Ze20 are indicated, together with the root-mean-squared error (RMSE), the median absolute deviation (MAD), and the bias of the mean and median with  $\tau_{\text{our study}} - \tau_{\text{relation of Zekollari(2020)}}$ .

applied definition.

Qualitatively, we can find similarities in the main controlling factors of response time. In Ze20, these are the glacier slope, the elevation range and the mass balance gradient. In our estimates, there is also the glacier slope (here mean area-weighted surface slope) and mass balance gradient important for all applied temperature perturbations (Fig. 4.14, legend). However, the elevation range is only used as predictor in the multilinear fit for  $\Delta T=+0.1^\circ\text{C}$  and  $\Delta T=+0.5^\circ\text{C}$ . While the mean ice thickness does not play any role in Ze20, it seems to be the most controlling factor for our response time estimates with  $\Delta T=+1^\circ\text{C}$ . In both approaches of Alpine glacier response times, there is a weak or nonexistent effect of the glacier area, volume or length on the volume response time. Another similarity is that response time decreases with larger climatic perturbations, although this was not further investigated in Ze20.

Another aspect concerns the definition of response time. It is unclear how to interpret and to apply an average response time of different shrinking and growing scenarios. Therefore, we preferred to analyse response time estimates for each  $\Delta T$  separately.

## 5.2 Comparison to literature and in between the experiments

In this section, our e-folding response time estimates are compared to the literature and in between the experiments. We first discuss the relation of response time to the glacier size (Ch. 5.2.1), to the slope (Ch. 5.2.2, and to the applied climatic perturbation (Ch. 5.2.3). Then,

relations to further variables and to the analytical approach of Jo89 are examined. Further, some real glacier response time estimates of our study are compared to estimates of other studies (Ch. 5.2.5).

### 5.2.1 Relation between glacier size and response time

The size of a glacier (volume, area, length) is not a parameter that can be used to describe differences in the response between glaciers.

In our study with the idealised experiments (Ch. 4.1), the response time decreases for longer glaciers on a constant slope (mainly driven by a larger mass balance at the terminus), while the response time increases for longer glaciers that have a flatter ablation area (mainly driven by the weaker mass flux), see Ch. 4.1.5.

Similarly, no consistent relationship between length and response time could be found for the temporal evolution of response time on the Hintereisferner. While for the strongest perturbations ( $\Delta T$ ), there seems to be an overall trend of decreasing response time for a shorter Hintereisferner, this is not anymore true for smaller  $\Delta T$  (Fig. 4.9).

For all Alpine glaciers, there is also no significant correlation between glacier size and response time visible, except for  $\Delta T=+1^\circ\text{C}$  (Fig. 4.13 a-f). In Ze20, size-related parameters only have an effect on the response time if they are themselves correlated to e.g. the mass balance at the terminus.

In the scaling approach of e.g. Bahr *et al.* (1998) the response time decreases for larger glacier size if the glacier shape and mass balance environment would not change (Table 2.1). However, already Bahr *et al.* (1998) argued that larger glaciers are usually flatter and counteract that effect. In Oerlemans (2012), no obvious relation between glacier length and response time was found as well when they used a scaling approach for length response time on 300 glaciers. The effect of size on response time is therefore described well in Harrison (2013) by 'although the larger of two glaciers on equal slopes will have the shorter response time, it does not follow in general that large glaciers respond faster than small ones, because of the sensitivity to slope'. In Fischer *et al.* (2014), they argue that south-exposed glaciers of the Swiss Alps are generally smaller and thinner. Therefore their response time is shorter, which is not directly visible from the estimates of our study.

In Raper and Braithwaite (2009) and Bach *et al.* (2018), where response times of world-wide glaciers were computed using very simplified block glacier experiments, no overall relationship between volume and response time was found. However, they found a positive correlation for some regions, while there was a negative correlation for other regions. In Raper and Braithwaite (2009), the volume response time increases with area in Axel Heiberg Island and Svalbard, hardly changes in Northern Scandinavia, Southern Norway and in the Alps, and even gets smaller in the Caucasus and in New Zealand. Whether regional differences in the size-response time relationship are visible for world-wide glaciers when using a less simplified numerical flowline model as OGGM should be analysed in a further study.

Consequently, from only comparing the area of different glaciers we cannot deduce which glacier has a longer response time, at least for Alpine glaciers, although this is sometimes incorrectly assumed.

### 5.2.2 Relations of glacier slope and mass balance gradient to the response time

There is a general consensus that both, steeper glaciers and larger mass balance gradients, are associated with shorter response times.

This was found in our study for the idealised experiments (Table 4.2) and for the Alpine glacier estimates (Fig. 4.13), where the mean area-weighted surface slope and the mass balance gradient are among the most important parameters that control the response time for all perturbations.

The rather hyperbolic relation of the response time with the mass balance gradient found in our study (Fig. 4.13 k), is also consistent with the scaling approaches that account for the mass-balance elevation feedback. These are summarized in Table 2.1 [(\*)2] with the mass balance gradient being in the denominator of Bahr *et al.* (1998); Oerlemans (2001); Harrison *et al.* (2001); and Lüthi (2009).

The logarithmic or hyperbolic relation between response time and slope (Fig. 4.13 l-s) is also visible in scatterplots of Haeberli (1995) for the Alpine glaciers' response time (using the formula of Jóhannesson, 1991, Eq. 4), of Bach *et al.* (2018) or Ze20. Similarly, the slope is a direct included parameter in the denominator of the formulas of Bahr *et al.* (1998); Oerlemans (2001); Roe and O'Neal (2009), see Table 2.1.

Therefore, the largest sensitivity of response time on the mass balance gradient (slope) was found for small slopes (mass balance gradients) (Fig. 4.2) which can be explained by the hyperbolic relation of both, the mass balance gradient and the slope. This is also consistent with Harrison *et al.* (2001) where it was mentioned that the mass-balance-elevation feedback is strongest for flat glaciers. To summarise, glaciers that are steeper and have larger mass balance gradients can more efficiently transfer mass and adjust to climatic changes, hence they have shorter response time (Oerlemans, 2012).

The effect of idealised glaciers melting into bedrock depressions and having for this reason longer response times was studied in depth in Ch. 4.1.4 and in Ch. 4.2.1 for very idealised Hintereisferner states with only one flowline, constant width and a linear mass balance.

For Alpine glaciers, an indication for that phenomenon could be that when applying low  $\Delta T$ , bed slope quantiles of the lowest 30% of elevation of the glacier ( $s_{30\%}$ ) explain some variance of response time. Hereby, response time increases for smaller  $s_{30\%}$  (Fig. 4.13 p).

To our knowledge, no other study analysed the possible effect of a bedrock depression on response time of glaciers, thus there is no literature to compare.

### 5.2.3 Relation between applied climatic perturbation and response time

For most of our experiments, applying larger perturbations in terms of  $\Delta \text{ELA} \uparrow \hat{=} \Delta T \uparrow$  results in shorter response times, ideal glaciers (Fig. 4.3 c1), Hintereisferner (Fig. 4.9), and Alpine glaciers (Fig. 4.11 a). This effect was also found in Zekollari and Huybrechts (2015) for the Morteratsch glacier and in Ze20 for Alpine glaciers.

For idealised glaciers on a constant slope, only minor decreases in response time occur for larger perturbations ( $\Delta \text{ELA} \uparrow$ ). These minor decreases are possibly related to short-term more negative mass balances at the terminus of transient glaciers because the ELAs had been raised up suddenly.

Most glaciers are steeper at their upper parts. Therefore, applying larger  $\Delta T$  results in steeper perturbed equilibrium glaciers (Fig. 4.12 f-i), which indicates why response time is generally getting much shorter for larger  $\Delta T$ . Those glaciers that are in their initial equilibrium very flat are most sensitive to  $\Delta T$  changes, as small slope increases on flat glaciers do have a larger impact than on already steep glaciers (Fig. 4.12 f-i).

For growing scenarios, i.e.  $\Delta \text{ELA} < 0$  or  $\Delta T < 0$ , response times are typically longer than for shrinking glaciers. This non-symmetric response to the sign of climatic perturbation was examined in our study for idealised glaciers (Fig. 4.3 c1). In other studies this was also found for real glaciers (see Oerlemans, 2001; Zekollari and Huybrechts, 2015; Zekollari *et al.*, 2020). We did not analyse the growing scenarios' response time further in our real glacier experiments.

Analytical or scaling approaches do not include a term for the magnitude of climatic perturbation and they assume that the perturbation is small enough in order that their equations can be linearised (Ch. 2.2).

How to decide which perturbation to use for numerical estimates might depend on the application. Some few glaciers have extremely long response times for small perturbations in our study, e.g. the 5% glaciers with longest response times have  $\tau \geq 237$  years for  $\Delta T=+0.1^\circ\text{C}$ . This seems to be rather unrealistic and possibly comes from influences on bedrock depressions. Therefore, the perturbation should possibly not be chosen too small. On the other hand, the e-folding response time concept has relied for most studies on the assumption of a small perturbation in order that the volume change can be described by an exponential function (e.g. Oerlemans, 2001; Leysinger Vieli and Gudmundsson, 2004), more in Ch. 5.3.

### 5.2.4 Relations between other variables and response time as well as comparison to Jo89

When applying a perturbation of  $\Delta T=+1^\circ\text{C}$ , the mean ice thickness is an important parameter in our study with a positive (linear) correlation to our Alpine response time estimates. The ice thickness is also in the numerator of analytical or scaling approaches from Jo89; Harrison et al. (2001); Lüthi (2009); Roe and O'Neal (2009); Raper and Braithwaite (2009), see Table 2.1. In Ze20, the mean or maximum ice thickness does not have an effect on the response time. Reasons are possibly that their ice thicknesses and response times are the average of four shrinking and four growing experiments (Ch. 5.1).

The analytical response time approach of Jo89 does not account for the mass-balance-elevation feedback and assumes a simplified geometry, still it can be a good approximation for large  $\Delta T$ .

For the response time evolution of Hintereisferner, it produced similar estimates compared to the numerically e-folding response time if large  $\Delta T$  are applied (Fig. 4.9).

While the approach of Jo89 can represent the qualitative response time trend for ideal glaciers with monotonously changing slopes (Fig. 4.5 A), "peak" response times for glaciers melting into a bedrock depression are not reproduced in the same way as the e-folding estimates (Fig. 4.5 B,C).

For the Alpine response time estimates, the approach of Jo89 is most similar to the e-folding response time for  $\Delta T=+1^\circ\text{C}$  (Fig. 5.4). For large  $\Delta T$ , the irregularities in the bed and the specific

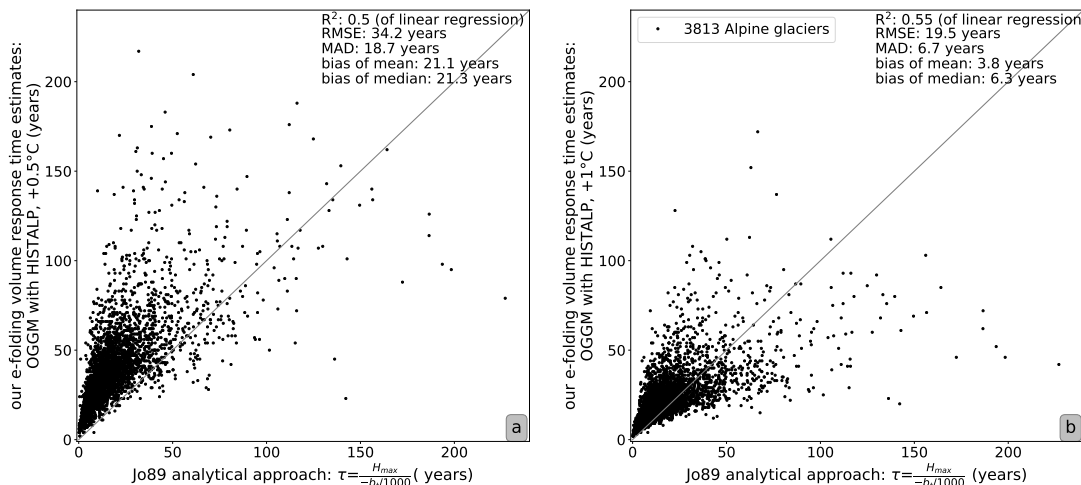


**Fig. 5.4: Scatterplot of Alpine glacier response times: analytical approach of Jo89 (Eq. 4) versus our e-folding estimates of OGGM with the HISTALP climate dataset and applied  $\Delta T$  of (a)  $+0.5^\circ\text{C}$  and (b)  $+1^\circ\text{C}$ . The indicated  $R^2$  are the square of the linear Pearson correlation coefficients (Wilks, 2011),  $p\text{-value} < 10^{-4}$ . The estimates of maximum ice thickness  $H_{max}$  and the mass balance at the terminus  $b_t$  for the Jo89 approach were taken from the initial equilibrium glacier state of the OGGM model.**

The measures of goodness of fit for the mean response time estimates of  $\Delta T=\{+0.5^\circ\text{C}, +1^\circ\text{C}\}$  of only those 792 Alpine glaciers that are above 1 km length of Ze20 are the following (same glaciers as in Fig. 5.2):  $R^2=0.6$ , RMSE= 30.0 years, MAD= 19.0 years, bias of mean= 20.5 years and bias of median= 20.6 years.

geometry of the glacier might be less important. Further, for large  $\Delta T$ , there are less glaciers with anomalously long response times.

However, due to the assumption of linear equations, the approach of Jo89 should, in theory, only be applied to a small perturbation. In practice, for lower  $\Delta T$  the Jo89 approach underestimates the real response time, probably because of the neglected mass-balance-elevation feedback, the assumption that mass balance changes are directly converted to tendencies on the terminus length and the simplified geometry (Ch. 2.2). The anomalously long e-folding response times of some glaciers for small  $\Delta T$  are also possibly related to the glaciers retreating into a bedrock depression, which are not represented right in Jo89 estimates (Fig. 4.5 B.1, Fig. 4.9).

To compare measures of goodness of fit between the analytical Jo89 approach and our estimates (Fig. 5.4) to the relation between Ze20 and our estimates (Fig. 5.2 a), we have to look at the same glaciers and apply the same  $\Delta T$ : the mean e-folding response time estimates of  $\Delta T=\{+0.5^{\circ}\text{C}, +1^{\circ}\text{C}\}$  of those Alpine glaciers that are above 1 km length of Ze20. In this case, the linear correlation coefficient is approximately equal, but RMSE, MAD, bias of mean and median are smaller between Ze20 and our OGGM HISTALP estimates than between Jo89 and our OGGM HISTALP estimates. Therefore, it seems that the discrepancies between e-folding response time estimates of the two studies (Ze20 vs our study) are smaller than those between the analytical approach of Jo89 and our e-folding estimates.

It has to be noted as well that the input for the Jo89 estimate was gained by bringing the glaciers first into equilibrium with the numerical flowline model of OGGM. Therefore, a numerical model is needed in this case anyway.

In Ze20, the difference between maximum and minimum height, the elevation range, is one of the parameters that control the response time. In our study, the elevation range is only for  $\Delta T=+0.1^{\circ}\text{C}$  and  $\Delta T=+0.5^{\circ}\text{C}$  among the three most important parameters of the multilinear fit with a hyperbolic relation of  $\frac{1}{x}$  (Fig. 4.14, legend).

The scaling approach of Lüthi (2009) uses also the elevation range in the denominator. Because the elevation range can be roughly expressed by the length of a glacier and its slope, it is indirectly also in other approaches that are listed in Table 2.1.

As many variables strongly correlate between each other, the multilinear fit only chooses one of a set of possible important predictors and the actual choice has no "physical meaning".

### 5.2.5 Direct comparison of response time estimates of real glaciers from other studies to our study

Apart from the Alpine glacier response time estimates of Ze20, only a handful of other studies computed e-folding volume response times for a few glaciers using a physically based numerical model. Most studies used analytical and scaling response time approaches with very simplified geometries of glaciers. Comparing estimates of response time of individual glaciers between studies is delicate, due to other applied definitions, assumptions, model setups and climatic perturbations. Still, a short juxtaposition is presented in the following.

Our Hintereisferner experiment with a glacier-specific calibration and a length-preserving approach gave response times between 105 and 65 years (over the entire period 1862–2003 and for  $\Delta T=\{+0.1^{\circ}\text{C}, \dots, +0.59^{\circ}\text{C}\}$ , Ch. 4.2.2). Whereas the bulk approach for all Alpine glaciers with the area-preserving approach gave a Hintereisferner response time of 78 to 52 years for  $\Delta T=\{+0.1^{\circ}\text{C}, \dots, +1^{\circ}\text{C}\}$  (Ch. 4.3). Discrepancies might come from the different calibrated mass-balance parameters (Ch. 3.1), from the different methods to get the glacier into equilibrium with a similar state as the transient glacier (Ch. 3.2), and from a changing response time over the studied period (Ch. 4.2.2).

The response time for Hintereisferner of Ze20 as an average of four shrinking and four growing scenarios is 51.4 years, while their respective average of only  $\Delta T=\{+0.5^{\circ}\text{C}, +1^{\circ}\text{C}\}$  is 50.3 years (personal communication with Harry Zekollari). These estimates are similar to the bulk approach of our study for large  $\Delta T$ .

In Haeberli (1995), the response time of Hintereisferner was estimated with the analytical approach of Jo89 to be around 80 years for the period 1920–1980. Applying the estimate of Jo89 on our equilibrium Hintereisferner states gives response times of in mean 70 years during the same period (Fig. 4.9). The estimates of Oerlemans (2012) that used an optimization procedure with glacier length records (2000–2005) got a response time estimate of 31 years for Hintereisferner. It is unclear, whether this is a length or volume response time scale. In any case, it is much shorter than what our study found.

With the same method, Oerlemans (2012) found a response time of only two years for the Kesselwandferner which is just located nearby the Hintereisferner. Although both glaciers have comparable mean slopes, their hypsometry and slope changes with altitude are different. The "Kesselwandferner has a relatively flat and wide accumulation area, but a steep and narrow tongue" (Oerlemans, 2012), compared to the flat tongue of Hintereisferner (Greuell, 1992). Conversely, in our study, the response time of Kesselwandferner is longer with 163 years for  $\Delta T=+0.1^{\circ}\text{C}$  and 60 years for  $\Delta T=+1^{\circ}\text{C}$  than of Hintereisferner. In the numerical estimate of Ze20, the mean response time of the shrinking Kesselwandferner scenario is 54 years and therefore similar to the mean of the shrinking Hintereisferner scenarios.

A scaling approach of Haeberli and Hoelzle (1995) that applied Eq. 4 of Jo89 estimated response times of a few decades (mostly 30–60 years) for Alpine glaciers that are longer than two kilometres. The scaling approach of Raper and Braithwaite (2009) got mean Alpine glacier response times of 73 years, whereas the respective estimates of Bach *et al.* (2018) are around 28 years. In our study using the OGGM HISTALP climate, the mean e-folding response time estimates over all Alpine glaciers and all four shrinking scenarios is 55 years, and a similar estimate with OGGM but the CRU climate gives 28 years. The corresponding only mean of shrinking scenarios in Ze20 is 32 years (Ch. 5.1).

Hence, response time estimates are very sensitive to the chosen definition, mass-balance dependent parameters, models and applied climatic perturbations. Consequently comparisons of absolute numbers between different studies is difficult or even impossible. Overall, we conclude that there exists no single response time for an individual glacier, as described in Benn and Evans (2014), and that the concept of response time should rather be applied only as a relative measure to compare the behaviour of different glaciers within one simulation and one dataset.

### **5.3 Volume against length e-folding response time and e-folding against asymptotic approach**

So far, we mostly analysed the e-folding volume response time. Here, it is compared to other approaches: to the e-folding length (Ch. 5.3.1), to the asymptotic volume (Ch. 5.3.2), and to the asymptotic length (Ch. 5.3.3) response time.

#### **5.3.1 Comparison between e-folding volume and length response time**

In our study, length response times are usually longer than volume response times for all experiments and climatic perturbations, especially if  $\Delta T>0.1^{\circ}\text{C}$ . In the idealised experiments, the ratio is in the mean around  $\tau_L/\tau_V=1.55$  with no clear dependency on the mass balance gradient (Fig. 4.2, right) and for flatter glaciers the ratio  $\tau_L/\tau_V$  is smaller (Fig. 4.3). In comparison, a ratio of  $\tau_L/\tau_V \sim 1.46$  was found with the numerical shallow-ice approximation glacier block experiments of Leysinger Vieli and Gudmundsson (2004) for retreating glaciers. Similarly, Zekollari and

Huybrechts (2015) got a ratio of  $\tau_L/\tau_V \sim 1.65$  for a full-Stokes response time estimate of the retreating Morteratsch glacier. In Oerlemans (2001), this effect was explained by the ice volume being more directly affected by mass balance changes than the glacier length. A mass balance change in the accumulation area has to travel first through the glacier before it reaches the terminus. Hence, the glacier length adjusts only after a certain "initial terminus response time scale" Pelt and Hedlund (2001). This delayed response of glacier length is extensively studied in Roe and Baker (2014), where an analytical three-stage model is developed (summary in Fig. 2.1).

The ratio  $\tau_L/\tau_V$  increases if a higher temperature perturbation or a larger ELA increase is applied: for idealised glaciers (Fig. 4.3 c2), for Hintereisferner response time evolution (not plotted,  $\tau_L/\tau_V(+0.1^\circ\text{C})=1.25$  and  $\tau_L/\tau_V(+0.59^\circ\text{C})=1.70$ ) as well as for Alpine glacier estimates (Fig. 4.11 b). Similarly, the total Alpine glacier area response time is 32 ( $\Delta T=+0.1^\circ\text{C}$ ) to 20 ( $\Delta T=+1^\circ\text{C}$ ) years longer than the total Alpine glacier volume response time (Fig. 4.10 b,d).

The ratio is smaller for growing glacier scenarios ( $\Delta \text{ELA} < 0$ ,  $\Delta T < 0$ ) with  $\tau_L/\tau_V \sim 1.3$  in idealised experiments (Fig. 4.3 c2). This was also found in Leysinger Vieli and Gudmundsson (2004),  $\tau_L/\tau_V \sim 1.28$ , and in Zekollari and Huybrechts (2015) for the growing Morteratsch glacier,  $\tau_L/\tau_V \sim 1.29$ .

For all alpine glaciers of our study, the mean difference between length and volume response time does not change much with the perturbation and is 17 years for  $\Delta T=+0.1^\circ\text{C}$  and 21 years for  $\Delta T=+1^\circ\text{C}$ . Hence, the increasing ratio of  $\tau_L/\tau_V$  for  $\Delta T \uparrow$  might mostly be caused by the volume response time getting smaller for  $\Delta T \uparrow$ .

Still, for small  $\Delta T$  and for the 1092 glaciers that still exist in their perturbed equilibrium state even for the highest perturbation, around 25% of the glaciers have similar or even lower length response times compared to volume estimates (Fig. 4.11). Those glaciers might have a specific geometry probably with a very thin tongue, or the estimated length response time is wrong due to the coarse resolution.

For  $\Delta T > 0.1^\circ\text{C}$ , the largest differences between length and volume response time occur for flat glaciers (not plotted). The possible reason is that ice velocities are smallest and thus perturbations need a longer time to reach the terminus.

Length response times of individual glaciers are more "noisy", i.e. visible on the length response time temporal evolution of Hintereisferner (Fig. 4.8). This is due to the numerical model that allows glacier length to change only in steps. The step size of idealised glaciers depends on the resolution and can have slight influences on the length response time (Fig. A.6). In the case of "real" glacier experiments, the resolution is fixed. Hence, for small perturbations, the total length change is only a small amount of gridpoint steps. The length, which corresponds to  $1 - \frac{1}{e}$  of the total length change, is often in between two possible gridpoint lengths. As the modelled glacier length only changes in steps and stays constant in between, it is unclear which year should be assigned as e-folding length response time. In our case we used the minimum year where the modelled length change was nearest to the e-folding length change. This is a rough approach and rather an underestimate.

A possible solution would be to apply a smoothing function beforehand. If this is not done, the length response times should only be interpreted when a large perturbation is applied. Hence, the problematic of stepwise length changes in numerical models is one of the reasons why a volume response time scale is a more appropriate scale. In addition, it is mostly the aim to find out how fast glacier mass diminishes, which can be better described by the volume than by the length of a glacier.

### 5.3.2 Comparison between e-folding and asymptotic volume response time

In our study, we use the e-folding volume response time, which is the time that an equilibrium glacier takes to adapt to  $1 - \frac{1}{e}$  of the total volume change after a climatic step change (Eq. 9). This time scale was used in all known literature for numerical response time estimates. In Jóhannesson (1997) and Leysinger Vieli and Gudmundsson (2004), the time constant of an exponential fit over the evolving volume change was introduced as an alternative approach (Eq. 8), but it was not further investigated. According to Jóhannesson (1997), both approaches should be applied only if the volume change can be described by an exponential curve. For analytical estimates, this is only valid for small perturbations according to the literature, more in Ch. 2.3. In the numerical estimate of Zekollari and Huybrechts (2015), the volume evolution was roughly exponential when applying large perturbations. Therefore, they used the same definition for smaller and larger perturbations. From the literature, it is however unclear and not indicated how well an exponential function fits to the modelled volume evolution.

In Fig. A.7 a, the scaled modelled volume change of Hintereisferner for the Alpine bulk-approach estimate from the initial ( $\frac{V_0 - V_1}{V_0} = 1$ ) to the perturbed equilibrium ( $\frac{V_1 - V_1}{V_0 - V_1} = 0$ ) and its exponential fits are shown for the different climatic perturbations. This is also presented for an other example glacier, the Vernagtferner (Fig. A.8), and for an idealised glacier with constant slope (Fig. A.2). Only when volume changes are scaled by  $\frac{V - V_1}{V_0 - V_1}$ , their evolution and goodness of fit can be directly compared between climatic perturbations and glaciers. The modelled volume changes slower in the first years and faster later on compared to the exponential fit. This occurs equally for all perturbations that we applied.

A possible measure of fit should not be an absolute value because a total error should be independent of glacier size. Therefore, we scaled here the RMSE and the maximum deviation between fit and modelled evolution by  $\frac{X - V_1}{V_0 - V_1}$ . With this approach, no clear tendency in the goodness of fit for real glaciers is visible. It seems that for all perturbations that we applied, the volume follows roughly similar an exponential evolution. The asymptotic volume response time is for most glaciers shorter than the e-folding estimate because the exponential fit overestimates the glacier changes at the beginning. A fit with more free parameters might explain better the evolution, but this is not subject of our study. The delayed volume changes at the beginning might be caused by the effect that the mass flux has to adjust to the initial small ice thickness changes in order that more volume gets lost (in a shrinking case). This was explained in the case of length changes in Roe and Baker (2014) for an analytical three-stage-model (Fig. 2.1).

In the ideal case, where the volume change fits perfectly to an exponential function, the asymptotic response time would be identical to the e-folding response time. Hence, an indication for a good fit could be if the two approaches are similar, which is analysed in the following.

For the experiments with idealised glaciers and also for the Hintereisferner response time estimates, the fitted exponential time constants are slightly shorter than the volume response time estimates with a mean  $\tau_{V,\text{asymptotic}} / \tau_{V,\text{e-folding}} \sim 0.95$ .

In idealised experiments of constant slope glaciers, it seems that the modelled volume evolution corresponds better to the exponential fit for the largest  $\Delta\text{ELA}$  (Fig. A.2 a). Hereby, the e-folding volume response time decreases slightly with increasing applied  $\Delta\text{ELA}$ , but only for strong perturbations. The volume asymptotic response time though does not change with the perturbation on idealised constant slope glaciers. Therefore, in this case, e-folding and asymptotic response times are most similar for larger perturbations.

However, for idealised glaciers with changing slopes or more "real" estimates the asymptotic response time changes with different perturbations almost identically as the e-folding response time (see e.g. Fig. 4.9 for Hintereisferner). Consequently, the asymptotic response time "constant" is also no constant on a glacier with changing slope if different perturbations are applied.

For all Alpine glaciers, the mean ratio of asymptotic to e-folding volume response time ranges between 0.94 for  $\Delta T=+0.1^\circ\text{C}$  and 0.92 for  $\Delta T=+1^\circ\text{C}$  (Fig. A.6 a). This ratio increases slightly

if only the 1092 glaciers are chosen that still exist in the perturbed glacier state even when  $\Delta T=+1^\circ\text{C}$  is applied. This is an indication that volume decrease can be more described by an exponential decreasing fit for those 1092 glaciers.

Overall, we can say that, for most glaciers independent of our applied climatic perturbation, the asymptotic response time is not much different from the e-folding volume response time. Therefore, we might be able to apply the same method for all applied perturbations in contrast to what the literature says (e.g. Jóhannesson, 1997). Nevertheless, if the assumption of an exponential volume change is valid depends on the scale of goodness of fit and the threshold to use. With this in mind, it seems to be still better to use the e-folding approach than the asymptotic one because the asymptotic approach needs more explicitly an exponential evolution.

### 5.3.3 Comparison between e-folding and asymptotic length response time

After applying a climatic perturbation, volume starts to change directly, but length adjustments only occur after a certain amount of time or very slowly in the first years. Therefore, a sigmoidal fit (Eq. 11) can explain better the length evolution, more in Ch. 2.2 and e.g. in Fig. A.7. Similar to the asymptotic volume response time, an asymptotic length response time can be computed as a combination of two fitting parameters of the sigmoidal function (derived in Eq. 11–13). For the Vernagtferner (Fig. A.8 b), the sigmoidal fit underestimates the initial length which indicates that an other free parameter might be necessary.

Due to the long periods of not changing glacier length in the model (coarse resolution), especially for small perturbations, estimated e-folding and asymptotic length response times are less similar than corresponding volume estimates (Fig. A.6). Hereby, asymptotic length response times are for most glaciers longer than e-folding length response times. This was also found for idealised glaciers with constant slope (Fig. A.2 b), and for the Hintereisferner temporal evolution (Fig. 4.8). For the smallest perturbation ( $\Delta T=+0.1^\circ\text{C}$ ), the ratios between asymptotic and e-folding length response time vary most between individual glaciers and are largest. A possible reason could be that for small  $\Delta T$  only minor glacier length changes of some gridpoints occur. Nevertheless, the newly introduced concept of an asymptotic length response time estimate by a sigmoidal fit could be used as an alternative to the e-folding length response time. However, the e-folding volume response time seems to be the more robust time scale compared to any kind of length response time.

## 5.4 Uncertainties, limitations and possible improvements

There are many uncertainties in the model itself as well as in the applied setup that influence response times of glaciers. Most were already mentioned in the respective chapters. Here, a short summary is given with some thoughts about possible improvements.

1. First of all, OGGM uses a shallow-ice-approximation (SIA) by computing a depth-integrated ice velocity. Hence, it ignores longitudinal and transverse stress gradients. In Leysinger Vieli and Gudmundsson (2004), a comparison of response times between a SIA and a higher-order model, in which the full-stress field is considered, was done for idealised block glaciers. While no differences of e-folding volume response times occurred for a medium to large glacier, for a small glacier the SIA response time was four years shorter. Still, they summarise that the effects of longitudinal stress gradients on the response time are small. In Zekollari and Huybrechts (2015) a higher-order ice flow model was used to estimate the response time of the Morteratsch glacier. They argued that the presence of basal motion leads to differences in response time between SIA models and more complex flow models. However, there is no study that analyses explicitly how response time changes between SIA and higher-order models on real glaciers.

A possible improvement could be to add a lateral drag parametrisation or basal sliding, which is implemented in OGGM (see Ch. 3.1), although those parametrisation have to be calibrated as well.

2. In addition, the default solver in OGGM does not conserve mass for very steep slopes. The "MUSCL superbee" solver of Jarosch *et al.* (2013) is strictly mass-conservative and numerically more robust but it works in OGGM only for non-changing bed shapes with a single flowline. In the idealised Hintereisferner experiment of a constant width, rectangular bed shape and one flowline, the response time estimates of the two solvers only differed slightly for a very long glacier (Fig. 4.6). Therefore, it is assumed that these errors are also small for the other experiments.

An other aspect is possible numerical instability. OGGM relies on an adaptive time stepping scheme that uses the *cfl\_condition* to find an appropriate time step (Ch. 3.1). We used here a low CFL-factor of 0.01 and set the minimum timestep to zero. For those settings, empirical tests did ensure stability, however a full stability analysis has to be done in the future.

3. Using OGGM with the default non-calibrated ice creep parameter  $A$  of Cu10 on all Alpine glaciers yields to a larger ice volume estimate compared to most other estimates. In this study, the  $A$ -parameter is tuned such that it corresponds to the Farinotti *et al.* (2019) Alpine glacier volume (Fig. A.5). Changing the  $A$ -parameter influences the response time because  $A$  is a measure of the stiffness of a glacier, see the sensitivity analysis of  $A$  for idealised experiments of constant slope glaciers (Fig. 4.3 b1).

We set  $A$  constant for all Alpine glaciers, although  $A$  depends on ice temperature. As Alpine glaciers are assumed to be isothermal, no change of  $A$  might occur in a single glacier but certainly between different glaciers. In the case of non-temperate glaciers, which are not analysed in this study, e.g. in Greenland,  $A$  might even change within layers of a single glacier. The highest values of  $A$  are found for non-temperate glaciers in the basal layers where the shear deformation is largest (Cu10). However, this occurs at scales that OGGM is not made for and at some point a global model has to do some compromises. It also has to be noted that OGGM uses  $A$  as calibration parameter to account for missing processes (such as sliding) and for uncertainties in the mass balance gradients.

4. As the ice thickness and the bed profile are unknown, they are computed via a volume inversion process in OGGM. Its calibration and validation is still work in process. The response time can be quite sensitive to bed slope changes, specifically for bedrock depressions. If those bedrock depressions are only an artefact of the model, they might produce a substantial source of uncertainty in the response time. Glacier bed topographies could be smoothed and the resulting response time changes could be analysed to estimate these uncertainties.

Applying only larger perturbations to estimate response times is a possible workaround, because the influence of a small bedrock depression gets less important if a larger part of the glacier melts (Fig. 4.5 B).

5. Moreover, there are large uncertainties in the climate itself and the mass balance calibration that can result in large variations in the Alpine glaciers' response time estimates. Different calibrated precipitation correction factors between e.g. HISTALP and CRU climate change the mass balance gradient of individual glaciers, which is an important controlling parameter for the response time (Fig. 5.1).

The calibration of the mass-balance parameters is in OGGM, however, only based on observational in-situ measurements with the traditional glaciological method provided by the WGMS (2017). Other models such as GloGEMflow of Zekollari *et al.* (2019) (applied for the

first Alpine glacier response time estimate in Ze20) use geodetic mass-balance estimates. A future version of OGGM that incorporates the information from geodetic measurements as well as the recently released ERA-5 land<sup>11</sup> dataset could diminish some uncertainties in the response time.

Other uncertainties in OGGM are discussed in the reference paper Maussion *et al.* (2019a).

6. Limitations of the response time application are given through its static definition that needs an initial glacier in equilibrium and a climatic step change. This is not valid for real-world glaciers, especially in the current age of climate warming. How to best estimate the response time of transient glaciers is therefore a controversial question (Ch. 3.2). Some kind of temperature bias has to be applied to have an initial glacier that has at least approximately a similar shape than the equilibrium glacier. However, the ice thickness distribution with altitude of a stable equilibrium glacier will be always different to a transient real-world glacier. Hence, the response time estimate is biased by its definition.
7. The original definition of an e-folding response time is only valid if the volume decreases in an exponential way. However, as already discussed in Ch. 5.3, it is unclear whether this is still a necessary assumption. The large response time sensitivity to the applied climatic perturbation, see e.g. Fig. 4.11 a, causes trouble when comparing response time estimates that use different perturbations. A redefinition that explicitly mentions the applied perturbation might be therefore reasonable.

In addition, a clear separation between scaling or analytical approaches to numerical approaches and between volume and length response time is important.

8. In this study, we only estimated the response time of glaciers for shrinking experiments with temperature perturbations. In a changing climate, however, other parameters such as the precipitation change as well. A more integrative realistic change of both, temperature and precipitation, might result in different response times.
9. With all these uncertainties and limitations, it was therefore not the aim to produce a perfect predictive model of the response time. The multilinear and random forest regression should be rather interpreted as a simple first estimate of how glacier characteristics control the response time. There are many possibilities to improve the prediction and to make it more robust (discussed in Ch. 4.3.3).

---

<sup>11</sup><https://confluence.ecmwf.int/display/CKB/ERA5-Land%3A+data+documentation> (last access: 14 February 2020)

## 6 Conclusion and Outlook

The aims of this thesis were to identify the strengths and weaknesses of the e-folding glacier response time, to better understand the mechanisms that influence the response time, and to compare the estimates between glaciers, different setups and studies.

All parameters that affect mass transfer in a glacier have an effect on the response time. For idealised experiments and alpine glacier estimates, the response time decreases with increasing slope and mass balance gradient of the initial glacier in a hyperbolic way. This is in line with previous studies. In case of large temperature perturbations on Alpine glaciers ( $\Delta T=+1^{\circ}\text{C}$ ), response time correlates (linearly) with the mean ice thickness of the initial glacier. This exhibits similarities to the analytical approach of Jo89 (Eq. 4) where the ice thickness is also in the numerator. Other driving factors include hypsometry, altitudinal slope changes, and bedrock depressions along the initial glacier. Idealised glaciers that retreat into a bedrock depression have much longer response times, specifically for small applied perturbations. This applies also for the modelled Hintereisferner (1862–2003), where the response time decreases only after an initial increase for small perturbations. Hence, in the case of bedrock depressions, glacier characteristics about the arrival state (perturbed equilibrium) can be more determinant for the response time estimate than those of the initial equilibrium state.

Due to the nature of a static response time definition, the temporally-evolving response time of Hintereisferner should be interpreted as response time changes of equilibrium glaciers with lengths fitting to the observations. Consequently, we cannot draw direct conclusions on how the climate-geometry imbalance has changed in reality.

For the studied set of glaciers, there is no clear relation between size (volume, area, length) and response time, which is in line with most previous studies. Though, scaling approaches of Bach *et al.* (2018) and Lüthi (2009) found correlations of glacier size and response time: dependent on the specific region, these were either positive or negative. A global study with numerical flowline models could further analyse whether such correlations do indeed exist.

For all our experiments with a realistic bed geometry, the response time is very sensitive to the applied temperature perturbation ( $\Delta T$ ). If glaciers are steeper in their upper part, which is the case for most Alpine glaciers, they have mostly shorter response times for larger applied  $\Delta T$ . In the Alps, the response of flat glaciers is most sensitive to  $\Delta T$ , possibly because the response time is more sensitive to perturbed equilibrium slope changes on flat glaciers compared to already relatively steep glaciers. Moreover, response time is less variable between different Alpine glaciers for larger  $\Delta T$ . When applying  $\Delta T=+0.1^{\circ}\text{C}$ , 50% of the 3863 studied glaciers have response times between 42 and 121 years. However, when applying  $\Delta T=+1^{\circ}\text{C}$ , 50% of the glaciers' response time is between 14 and 29 years with the used HISTALP dataset and the mass balance calibration of the OGGM model.

We performed a random forest regression taking initial climatic and geometric characteristics, as well as the applied  $\Delta T$  as predictors. With a five-fold cross-validation on Alpine glaciers, for all four perturbations together, we obtained on average a median absolute deviation of 4 years and a  $R^2$  adjusted of 0.76. Area-weighted surface slope, mass balance gradient, and temperature perturbation itself were among the most important factors that describe the variance in the response time. As long as response time is not arbitrarily defined by a certain  $\Delta T$ , the large dependency on  $\Delta T$  pleads for adding  $\Delta T$  to existing formulas of response time prediction.

E-folding length (and area) response time is longer than volume response time for most glaciers. Length evolution can be described best by a sigmoidal fit and a combination of its fitting constants gives a newly defined asymptotic length response time. However, length response time is less robust, therefore we set the focus in our study to the e-folding volume response time.

On the one hand, if a too small  $\Delta T$  is applied to compute a response time, there might be unwanted influences of bedrock depressions. On the other hand, the original definition of e-folding response time is constrained to only exponential volume changes. In many studies, this was assumed to occur only for a small perturbation ( $\Delta T$ ). Our findings suggest that a single glacier's volume evolution after a sudden climatic step change is approximately exponential for perturbation magnitudes of  $\Delta T = \{+0.1^\circ\text{C}, \dots, +1^\circ\text{C}\}$ . The small discrepancies between e-folding and asymptotic response time scale (i.e. fitting constant of an exponential function of volume evolution), independent of applied  $\Delta T$ , are further evidence for an exponential volume evolution. In addition, it is not strictly necessary to assume that the volume evolution is exponential, given that response time is just a construct to compare the glaciers' response speed. Hence, which  $\Delta T$  should be applied might simply depend on the specific application of response time.

In our study, median discrepancies between Alpine glacier response time estimates of two climate datasets (HISTALP and CRU) with their respective calibration parameters in OGGM are larger than variations to another model used in Ze20. However, the response time estimates using the same model correlate better with each other than with the estimates of Ze20.

To conclude, the response time is not constant for a single glacier. It varies over time and for different applied climatic perturbations (here  $\Delta T$ ), studies, and model calibration. Consequently, we recommend using the response time only as a relative number. The static definition of the response time as a measure of response speed between two equilibrium states is another factor that complicates its interpretation and direct application.

The response time is always going to be a simplification of what complex numerical models are able to predict nowadays. Which insights about glacier and climate change in general can the concept of response time still give us? When being aware of its limitations, the response time can be a simple valuable tool to compare the response of different individual glaciers to a changing climate under "laboratory conditions" and to analyse the controlling geometric and climatic parameters of the glaciers.

It could help to better understand how well glaciers of the past can be reconstructed (see Eis *et al.*, 2019). A starting point could be to study how the correlation between response time and reconstructability changes with different applied perturbations  $\Delta T$  and whether there is an influence of bedrock depressions on the reconstructability of a glacier.

Moreover, many studies used analytical response time estimates to calibrate analytical models and the new insights of this study could improve those models.

The large differences in the mass balance gradient between glacier regions in the world (Raper and Braithwaite, 2009) suggest strong regional discrepancies in the response times. In order to analyse regional differences in the response time and its controlling factors, a next step is to estimate the response time of all glaciers in the world using OGGM. Hereby, relative response time changes with  $\Delta T$  and response time itself could be a feature to cluster worldwide glaciers into similarly behaving groups of response time, e.g. with the K-Means clustering algorithm. These insights could be used to improve the calibration of numerical global mass balance models.

Another future task is to analyse whether response time has a predictive value for other aspects of glaciology such as the current rate of volume change estimated by geodetic methods.

Finally, one of the most important questions is to understand how the current glaciers' response evolves in the future for different climate change scenarios: Which glaciers respond faster or slower as they retreat with the ongoing climate change and what are their regional differences? How does the meltwater of individual glaciers change and affect existing fresh water reservoirs? How fast will future sea-level rise occur? We hope that better comprehension of the theoretical construct of glaciers' response time might help to answer these real-world urgent questions.

## A Appendix

### Abbreviations & Symbols

Table A.1: List of abbreviations

Notation	Description
Cu10	Cuffey and Paterson (2010)
Ho19	Hooke (2019)
Jo89	Jóhannesson <i>et al.</i> (1989)
Ze20	Zekollari <i>et al.</i> (2020)
AAR	Accumulation Area Ratio
CFL	Courant-Friedrichs-Lowy condition
DEM	Digital Elevation Model
ELA	Equilibrium Line Altitude (m)
MAD	Median Absolute Deviation
OGGM	Open Global Glacier Model
RGI	Randolph Glacier Inventory
RMSE	Root-Mean-Square Error
SIA	Shallow Ice Approximation

**Table A.2:** List of often used symbols

Notation	Description
$\tau$	response time (years) if not otherwise stated the e-folding volume response time (Eq. 9)
$A$	ice creep parameter of the Glen's flow law (Eq. 1) default value: $A_0=2.4 \cdot 10^{-24} (\text{s}^{-1} \text{Pa}^{-3})$
$t_{\text{star}}$	glacier-specific mass balance calibration parameter of OGGM, represents center of a 31 year climate period where today's glacier would be approx. in equilibrium (year)
$L, l$	length of the glacier (m or km)
$S_c$	cross-section area of the glacier ( $\text{m}^2$ )
$S_A$	surface area of the glacier ( $\text{m}^2$ or $\text{km}^2$ )
$w$	width of the glacier (m)
$H, h$	ice thickness of the glacier (m) with the maximum height $H_{\max}$ and mean height $\bar{H}$
$V$	volume of the glacier ( $\text{m}^3$ or $\text{km}^3$ )
$B$	net mass balance over entire glacier ( $\text{mm w.e. yr}^{-1} \hat{=} \text{kg m}^{-2} \text{yr}^{-1}$ )
$b_t$	mass balance at the terminus ( $\text{mm w.e. yr}^{-1} \hat{=} \text{kg m}^{-2} \text{yr}^{-1}$ ) (strictly negative for an equilibrium glacier)
$\beta$	mass balance gradient with altitude ( $\text{mm w.e. yr}^{-1} \text{m}^{-1}$ ) of ablation area (real glaciers) or entire area (if a linear mass balance is applied)
$s$	surface slope ratio of altitudinal to horizontal difference (no unit)
$s_{X\%}$	surface slope ratio of the lowest X% of elevation of the glacier (no unit)
$\text{index}_0$	characteristic of the initial equilibrium glacier state
$\text{index}_1$	characteristic of the perturbed equilibrium glacier state (after applying a climatic step change)
$\Delta T$	climatic step change as temperature perturbation ( $^{\circ}\text{C}$ )
$\Delta \text{ELA}$	climatic step change as equilibrium line altitude increase (m)

## A.1 Idealised experiments: resolution sensitivity & asymptotic response times

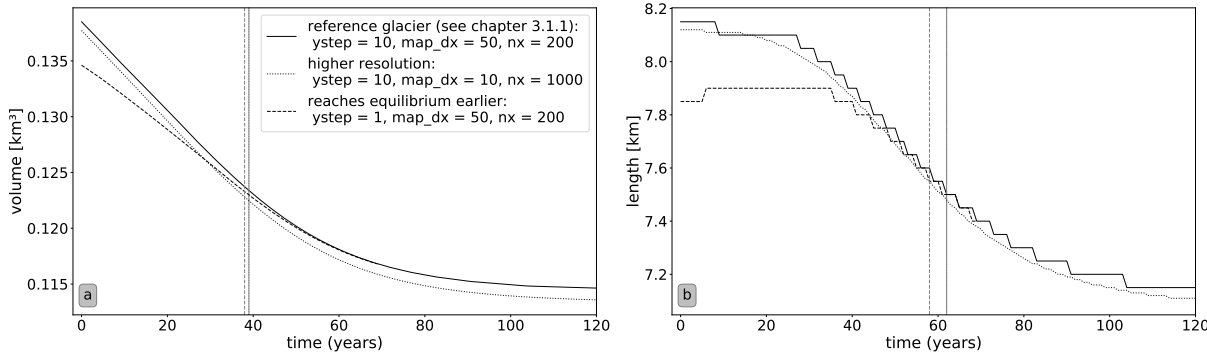


**Fig. A.1:** Differences in the (a) volume and (b) length evolution for different resolutions (*map\_dx*) and for two different *ystep*. *ystep* describes how often to check whether the glacier has reached equilibrium. The corresponding response times are depicted as vertical lines.

From these experiments, it can be seen that, if the model assumes too early that the glacier is in equilibrium, e.g. low *ystep* or high *rate* (in Fig. A.1 kept constant), specifically the length response time can be smaller. This results from the fact that the initial equilibrium volume is too small and the final volume after the perturbation is too high. For steeper glaciers or higher mass balance gradients, this sensitivity is less pronounced.

If the parameter *map\_dx* (metres per grid point) is decreased and *nx* (amount of grid points) is increased (to define the same bed length), the resolution is raised. Hence, a smoother length evolution is simulated. In this experiment, this results in neither volume nor length response time changes. If we would want to analyse the length response time more in detail, a higher resolution might still be necessary, e.g. *map\_dx* = 10 and *nx* = 1000. However for real glaciers we can only take the resolution that we have. Therefore, we used equally for the idealised experiment the more coarse resolution of *map\_dx* = 50 and *nx* = 200, which needs less computational power.

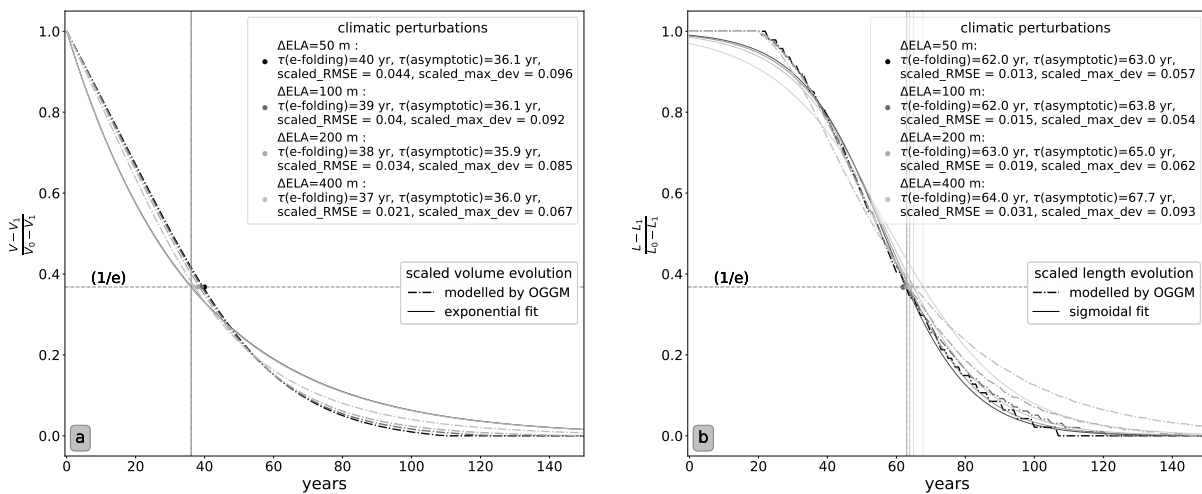


**Fig. A.2:** Idealised glacier of constant slope after raising the ELA by  $\Delta\text{ELA}=\{+50\text{ m}, \dots, +400\text{ m}\}$ : (a) scaled volume,  $V$ , and (b) length,  $L$ , evolution. The corresponding e-folding (see Eq. 9) and asymptotic (see Eq. 8 for volume and Eq. 10 & 13 for length) response times are indicated. The root-mean-square error (RMSE) and the maximum deviation ("fitted"- "modelled" values) are scaled to the volume change by  $\frac{X - X_0}{X_0 - X_1}$  for  $X \in \{V, L\}$ . The index  $_0$  corresponds to the initial equilibrium state and the index  $_1$  to the perturbed equilibrium. The used idealised glacier is the reference glacier described in Ch. 4.1.1.

## A.2 Hintereisferner: applied climate and length-preserving temperature bias (1862–2003)

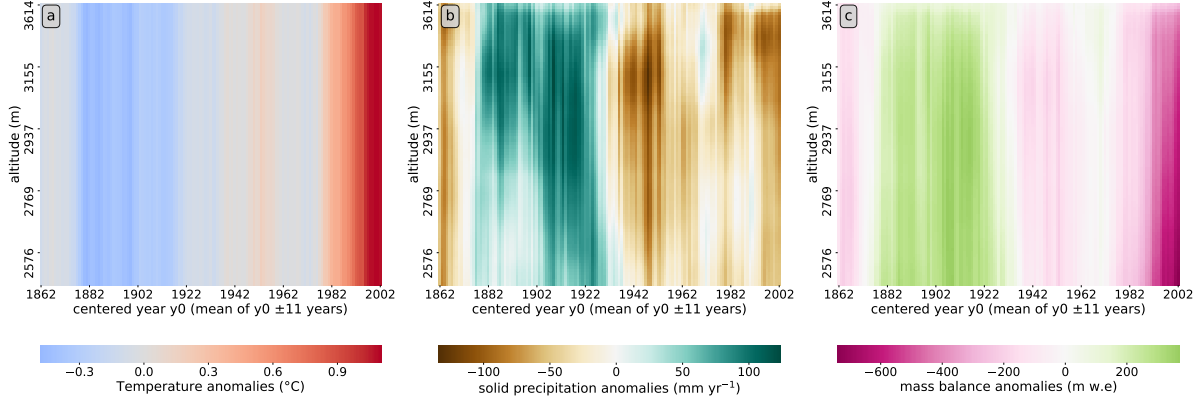


**Fig. A.3:** Climatological anomaly height profiles of the mean 23-year climate of Hintereisferner with centred years from 1862 to 2003 (as extracted from the HISTALP dataset using the Hintereisferner-specific calibration parameters of  $A=3A_0$ ,  $p_f=1.2$ ,  $\epsilon=-100$  and the default other parameters, see Eq. 14). The (c) mass balance anomaly is a mixed signal between (a) temperature and (b) solid precipitation anomaly.

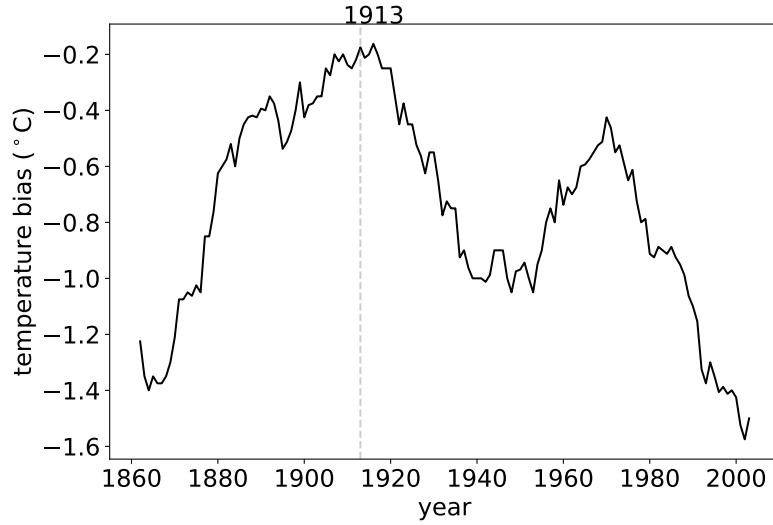


**Fig. A.4:** Applied temperature bias to build an equilibrium Hintereisferner with the same lengths as a fit from observations. The Hintereisferner-specific OGGM parameters  $A=3A_0$ ,  $p_f=1.2$ ,  $\epsilon=-100$  and the HISTALP climate (mean of 23 years), as shown in Fig. A.3, were applied. The mass balance calibration parameter  $tstar$  was here the year 1913.

### A.3 Alps: $A$ -calibration and the asymptotic response time estimates

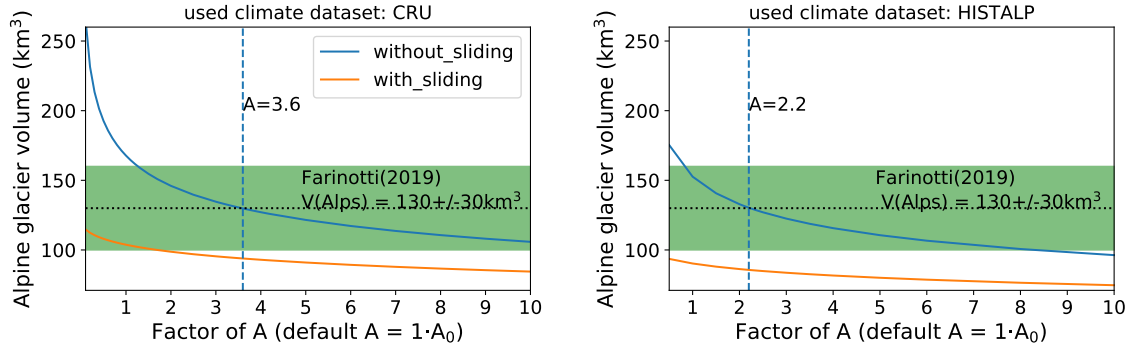


**Fig. A.5:** Calibration of the Alps total glacier ice volume from the inversion process (sum of 3927 glaciers) from OGGM to the Farinotti *et al.* (2019) Alps total glacier ice volume intercomparison estimate ( $130 \pm 30 \text{ km}^3$ ) by tuning the ice creep parameter  $A$ .

(left): Using the model-default CRU dataset, the best estimate would be achieved using  $A=3.6A_0$  without sliding ( $f_s=0$ ) with an Alpine volume estimate of  $V=129.8 \text{ km}^3$ . (right): For the HISTALP dataset with different default parameters for the Alps, the best agreement is for  $A=2.2A_0$  and without sliding with an Alpine volume estimate of  $V=130.3 \text{ km}^3$ . The with\_sliding estimates include parametrisation of Oerlemans (1997) with  $f_s=5.7 \times 10^{-20}$  (see Eq. 17). Both estimates were done without taking any lateral drag parametrisation into account. If a lateral drag parametrisation of Adhikari and J. Marshall (2012) would have been added, a higher  $A$ -parameter would be necessary to get the same ice volume of the Alps: around  $8A_0$  without sliding and  $A=1.7A_0$  with sliding (if  $f_s=5.7 \times 10^{-20}$ ).

The chosen parameters that were used for the results of the Alpine glaciers using HISTALP were hence,  $p_f=1.75$ ,  $T_{\text{melt}}=-1.75^\circ\text{C}$  with  $A=2.2A_0$  (Eq. 14). In Ch. 5.1, a short comparison of the response time using the CRU dataset was done where the parameters  $p_f=2.5$ ,  $T_{\text{melt}}=-1^\circ\text{C}$  with  $A=3.6A_0$  were used.

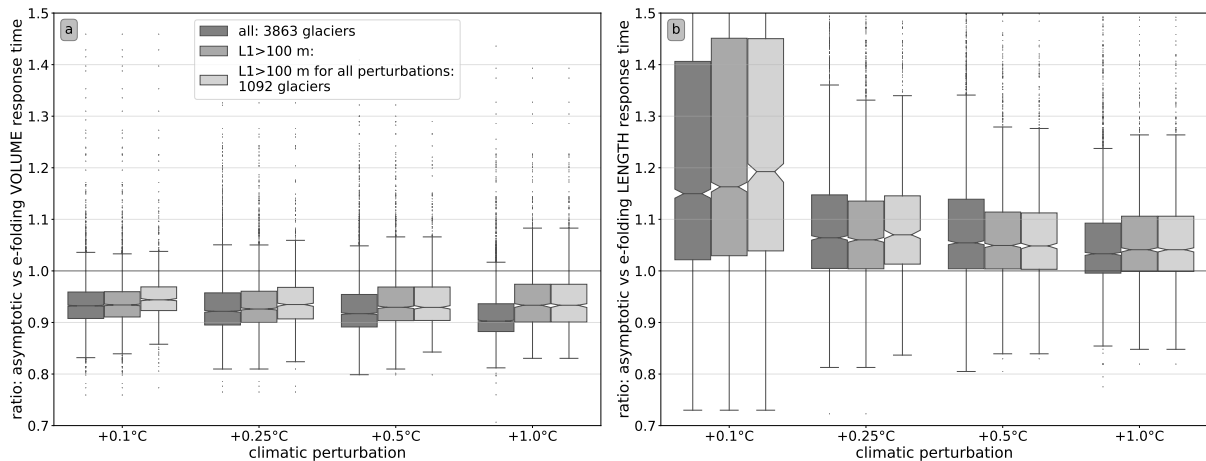


**Fig. A.6:** Ratio of asymptotic (Eq. 8 & Eq. 10/13) to e-folding (Eq. 9) response time estimates of (a) volume and (b) length for Alpine glaciers.

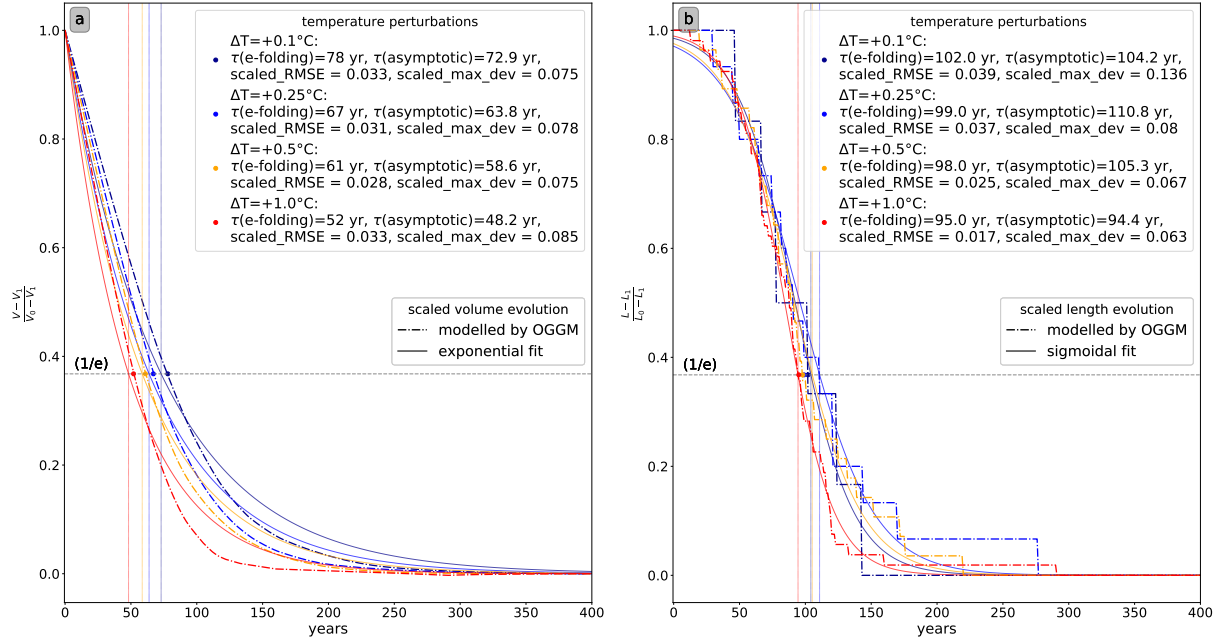


**Fig. A.7: Hintereisferner:** (a) scaled volume,  $V$ , and (b) length,  $L$ , evolution after a climatic step temperature perturbation change of  $\Delta T$  with (a) exponential and (b) sigmoidal fit using the bulk-approach calibration of Alpine glaciers. The corresponding e-folding (see Eq. 9) and asymptotic (see Eq. 8 for volume and Eq. 10 & 13 for length) response times are indicated. The root-mean-square error (RMSE) and the maximum deviation ("fitted"- "modelled" values) are scaled to the volume change by  $\frac{X - X_0}{X_0 - X_1}$  for  $X \in \{V, L\}$ . The index<sub>0</sub> corresponds to the initial equilibrium state and the index<sub>1</sub> to the perturbed equilibrium.

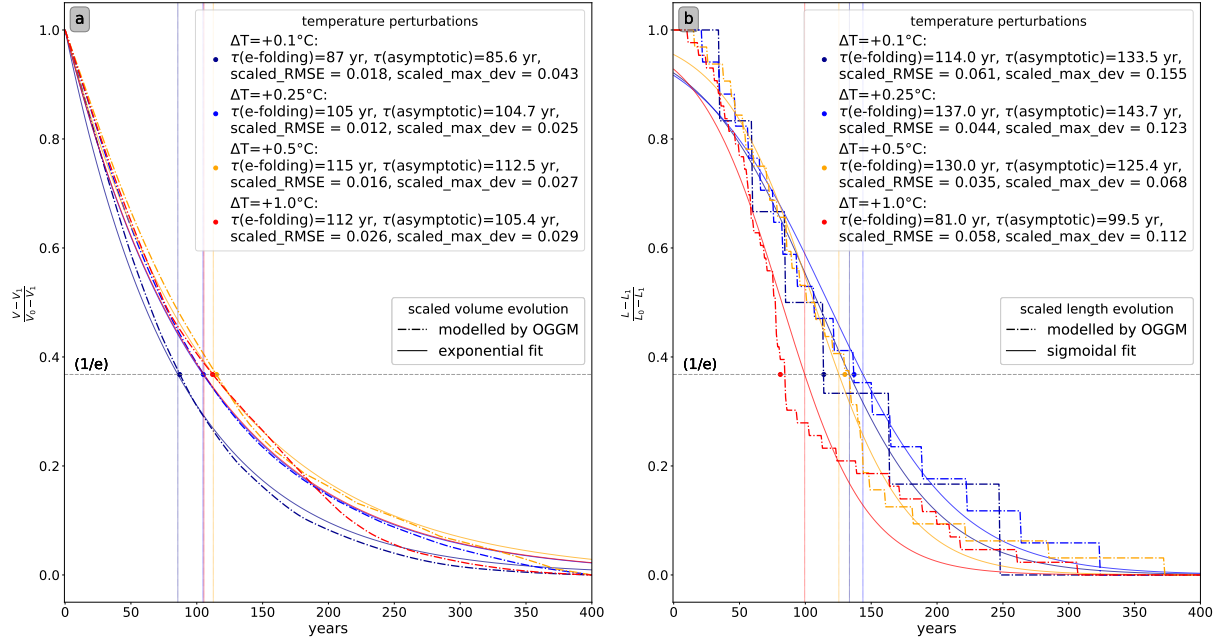


**Fig. A.8: Vernagtferner:** (a) scaled volume,  $V$ , and (b) length,  $L$ , evolution after a climatic step temperature perturbation change of  $\Delta T$  with (a) exponential and (b) sigmoidal fit using the bulk-approach calibration of Alpine glaciers (same as in Fig. A.7).

## Bibliography

- Adhikari, S. and J. Marshall, S.** (2012). Parameterization of lateral drag in flowline models of glacier dynamics. *Journal of Glaciology*, 58(212):1119–1132. <https://doi.org/10.3189/2012JoG12J018>.
- Anderson, B., Lawson, W., and Owens, I.** (2008). Response of Franz Josef Glacier Ka Roimata o Hine Hukatere to climate change. *Global and Planetary Change*, 63(1):23–30. <https://doi.org/10.1016/j.gloplacha.2008.04.003>.
- Auer, I., Böhm, R., Jurkovic, A., Lipa, W., Orlik, A., Potzmann, R., Schöner, W., Ungersböck, M., Matulla, C., Briffa, K., Jones, P., Efthymiadis, D., Brunetti, M., Nanni, T., Maugeri, M., Mercalli, L., Mestre, O., Moisselin, J.-M., Begert, M., Müller-Westermeier, G., Kveton, V., Bochnicek, O., Stastny, P., Lapin, M., Szalai, S., Szentimrey, T., Cegnar, T., Dolinar, M., Gajic-Capka, M., Zaninovic, K., Majstorovic, Z., and Nieplova, E.** (2007). HISTALP—historical instrumental climatological surface time series of the Greater Alpine Region. *International Journal of Climatology*, 27(1):17–46. <https://doi.org/10.1002/joc.1377>.
- Bach, E., Radic, V., and Schoof, C.** (2018). How sensitive are mountain glaciers to climate change? Insights from a block model. *Journal of Glaciology*, 64(244):247–258. <https://doi.org/10.1017/jog.2018.15>.
- Bahr, D. B., Pfeffer, W. T., and Kaser, G.** (2015). A review of volume-area scaling of glaciers. *Reviews of Geophysics*, 53(1):95–140. <https://doi.org/10.1002/2014RG000470>.
- Bahr, D. B., Pfeffer, W. T., Sassolas, C., and Meier, M. F.** (1998). Response time of glaciers as a function of size and mass balance: 1. Theory. *Journal of Geophysical Research: Solid Earth*, 103(B5):9777–9782. <https://doi.org/10.1029/98jb00507>.
- Benn, D. and Evans, D. J.** (2014). Glaciers and glaciation. Routledge. <http://dro.dur.ac.uk/6883/>.
- Böðvarsson, G.** (1955). On the flow of ice-sheets and glaciers.
- Breiman, L.** (2001). Random forests. *Machine learning*, 45(1):5–32.
- Budd, W. F., Keage, P. L., and Blundy, N. A.** (1979). Empirical studies of ice sliding. *Journal of Glaciology*, 23(89):157–170. <https://doi.org/10.3189/S0022143000029804>.
- Burke, E. E. and Roe, G. H.** (2013). The absence of memory in the climatic forcing of glaciers. *Climate Dynamics*, 42(5-6):1335–1346. <https://doi.org/10.1007/s00382-013-1758-0>.
- Cogley, J. G., Hock, R., and Rasmussen, L.** (2011). Glossary of glacier mass balance and related terms. *Journal of Glaciology*. [https://www.research.manchester.ac.uk/portal/files/53855620/Glossary\\_of\\_glacier\\_mass\\_balance.pdf](https://www.research.manchester.ac.uk/portal/files/53855620/Glossary_of_glacier_mass_balance.pdf).
- Cuffey, K. M. and Paterson, W. S. B.** (2010). The physics of glaciers, 4th edition. Academic Press.
- Eis, J., Maussion, F., and Marzeion, B.** (2019). Initialization of a global glacier model based on present-day glacier geometry and past climate information: an ensemble approach (under review). *The Cryosphere Discussions*, pages 1–21. <https://www.the-cryosphere-discuss.net/tc-2019-68/>.
- Elsberg, D. H., Harrison, W. D., Echelmeyer, K. A., and Krimmel, R. M.** (2001). Quantifying the effects of climate and surface change on glacier mass balance. *Journal of Glaciology*, 47(159):649–658. <https://doi.org/10.3189/172756501781831783>.

- Farinotti, D., Brinkerhoff, D. J., Clarke, G. K., Fürst, J. J., Frey, H., Gantayat, P., Gillet-Chaulet, F., Girard, C., Huss, M., Leclercq, P. W., Linsbauer, A., Machguth, H., Martin, C., Maussion, F., Morlighem, M., Mosbeux, C., Pandit, A., Portmann, A., Rabatel, A., Ramsankaran, R., Reerink, T. J., Sanchez, O., Stentoft, P. A., Singh Kumari, S., Van Pelt, W. J., Anderson, B., Benham, T., Binder, D., Dowdeswell, J. A., Fischer, A., Helffricht, K., Kutuzov, S., Lavrentiev, I., McNabb, R., Hilmar Gudmundsson, G., Li, H., and Andreassen, L. M.** (2017). How accurate are estimates of glacier ice thickness? Results from ITMIX, the Ice Thickness Models Intercomparison eXperiment. *Cryosphere*, 11(2):949–970. <https://doi.org/10.5194/tc-11-949-2017>.
- Farinotti, D., Huss, M., Bauder, A., Funk, M., and Truffer, M.** (2009). A method to estimate the ice volume and ice-thickness distribution of alpine glaciers. *Journal of Glaciology*, 55(191):422–430. <https://doi.org/10.3189/002214309788816759>.
- Farinotti, D., Huss, M., Fürst, J. J., Landmann, J., Machguth, H., Maussion, F., and Pandit, A.** (2019). A consensus estimate for the ice thickness distribution of all glaciers on Earth. *Nature Geoscience*, 12(3):168–173. <https://doi.org/10.1038/s41561-019-0300-3>.
- Fischer, M., Huss, M., Barboux, C., and Hoelzle, M.** (2014). The New Swiss Glacier Inventory SGI2010: Relevance of Using High-Resolution Source Data in Areas Dominated by Very Small Glaciers. *Arctic, Antarctic, and Alpine Research*, 46(4):933–945. <https://doi.org/10.1657/1938-4246-46.4.933>.
- Geist, T. and Stotter, J.** (2007). Documentation of glacier surface elevation change with multi-temporal airborne laser scanner data—case study: Hintereisferner and kesselwandferner, tyrol, austria. *Zeitschrift fur Gletscherkunde und Glazialgeologie*, 41:77–106.
- Greuell, W.** (1992). Hintereisferner, Austria: mass-balance reconstruction and numerical modelling of the historical length variations. *Journal of Glaciology*, 38(129):233–244. ISSN 0022-1430. <https://doi.org/10.3189/S0022143000003646>.
- Haeberli, W.** (1995). Glacier fluctuations and climate change detection. *Geografia Fisica e Dinamica Quaternaria*, 18(2):191–199.
- Haeberli, W. and Hoelzle, M.** (1995). Application of inventory data for estimating characteristics of and regional climate-change effects on mountain glaciers: a pilot study with the european alps. *Annals of Glaciology*, 21:206–212. <https://doi.org/10.3189/S0260305500015834>.
- Harris, I., Jones, P. D., Osborn, T. J., and Lister, D. H.** (2014). Updated high-resolution grids of monthly climatic observations—the cru ts3. 10 dataset. *International journal of climatology*, 34(3):623–642.
- Harrison, W. D.** (2013). How do glaciers respond to climate? Perspectives from the simplest models. *Journal of Glaciology*, 59(217):949–960. <https://doi.org/10.3189/2013JoG13J048>.
- Harrison, W. D., Elsberg, D. H., Echelmeyer, K. A., and Krimmel, R. M.** (2001). On the characterization of glacier response by a single time-scale. *Journal of Glaciology*, 47(159):659–664. <https://doi.org/10.3189/172756501781831837>.
- Harrison, W. D., Raymond, C. F., Echelmeyer, K. A., and Krimmel, R. M.** (2003). A macroscopic approach to glacier dynamics. *Journal of Glaciology*, 49(164):13–21. <https://doi.org/10.3189/172756503781830917>.
- Haylock, M., Hofstra, N., Klein Tank, A., Klok, E., Jones, P., and New, M.** (2008). A european daily high-resolution gridded data set of surface temperature and precipitation for 1950–2006. *Journal of Geophysical Research: Atmospheres*, 113(D20).

- Herla, F., Roe, G. H., and Marzeion, B.** (2017). Ensemble statistics of a geometric glacier length model. *Annals of Glaciology*, 58(75pt2):130–135. ISSN 0260-3055. <https://doi.org/10.1017/aog.2017.15>.
- Hooke, R. L.** (2019). Principles of glacier mechanics. Cambridge university press. <https://www.cambridge.org/core/books/principles-of-glacier-mechanics/F803D613F524EB08749846B473F4B285>.
- Huss, M. and Hock, R.** (2018). Global-scale hydrological response to future glacier mass loss. *Nature Climate Change*, 8(2):135–140. <https://doi.org/10.1038/s41558-017-0049-x>.
- Hutter, K.** (1981). The effect of longitudinal strain on the shear stress of an ice sheet: in defence of using stretched coordinates. *Journal of Glaciology*, 27(95):39–56.
- Hutter, K.** (1983). Theoretical glaciology: material science of ice and the mechanics of glaciers and ice sheets. Springer Netherlands, 510 pp.
- Jarosch, A. H., Schoof, C. G., and Anslow, F. S.** (2013). Restoring mass conservation to shallow ice flow models over complex terrain. *Cryosphere*, 7(1):229–240. <https://doi.org/10.5194/tc-7-229-2013>.
- Jarvis, A., Reuter, H. I., Nelson, A., Guevara, E., et al.** (2008). Hole-filled srtm for the globe version 4, available from the cgiar-csi srtm 90m database. <https://cigarcsi.community/data/srtm-90m-digital-elevation-database-v4-1/>.
- Jóhannesson, T.** (1991). Modelling the Effect of Climatic Warming on the Hofsjökull Ice Cap, Central Iceland. *Hydrology Research*, 22(2):81–94. ISSN 0029-1277. <https://doi.org/10.2166/nh.1991.0006>.
- Jóhannesson, T.** (1997). The response of two Icelandic glaciers to climatic warming computed with a degree-day glacier mass-balance model coupled to a dynamic glacier model. *Journal of Glaciology*, 43(144):321–327. <https://doi.org/10.3189/S0022143000003270>.
- Jóhannesson, T., Raymond, C., and Waddington, E.** (1989). Time-scale for adjustment of glaciers to changes in mass balance. *Journal of Glaciology*, 35(121):355–369. <https://doi.org/10.3189/S002214300000928X>.
- Kaser, G., Grosshauser, M., and Marzeion, B.** (2010). Contribution potential of glaciers to water availability in different climate regimes. *Proceedings of the National Academy of Sciences*, 107(47):20223–20227. [www.pnas.org/cgi/doi/10.1073/pnas.1008162107](http://www.pnas.org/cgi/doi/10.1073/pnas.1008162107).
- Kienholz, C., Rich, J. L., Arendt, A. A., and Hock, R.** (2014). A new method for deriving glacier centerlines applied to glaciers in Alaska and northwest Canada. *Cryosphere*, 8(2):503–519. <https://doi.org/10.5194/tc-8-503-2014>.
- Leclercq, P. W. and Oerlemans, J.** (2012). Global and hemispheric temperature reconstruction from glacier length fluctuations. *Climate Dynamics*, 38(5-6):1065–1079. ISSN 0930-7575. <https://doi.org/10.1007/s00382-011-1145-7>.
- Leclercq, P. W., Oerlemans, J., Basagic, H. J., Bushueva, I., Cook, A. J., and Le Bris, R.** (2014). A data set of worldwide glacier length fluctuations. *The Cryosphere*, 8(2):659–672. ISSN 1994-0424. <https://doi.org/10.5194/tc-8-659-2014>.
- Leysinger Vieli, G. J.-M. C. and Gudmundsson, G. H.** (2004). On estimating length fluctuations of glaciers caused by changes in climatic forcing. *Journal of Geophysical Research: Earth Surface*, 109(F1):1–14. <https://doi.org/10.1029/2003jf000027>.

- Lüthi, M. P.** (2009). Transient response of idealized glaciers to climate variations. *Journal of Glaciology*, 55(193):918–930. [https://www.cambridge.org/core/product/identifier/S0022143000205844/type/journal\\_article](https://www.cambridge.org/core/product/identifier/S0022143000205844/type/journal_article).
- Marzeion, B., Cogley, J. G., Richter, K., and Parkes, D.** (2014a). Attribution of global glacier mass loss to anthropogenic and natural causes. *Science*, 345(6199):919–921. ISSN 0036-8075. <https://doi.org/10.1126/science.1254702>.
- Marzeion, B., Jarosch, A. H., and Gregory, J. M.** (2014b). Feedbacks and mechanisms affecting the global sensitivity of glaciers to climate change. *The Cryosphere*, 8(1):59–71. ISSN 1994-0424. <https://doi.org/10.5194/tc-8-59-2014>.
- Marzeion, B., Jarosch, A. H., and Hofer, M.** (2012). Past and future sea-level change from the surface mass balance of glaciers. *Cryosphere*, 6(6):1295–1322. <https://doi.org/10.5194/tc-6-1295-2012>.
- Marzeion, B., Kaser, G., Maussion, F., and Champollion, N.** (2018). Limited influence of climate change mitigation on short-term glacier mass loss. *Nature Climate Change*, 8(April):1–4. <http://dx.doi.org/10.1038/s41558-018-0093-1>.
- Maussion, F., Butenko, A., Champollion, N., Dusch, M., Eis, J., Fourteau, K., Gregor, P., Jarosch, A. H., Landmann, J., Oesterle, F., Recinos, B., Rothenpieler, T., Vlug, A., Wild, C. T., and Marzeion, B.** (2019a). The Open Global Glacier Model (OGGM) v1.1. *Geoscientific Model Development*, 12(3):909–931. <https://doi.org/10.5194/gmd-12-909-2019>.
- Maussion, F., Roth, T., Dusch, M., Recinos, B., Vlug, A., Marzeion, B., Oberrauch, M., Eis, J., Landmann, J., Jarosch, A., Bartholomew, S. L., Champollion, N., Castellani, M., Gregor, P., Antonub, Smith, S., and Rounce, D.** (2019b). Oggm/oggm: v1.1.2. <https://doi.org/10.5281/zenodo.3406019>.
- Nye, J. F.** (1960). The response of glaciers and ice-sheets to seasonal and climatic changes. *Proceedings of the Royal Society of London. Series A. Mathematical and Physical Sciences*, 256(1287):559–584.
- Nye, J. F.** (1963). On the Theory of the Advance and Retreat of Glaciers. *Geophysical Journal International*, 7(4):431–456. <https://doi.org/10.1111/j.1365-246X.1963.tb07087.x>.
- Oerlemans, J.** (1997). Climate sensitivity of Franz Josef Glacier, New Zealand, as revealed by numerical modeling. *Arctic and Alpine Research*, 29(2):233–239.
- Oerlemans, J.** (2001). Glaciers and climate change. CRC Press.
- Oerlemans, J.** (2005). Atmospheric science: Extracting a climate signal from 169 glacier records. *Science*, 308(5722):675–677. <https://doi.org/10.1126/science.1107046>.
- Oerlemans, J.** (2007). Estimating response times of Vadret da Morteratsch, Vadret da Palü, Briksdalsbreen and Nigardsbreen from their length records. *Journal of Glaciology*, 53(182):357–362. <https://doi.org/10.3189/002214307783258387>.
- Oerlemans, J.** (2008). Minimal glacier models. Igitur Universiteitsbibliotheek Utrecht.
- Oerlemans, J.** (2012). Linear modelling of glacier length fluctuations. *Geografiska Annaler, Series A: Physical Geography*, 94(2):183–194. <https://doi.org/10.1111/j.1468-0459.2012.00469.x>.
- Oerlemans, J.** (2018). Modelling the late Holocene and future evolution of Monaco-breen, northern Spitsbergen. *Cryosphere*, 12(9):3001–3015. <https://doi.org/10.5194/tc-12-3001-2018>.

- Oppenheimer, M., Glavovic, B., Hinkel, J., van de Wal, R., Magnan, A. K., Abd-Elgawad, A., Cai, R., Cifuentes-Jara, M., Deconto, R. M., Ghosh, T., Isla, F., Marzeion, B., Meyssignac, B., and Sebesvari, Z.** (2019). Sea level rise and implications for low lying islands, coasts and communities. In: *IPCC Special Report on the Ocean and Cryosphere in a Changing Climate* [H.-O. Pörtner, D.C. Roberts, V. Masson-Delmotte, P. Zhai, M. Tignor, E. Poloczanska, K. Mintenbeck, A. Alegría, M. Nicolai, A. Okem, J. Petzold, B. Rama, N.M. Weyer (eds.)]. In press. [https://report.ipcc.ch/srocc/pdf/SROCC\\_FinalDraft\\_Chapter4.pdf](https://report.ipcc.ch/srocc/pdf/SROCC_FinalDraft_Chapter4.pdf).
- Otto, J.-C.** (2019). Proglacial Lakes in High Mountain Environments, pages 231–247. Springer International Publishing. ISBN 978-3-319-94184-4. [https://doi.org/10.1007/978-3-319-94184-4\\_14](https://doi.org/10.1007/978-3-319-94184-4_14).
- Pedregosa, F., Varoquaux, G., Gramfort, A., Michel, V., Thirion, B., Grisel, O., Blondel, M., Prettenhofer, P., Weiss, R., Dubourg, V., Vanderplas, J., Passos, A., Cournapeau, D., Brucher, M., Perrot, M., and Duchesnay, E.** (2011). Scikit-learn: Machine learning in Python. *Journal of Machine Learning Research*, 12:2825–2830.
- Peltz, M. S. and Hedlund, C.** (2001). Terminus behavior and response time of North Cascade glaciers, Washington, U.S.A. *Journal of Glaciology*, 47(158):497–506. <https://doi.org/10.3189/172756501781832098>.
- Pfeffer, W. T., Arendt, A. A., Bliss, A., Bolch, T., Cogley, J. G., Gardner, A. S., Hagen, J.-O., Hock, R., Kaser, G., Kienholz, C., and et al.** (2014). The randolph glacier inventory: a globally complete inventory of glaciers. *Journal of Glaciology*, 60(221):537–552. <https://doi.org/10.3189/2014JoG13J176>.
- Pfeffer, W. T., Sassolas, C., Bahr, D. B., and Meier, M. F.** (1998). Response time of glaciers as a function of size and mass balance: 2. Numerical experiments. *Journal of Geophysical Research: Solid Earth*, 103(B5):9783–9789. <http://doi.wiley.com/10.1029/98JB00508>.
- Raper, S. C. and Braithwaite, R. J.** (2009). Glacier volume response time and its links to climate and topography based on a conceptual model of glacier hypsometry. *Cryosphere*, 3(2):183–194. <https://doi.org/10.5194/tc-3-183-2009>.
- Richardson, S. D. and Reynolds, J. M.** (2000). An overview of glacial hazards in the himalayas. *Quaternary International*, 65:31–47.
- Roe, G. H.** (2011). What do glaciers tell us about climate variability and climate change? *Journal of Glaciology*, 57(203):567–578. [https://www.cambridge.org/core/product/identifier/S0022143000205649/type/journal\\_article](https://www.cambridge.org/core/product/identifier/S0022143000205649/type/journal_article).
- Roe, G. H. and Baker, M. B.** (2014). Glacier response to climate perturbations: an accurate linear geometric model. *Journal of Glaciology*, 60(222):670–684. [https://www.cambridge.org/core/product/identifier/S0022143000203031/type/journal\\_article](https://www.cambridge.org/core/product/identifier/S0022143000203031/type/journal_article).
- Roe, G. H. and Baker, M. B.** (2016). The response of glaciers to climatic persistence. *Journal of Glaciology*, 62(233):440–450. [https://www.cambridge.org/core/product/identifier/S0022143016000046/type/journal\\_article](https://www.cambridge.org/core/product/identifier/S0022143016000046/type/journal_article).
- Roe, G. H. and O’Neal, M. A.** (2009). The response of glaciers to intrinsic climate variability: observations and models of late-Holocene variations in the Pacific Northwest. *Journal of Glaciology*, 55(193):839–854. <https://doi.org/10.3189/002214309790152438>.
- Span, N. and Fischer, A.** (2005). Radarmessungen der Eisdicke österreichischer Gletscher [1995–1998]: Messungen 1995 bis 1998 (Bd. 1). Zentralanstalt für Meteorologie und Geodynamik.

- Strobl, C., Boulesteix, A.-L., Kneib, T., Augustin, T., and Zeileis, A.** (2008). Conditional variable importance for random forests. *BMC Bioinformatics*, 9(307). <http://www.biomedcentral.com/1471-2105/9/307>.
- Strobl, C., Boulesteix, A.-L., Zeileis, A., and Hothorn, T.** (2007). Bias in random forest variable importance measures: Illustrations, sources and a solution. *BMC bioinformatics*, 8(1):25.
- Strobl, C., Hothorn, T., and Zeileis, A.** (2009). Party on! A new, conditional variable importance measure available in the party package. <https://epub.ub.uni-muenchen.de/9387/1/techreport.pdf>.
- van de Wal, R. S. W. and Oerlemans, J.** (1995). Response of valley glaciers to climate change and kinematic waves: a study with a numerical ice-flow model. *Journal of Glaciology*, 41(137):142–152. ISSN 0022-1430. <https://doi.org/10.3189/S0022143000017834>.
- WGMS** (2017). Fluctuations of glaciers database. *World Glacier Monitoring Service, Zurich, Switzerland*. [https://wgms.ch/products\\_fog/](https://wgms.ch/products_fog/).
- Wilks, D. S.** (2011). Statistical methods in the atmospheric sciences, volume 100. Academic press. <https://www.elsevier.com/books/statistical-methods-in-the-atmospheric-sciences/wilks/978-0-12-385022-5>.
- Zekollari, H., Huss, M., and Farinotti, D.** (2019). Modelling the future evolution of glaciers in the European Alps under the EURO-CORDEX RCM ensemble. *Cryosphere*, 13(4):1125–1146. ISSN 19940424. <https://doi.org/10.5194/tc-13-1125-2019>.
- Zekollari, H., Huss, M., and Farinotti, D.** (2020). On the Imbalance and Response Time of Glaciers in the European Alps. *Geophysical Research Letters*, 47(2):e2019GL085578. ISSN 0094-8276. <https://doi.org/10.1029/2019GL085578>.
- Zekollari, H. and Huybrechts, P.** (2015). On the climate-geometry imbalance, response time and volume-area scaling of an alpine glacier: insights from a 3-D flow model applied to Vadret da Morteratsch, Switzerland. *Annals of Glaciology*, 56(70):51–62. [https://www.cambridge.org/core/product/identifier/S0260305500250325/type/journal\\_article](https://www.cambridge.org/core/product/identifier/S0260305500250325/type/journal_article).
- Zemp, M., Huss, M., Thibert, E., Eckert, N., McNabb, R., Huber, J., Barandun, M., Machguth, H., Nussbaumer, S. U., Gärtner-Roer, I., Thomson, L., Paul, F., Maussion, F., Kutuzov, S., and Cogley, J. G.** (2019). Global glacier mass changes and their contributions to sea-level rise from 1961 to 2016. *Nature*, 568(7752):382–386. <http://www.nature.com/articles/s41586-019-1071-0>.



## Acknowledgments

First of all, I would like to thank my supervisor Fabien Maussion for offering me this thesis subject, for helping to sort my ideas with a lot of patience and for all the inspiring discussions that we had. I am grateful that I got the opportunity to use the Open Global Glacier Model (OGGM) and that I could discover the depths of its code.

Furthermore, I want to thank Matthias Dusch for answering me numerous questions about the OGGM code. He performed also the Hintereisferner-specific length-fitting model calibration of OGGM that I used in Ch. 4.2.2.

The computational results for the Alpine glaciers have been achieved using the cluster of the University of Bremen.

Next, I wish to show my gratitude to my study colleagues for the great time that we spent together. Special thanks go to Zora Schirmeister for the many fruitful study projects, as well as for our adventures in the mountains together.

Moreover, I would like to thank Valentin Marteau, my parents and my siblings for assisting and encouraging me - each one - in their way.

I am glad that I could live in a place such as Innsbruck: a balanced combination of intensive studies and extensive exercises in nature kept me both, motivated and fulfilled, during my Master studies.

*"Life is like riding a bicycle. In order to keep your balance, you must keep moving."*

Albert Einstein

